IDENTIFICATION OF THE RNA BINDING PROTEIN RBM3 AS A NOVEL EFFECTOR OF β-CATENIN SIGNALING AND COLON CANCER STEM CELLS

By

Anand Venugopal

Submitted to the graduate degree program in Molecular and Integrative Physiology and the Graduate Faculty of the University of Kansas in partial fulfillment of the requirements for the degree of Doctor of Philosophy.

_____
Chairperson Shrikant Anant, Ph.D.

_____
Roy Jensen, M.D.

_____
Andrew Godwin, Ph.D.

_____
Danny Welch, Ph.D.

_____
John Wood, Ph.D.

Date Defended: March 14, 2014

The Dissertation Committee for Anand Venugopal

certifies that this is the approved version of the following dissertation:

IDENTIFICATION OF THE RNA BINDING PROTEIN RBM3 AS A NOVEL EFFECTOR OF β-CATENIN SIGNALING AND COLON CANCER STEM CELLS

_____

Chairperson Shrikant Anant, Ph.D.

Date approved: March 14, 2014

Abstract

The intestinal epithelium is one of the fastest renewing tissues within the adult. This renewal is primarily driven by the intestinal epithelial stem cell compartment and homeostasis of this compartment needs to be strictly maintained. Loss of regulation can lead to hyperplasia and subsequent malignant transformation. Moreover, cancers are also thought to contain a stem cell population which maintains long term tumor viability and recurrence following therapy. Therefore, a thorough understanding of the molecular machinery that governs stem cell homeostasis can further our understanding of colon cancer initiation and progression. The RNA binding protein RBM3 is upregulated in many solid tumors including colon, prostate and breast. It also serves as a proto-oncogene inducing the malignant transformation of normal cells when overexpressed. To further characterize the mechanism, we overexpressed RBM3 in DLD-1 and HCT 116 colon cancer cell lines. We show that RBM3 overexpression is capable of increasing the cancer stem cell phenotype as measured by side population assay, spheroid formation and expression of the putative stem cell markers DCLK1, LGR5 and CD44. Interestingly, RBM3 also increases chemoresistance through increased multidrug efflux and quiescence, both characteristics commonly attributed to cancer stem cells. Moreover, RBM3 overexpression appears to increase activity of the β-catenin signaling cascade, a pathway critical for the maintenance of stem cell self-renewal and implicated in the pathogenesis of colon cancer. We also show that RBM3 overexpression decreases the activity of GSK3β, a member of the destruction complex known to suppress β-catenin levels within the cell. Consistent with this, pharmacologic inhibition of GSK3β similarly phenocopies RBM3 induced β-catenin transcriptional activity. Taken together, we conclude that RBM3 overexpression is capable of

increasing the cancer stem cell population. We also show a novel role for RBM3 in increasing β-catenin signaling activity. Based on these data, we infer that the overexpression of RBM3 observed within solid tumors may be critical for maintaining self-renewal within the cancer stem cells and necessary for long term viability of tumor formation.

Dedication

Dedicated to my fiancée Jessica,

I treasure every step we take together

Your endless love is my foundation

Acknowledgements

First and foremost, I want to thank Dr. Shrikant Anant for his mentorship. Thank you for providing me to opportunities to develop my scientific career. You always allowed me the independence to pursue my own ideas and when I needed it, you pushed me beyond the limits of my own comfort to achieve what I never thought would be possible. Without question, you provided the resources I needed to pursue each of my ideas. You taught me how much more there is to science than just performing experiments. I cannot thank you enough for your guidance when I was lost, your encouragement when I was in doubt, your patience when I was trying, and most of all for providing me a home for the past four years. The lessons I have learned under your mentorship, I will carry with me for the rest of my life.

I would also like to thank Dr. Shahid Umar for his dedication to my training. For some reason that eludes me, you have devoted more time and energy in guiding me through my research than I ever deserved. I am consistently amazed by the passion and thoroughness that you display towards your research. Thank you for always finding the time to appraise and advise me on my research.

I want to express my gratitude to Dr. Roy Jensen. Thank you for being my advocate in the early months of my career. Thank you for providing a laboratory for me to work in while I awaited the opening of Dr. Anant's new lab. Finally, thank you for serving on my committee and continuing to provide valuable advice for my research.

I would like to thank all of the members of my lab. To Dr. Satish Ramalingam, Mrs. Priya Ponnurangam, Dr. Partha Rangarajan, Mr. David Standing, Mr. Naveen Neradugomma, Dr.

Prabhu Ramamoorthy, Dr. Gaurav Kaushik, Ms. Lauren Larsen, and Ms. Dannita Youngblood. You have all been an integral part of my life for the past four years. I truly value the scientific discourse and companionship we have shared.

I am especially grateful to Dr. Dharma Subramaniam for expanding my scientific techniques. Thank you for assisting me with the technical aspects of lab work that I would never have been able to learn on my own. I am also grateful for your willingness to help me at any time of day or night and for always being there to listen.

I want to thank Dr. Deep Kwatra for training me with much of the drug resistance work. Because of you I was able to efficiently complete these experiments. I am also grateful for your ever-present optimism. In light of good news and bad, it has helped to lift my spirits.

I am grateful to the members of my committee. Dr. Roy Jensen, Dr. Andrew Godwin, Dr. Danny Welch and Dr. John Wood, thank you for serving on my dissertation advisory committee. Thank you for providing the constructive criticism on my project to help develop it as best I could. I greatly value your input and guidance as I develop my career.

I want to thank Dr. Paul Cheney for your endless support of myself as well as all of the students within the department. Your commitment to the students and to the Physiology Society has been priceless. Thank you for helping to ensure that the years we students spend within the Physiology Department are the best they could possibly be.

I want to thank Ms. Shari Standiferd for always helping to guide me through the jungle of paperwork that always seems to overwhelm me. Your thorough administrative knowledge, your efficiency and most of all your unfailing willingness to help have allowed me to perform my work, serve my fellow students and move through this program with minimal interruption.

I want to express my gratitude to the leadership of the MD/PhD Program. To Dr. Timothy Fields and Dr. Brenda Rongish, thank you for always looking out for us. Also, I would like to thank Mrs. Janice Fletcher for making sure we make it through the many jarring transitions that we experience as we move through this program.

I also thank the National Institute of Digestive and Diabetic and Kidney Diseases for sponsoring my research of RNA binding proteins in intestinal stem cells and for generously funding my training as a physician scientist.

I cannot express my gratitude to my parents enough. Thank you for providing me guidance when I least wanted it, but most needed it. Thank you for your unwavering support in everything I do. And thank you for allowing me the freedom to make my own mistakes and find my own path.

Finally, thank you to my fiancée, Jessica Johnson. You are a constant inspiration in my life. I want you to know how much I love you and how grateful I am that you are sharing this journey with me.

Table of Contents

List of Tables and Figures

Chapter I: Introduction

Chapter II: Overexpression of RBM3 increases stem cell characteristics and chemoresistance in colon cancer cells

Chapter III: RBM3 overexpression generates an increase in β-catenin signaling

Chapter IV: RBM3 induces a quiescent state in colon cancer cells

List of Abbreviations

5-FU	5-fluorouracil
7AAD	7-amino actinomycin D
ABC	ATP binding cassette
ADM	Doxorubicin
AF488	AlexaFluor 488
AF647	AlexaFluor 647
ALDH1A1	Aldehyde dehydrogenase 1A1
AML	Acute myeloid leukemia
APC	Adenomatous polyposis coli
APCF	Allophycocyanin
BCRP	Breast cancer resistance protein
bFGF	Basic recombinant fibroblast growth factor
BIO	6-bromoindirubin-3'-oxime
BMI1	B lymphoma Mo-MLV insertion region 1 homolog
BrdU	Bromo-deoxy uridine
βTrCP	β transducing repeat containing protein
CBC	Crypt basal columnar cell
CK1	Casein kinase 1
COX-2	Cyclooxygenase 2
CSC	Cancer stem cell
DAPT	N-[N-(3,5-Difluorophenacetyl)-L-alanyl]-S-phenylglycine t-butyl ester
DCLK1	Doublecortin containing calmodulin-like kinase 1
DCV	DyeCycle violet
DLL	Delta-like
DMEM	Dulbecco's modified Eagle medium
Dox	Doxycycline
EGF	Epidermal growth factor
EMT	Epithelial-to-mesenchymal transition
FACS	Fluorescence activated cell sorting
FAP	Familial adenomatous polyposis
FBS	Fetal bovine serum
FSC	Forward scatter
G6PDH	Glucose-6-phosphate dehydrogenase
GAPDH	Glyceraldehyde phosphate dehydrogenase
GFP	Green fluorescent protein
GM-CSF	Granulocyte monocyte colony stimulating factor
GSK3β	Glycogen synthase kinase 3β
HDAC	Histone de-acetylase
HIF	Hypoxia inducible factor

HSC	Hematopoietic stem cell
HuR	Human antigen R
IF	Immunofluorescence
IHC	Immunohistochemistry
IL-8	Interleukin 8
iPSC	Induced pluripotent stem cell
ISC	Intestinal stem cell
LEF	Lymphoid enhancer binding factor
LGR5	Leucine-rich repeat-containing G-protein coupled receptor 5
LOH	Loss of heterozygosity
LPS	Lipopolysaccharide
LRC	Label retaining cell
LRP	Low density lipoprotein related protein
MIN	Multiple intestinal neoplasia
MOI	Mean of infection
MRP	Multidrug resistance protein
Msi1	Musashi1
NICD	Notch intracellular domain
NS-398	N-[2-(Cyclohexyloxy)-4-nitrophenyl]methanesulfonamide
PBS	Phosphate buffered saline
PE	Phycoerythrin
PGE2	Prostaglandin E2
Pgp	Phospho-glycoprotein
RBM3	RNA binding motif containing protein 3
SCID	Severe combined immune deficient
SELEX	Systematic evolution of ligands by exponential enrichment
SEM	Standard error of mean
siCTNNB1	Small interfering RNA for *CTNNB1*
siRNA	Small interfering RNA
siSCR	Non-specific small interfering RNA
SP	Side population
SSC	Side scatter
TCF	Transcription factor
UTR	Untranslated region
VEGF	Vascular endothelial growth factor

Chapter I: Introduction

Intestinal epithelial renewal

The intestinal epithelium is one of the fastest renewing tissues in adult mammals (Heath, 1996). It is composed of a one cell thick layer of epithelial cells that serves the functions of nutrient and water absorption, mucous secretion, and barrier formation. This epithelial layer is turned over approximately every three to four days and requires a high rate of proliferation to maintain this rate of turnover. Small shifts in the proliferative rate can result in significant changes to normal intestinal function and hence disease. A decrease in intestinal epithelial renewal may result in wasting disease or loss of intestinal barrier function, and more importantly, hyperplastic proliferation can result in the formation of intestinal malignancies. As such, intestinal epithelial renewal needs to be tightly regulated. It is important to understand the signaling pathways that regulate intestinal epithelial renewal and in turn the factors that can influence the activity of these signaling pathways in order to further understand the pathogenesis and mechanisms of disease states such as colorectal cancer.

This study is primarily focused on stem cells as they relate to colon cancer. We begin this discussion with an overview of the current knowledge of the stem cell in the context of normal adult intestinal physiology and progress into implications of this evidence in the study of cancer.

Intestinal epithelial architecture, hierarchy and the intestinal stem cell

The intestinal epithelial layer is composed of crypts of Lieberkühn which are invaginations of the intestinal surface, and villi which are protrusions of the intestinal surface (Figure 1). This surface from the crypt base to the villus apex composes the crypt-villus axis. The majority of proliferation occurs at a proliferative zone near the crypt base called the transit amplifying

Figure 1

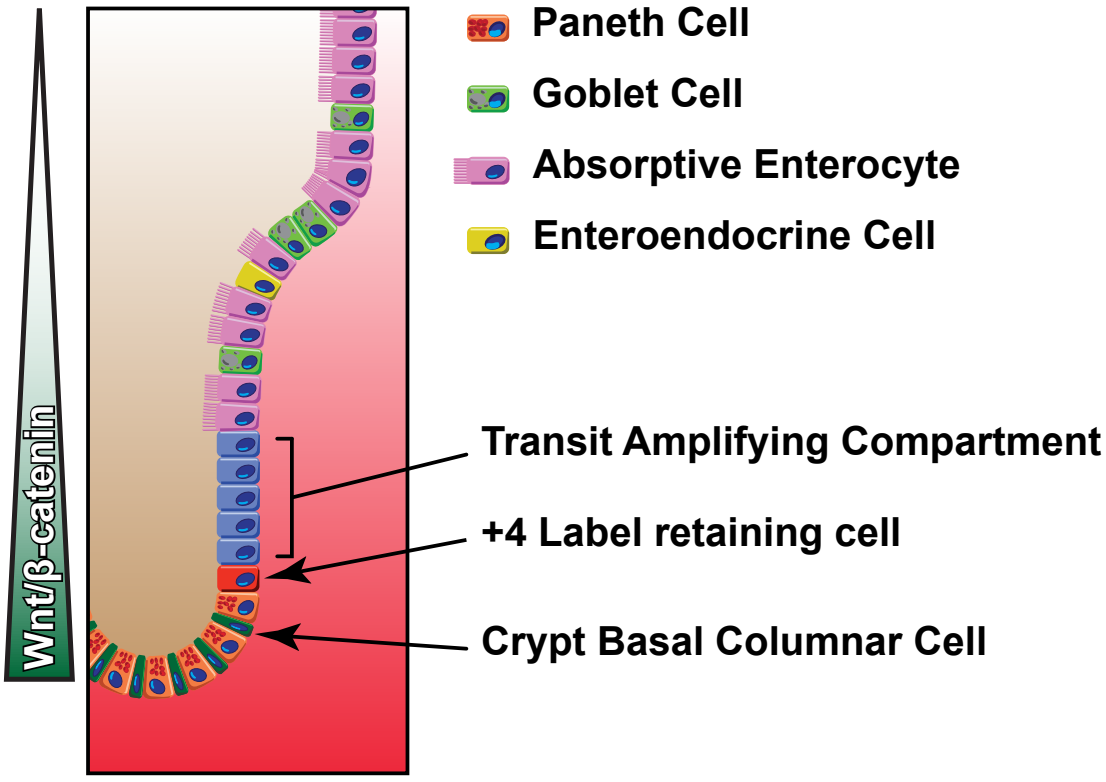
Wnt/β-catenin
Paneth Cell
Goblet Cell
Absorptive Enterocyte
Enteroendocrine Cell
Transit Amplifying Compartment
+4 Label retaining cell
Crypt Basal Columnar Cell

Figure 1: Schematic diagram of the crypt-villus axis of the small intestine. Depicted are the +4 LRC, the CBC and the transit amplifying compartment. Additionally, intensity of the Wnt/β-catenin signaling cascade is represented on the left. The colon differs from the small intestine in that there are no villi, the goblet cells are present in greater abundance and paneth cells are absent.

compartment. Cells reside within this region for approximately two days dividing several times, then terminally differentiate into one of three lineages: enterocyte, goblet cell or enteroendocrine cell and ascend along the crypt-villus axis for approximately three days until undergoing spontaneous apoptosis at or near the villus apex (Hall et al., 1994). There is also one differentiated cell type – the paneth cell – which resides at the crypt bottom. Additionally there are a few differences between the architecture of the large and small intestine. Notably, relative to the small intestine, the large intestine has no villus structures, the proportion of mucus secreting goblet cells is significantly increased and the crypt bases contain no paneth cells.

In order to understand the driving force of intestinal renewal, it was shown that at the bases of crypts exist a small population of intestinal stem cells (ISCs) through several different studies. One of the original studies illustrated that the entire epithelium of each crypt clonal in origin. Using immunohistochemistry (IHC) to measure glucose-6-phosphate dehydrogenase (G6PDH) activity in mice with a heterozygous mutation for G6PDH following treatment with a colonic mutagen, it was revealed that loss of heterozygosity (LOH) occurred across entire crypts (Griffiths et al., 1988). This finding rather than sporadic LOH along crypts implied that the epithelial lining of crypts arose in a clonal fashion. Additionally, by observing crypts of chimeric mice, it was observed that crypts originate as polyclonal structures, but over time, become monoclonal (Schmidt et al., 1988). These studies imply that the entire epithelium of each intestinal crypt must arise from a very limited number of cells residing within the crypt that give rise to a clonal population of differentiated epithelial cells.

Stem cells are cells with the capacity to give rise to differentiated cell lineages and the capacity to generate at least one daughter cell that maintains the stem cell phenotype (self-renewal) (Wagers and Weissman, 2004). Indeed in the intestinal crypt two discrete populations of cells

have been elucidated which both have the capacity to self-renew and which generate the full spectrum of differentiated intestinal epithelial lineages. However, these two populations are characterized with distinct niches and different proliferative capacity. The first identified population was observed through label retention studies. Potten, *et al.* demonstrated that following treatment with a nucleoside analogue, there was a small population of cells near the base of the crypt that retained the nucleoside label for up to four weeks (Potten et al., 1978). These cells referred to as label retaining cells (LRCs) are located approximately four cells from the base of the crypt in the supra-paneth region also known as the +4 position. The +4 LRC represents a subpopulation of quiescent stem cells within the crypt (Potten et al., 1997). These LRCs are also insensitive to inactivation of CDC25 (a protein required to drive cell cycle progression) further suggesting that the LRCs represent a quiescent stem cell pool (Lee et al., 2009).

More recently discovered is the population of crypt basal columnar cells (CBCs) that lie at the very base of the crypt. CBCs were originally described as a cycling population of cells residing between paneth cells within the base of the crypt (Cheng and Leblond, 1974). They are also morphologically distinct from the +4 LRCs as they are interspersed between paneth cells, contain very little cytoplasm and have a sliver-like shape (Barker et al., 2007). Additionally, CBCs harvested through laser capture microdissection have been shown to share gene signatures with hematopoietic stem cells (HSCs) and neural stem cells (Stappenbeck et al., 2003). Later studies showed that these cells represent a long lived but rapidly cycling ISC pool that is capable of generating the differentiated epithelial lineages (Barker et al., 2007). In contrast to LRCs, CBCs are indeed sensitive to loss of CDC25 and show loss of cell cycle progression and differentiation following CDC25 deletion (Lee et al., 2009). Finally, it was shown that the CBC population isn't

strictly necessary for maintaining intestinal epithelial homeostasis (Tian et al., 2011). In fact, diphtheria toxin directed ablation of the CBC compartment was compensated for by expansion of the +4 LRC population which later regenerated the CBC population. This study provides evidence for a hierarchical relationship with the quiescent +4 LRC giving rise to the rapidly cycling CBC (Tian et al., 2011). On the other hand, +4 LRCs have been shown to be especially susceptible to radiation based injury, presumably to protect the genomic integrity of the cell responsible for producing the entire progeny of the crypt (May et al., 2008; Potten, 1977). CBCs on the other hand, have been shown to be indispensable for crypt regeneration following radiation injury, implying that +4 LRCs undergo apoptosis more readily in the context of genotoxic injury, at which point CBCs can serve as the reserve population for the +4 LRCs (Metcalfe et al., 2013). Current evidence suggests that the CBC and LRC populations serve to compensate for loss of eachother under certain contexts, however the exact role that each distinct stem cell population plays in maintaining intestinal epithelial homeostasis and oncogenic transformation as well as the interplay between the quiescent and rapidly cycling stem cell pool is not yet fully understood.

In order to further characterize the functional roles of these distinct ISC populations, large efforts have been made to identify and isolate LRCs and CBCs. Concomitantly with the studies that revealed some of the functional roles and niches of the LRCs and CBCs, studies were conducted which revealed specific markers for these populations. One of the initially identified stem cell markers of the LRC population was B lymphoma Mo-MLV insertion region 1 homolog (Bmi-1) (Sangiorgi and Capecchi, 2008). Bmi-1 was originally found to be an important regulator of the proliferation of HSCs as well as a marker of neural stem cells (Lessard and Sauvageau, 2003; Molofsky et al., 2003). Later studies showed that Bmi-1 also marks the +4 LRC and that these

cells were capable of self-renewal and differentiation as demonstrated by their ability to generate the four lineages of the small intestine. A Bmi-1 specific expression of diphtheria toxin receptor results in crypt degeneration following administration of diphtheria toxin (Sangiorgi and Capecchi, 2008). This observation serves to further validate the stem cell properties of the +4 LRC as well as implicates Bmi-1 expression as a marker of the LRC. Additionally, one of the more recently discovered markers of the LRC is doublecortin containing calmodulin-like kinase 1 (DCLK1) which is expressed in discrete cells at the +4 position in the intestinal crypt (Giannakis et al., 2006; May et al., 2008).

A potential stem cell marker known to identify cells of the CBC niche is the Leucine-rich repeat-containing G-protein coupled receptor 5 (LGR5). LGR5 was first identified as a target of the Wnt/β-catenin pathway that is highly upregulated at the crypt base. Additionally, lineage tracing experiments using the LGR5 promoter to activate LacZ expression showed discrete clonal ribbons of LacZ positive cells implying that LGR5 positive cells could generate a crypt of clonal origin with all four differentiated epithelial lineages (Barker et al., 2007). A more in depth discussion on the relation between these stem cell markers and intestinal tumorigenesis is discussed in the following section.

There are however, some largely important questions arising when investigating these stem cell markers. First, are these markers truly markers of stem cells or are they just upregulated in stem cells leading to and enrichment rather than a distinctive marking of stem cells? Additionally, while many stem cell markers have been elucidated, it is unclear what their functional relevance is in the stem cell. The question remains whether expression of these markers can induce or maintain the stem cell phenotype or if the stem cell phenotype leads to expression of these

markers. While these questions remain largely outside of the scope of the current study, they are an important aspect of ISC physiology that warrants investigation.

Cancer stem cells

The cancer stem cell (CSC) is a cell type with similar properties to physiologic stem cells with the capacity to self-renew (usually measured as capacity to generate long lived tumors), the capacity to differentiate (usually measured as the capacity to generate phenotypically distinct progeny) and generally considered to have the capacity to initiate tumor formation. The CSC model necessitates a hierarchical relationship within the tumor where CSCs generate progeny that proliferate and to a limited extent differentiate. Early evidence for this paradigm comes from observations that the proliferative index of tumors is inversely correlated with the degree of differentiation of the tumor cells and that clonal markers of cancer initiation appear within multiple cell lineages (Buick and Pollak, 1984; Fialkow et al., 1977).

The first isolation of the cancer stem cell (CSC) population was demonstrated by Lapidot, et al. using mouse acute myeloid leukemia (AML) cells. It was observed that cells positive for CD34 and negative for CD38 (CD34+/CD38-) made up a small fraction of the overall population of leukemia cells, however, isolation of this small cell population and transplantation into severe combined immune deficient (SCID) mice resulting in recapitulation of the original AML containing the differentiated spectrum of tumor cells (Lapidot et al., 1994). Importantly, the recapitulation of the tumor was established using far fewer seeding cells implying that there is a very limited portion of cells within a given neoplasm that are capable of initiating tumor formation. This study also implied that the stem cell hierarchy is not only relevant in the

physiologic context, but tumors may also subscribe to a hierarchy where CSCs give rise to proliferative progeny that make up the bulk of the tumor.

Tumor initiating cells have been demonstrated in a number of other solid tumors including breast and colon. For example, cells from primary breast cancers were examined for cell surface marker expression and it was found that cells with the $CD44^{+}/CD24^{Lo}/Lineage^{-}$ phenotype were capable of initiating tumors in xenografts while alternate phenotypes yielded no significant tumor initiating capacity (Al-Hajj et al., 2003). These studies also showed that the tumors recapitulated by the $CD44^{+}/CD24^{Lo}/Lineage^{-}$ were capable of generating heterogenous tumors, implying capacity to differentiate, and long lived tumors, implying capacity to self-renew. In contrast to this work, additional studies suggest that the CD44+/CD24+/ESA+ cell population may be the stem cell population in pancreatic tissue (Li et al., 2007).

As a loss of homeostasis of the stem cell population is thought to be responsible for the initiation of some tumors, it is important to understand the concepts underlying stem cell compartment expansion. Generally speaking, there are two primary routes to increasing the stem cell population. First, regulation pathways within existing stem cells could cease to function adequately, as in the case of overactivation of the Wnt/β-catenin pathway, which results in increased symmetric divisions. Under the conditions of symmetric divisions, both daughter cells retain an undifferentiated state with stem cell characteristics (Figure 2). It has been demonstrated that under physiologic conditions, the majority of ISC divisions are asymmetric divisions giving rise to a single stem daughter cell and one daughter cell fated to terminally differentiate with a small portion of stem cell divisions being symmetric divisions. Using epigenetic methylations signatures for individual human colon crypts, Yakiba *et al.* deduced that ISCs undergo asymmetric divisions approximately 95% of the time with the expression and increased divisions

Figure 2

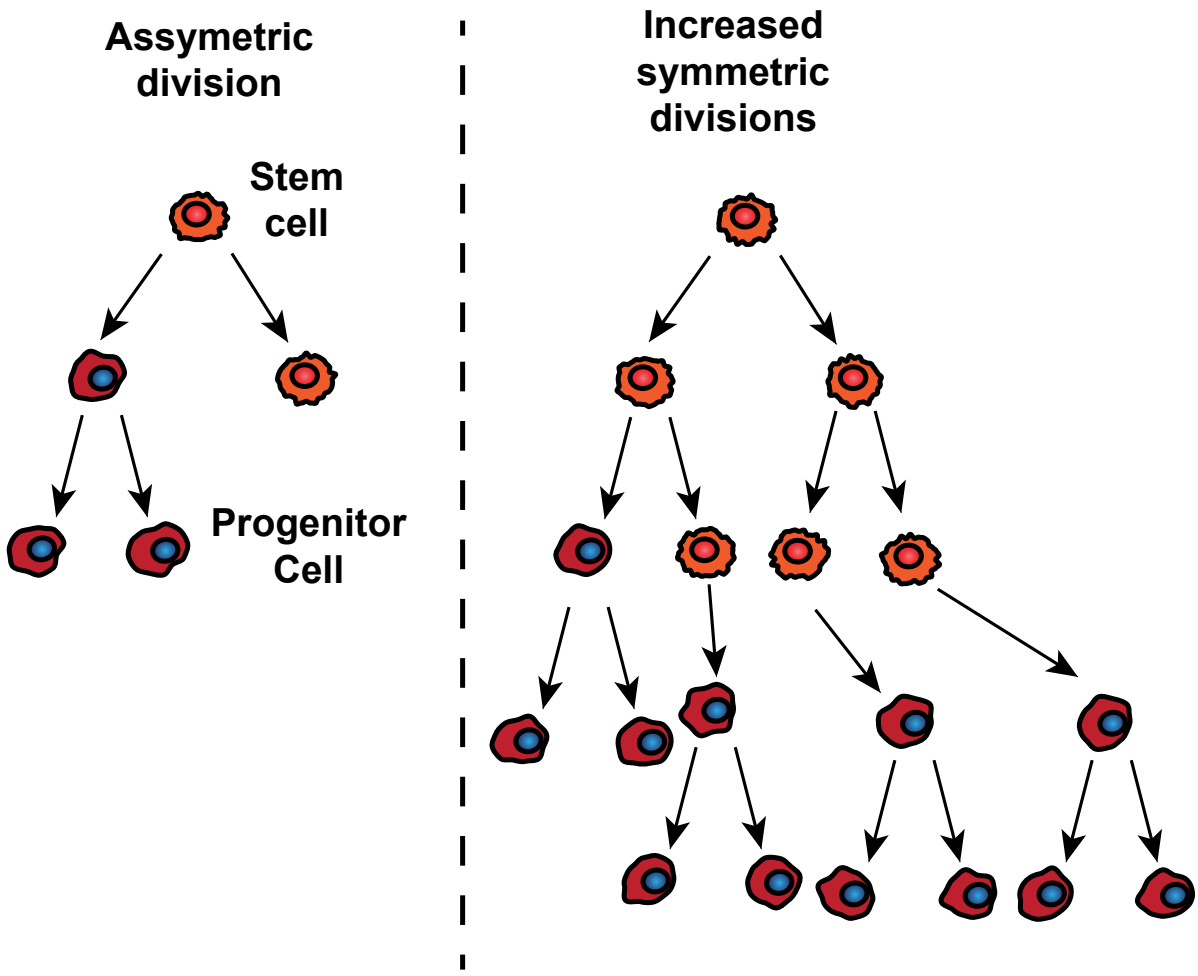
Assymetric division
Stem cell
Progenitor Cell
Increased symmetric divisions

Figure 2: Diagrammatic representation of the expansion of the stem cell compartment resulting in increase in proliferative progeny. Left is a representation of asymmetric division giving rise proliferative progeny. Right is dysregulation of stem cell homeostasis resulting in increased stem cell population and increased proliferative progeny.

or spontaneous extinction of the stem cell (Yatabe et al., 2001). Presumably the small percentage of symmetric divisions allows for crypt fission to regenerate lost neighboring crypts due to degeneration of injury.

Second, it is possible that cells fated to terminally differentiate retain some amount of plasticity and, due to dysregulated signaling pathways, undergo dedifferentiation where they reacquire stem cell characteristics. In support of this, it was recently shown that by overexpressing an inflammatory signaling mediator, NFκB, and inducing a secondary effect of Wnt activation, non-stem cells within the crypt were capable of dedifferentiating to stem-like cells with tumor initiating characteristics (Schwitalla et al., 2013). This concept of cellular plasticity and dedifferentiation implies that the stem cell to progenitor cell hierarchy is in fact not unidirectional but rather bidirectional with progenitor cells retaining a limited capacity to acquire stem cell properties.

These studies demonstrate that the CSC is an important part of the regulation of cancer in general. Also, it is currently poorly understood how CSCs can serve a role in initiating malignant progression. It is possible that only ISCs that have become dysregulated are capable of malignant transformation, or it is possible that ISC progeny can display a limited capacity to dedifferentiate and attain cancer initiating properties.

Stem cell markers for CSCs

In order to further understand roles of CSCs in cancer initiation and progression, several stem cell markers have been implicated with the CSC phenotype. Recent studies have demonstrated that the ISC markers LGR5 and DCLK1 serve major roles in colon cancer pathogenesis. For

example, using the LGR5 promoter driven deletion of the tumor suppressor adenomatous polyposis coli (APC) showed that LGR5-positive cells with loss of the tumor suppressing effects of APC leads to malignant transformation within days and generate long lived adenomas with unimpeded growth over weeks (Barker et al., 2009). On the other hand, APC deletion in transit amplifying cells showed adenoma formation that rapidly stalled. These studies suggest that loss of appropriate stem cell signaling in the physiologic ISC is a driving factor behind intestinal tumorigenesis. It also suggests that the progeny of ISCs fated to terminally differentiate have limited capacity to initiate malignant transformation and maintain tumor formation as they have limited self-renewal capacity.

A similar study crossing a well-established genetic mouse model for colon cancer, the $APC^{Min/+}$ mouse, with a DCLK1 promoter driven LacZ lineage tracer revealed that adenoma formation within the mouse intestine originated from a DCLK1-positive CSC (Nakanishi et al., 2013). Interestingly, the parallel experiment using LGR5 lineage tracing in $APC^{Min/+}$ mouse showed most of the normal intestine showed LacZ expression with focally higher expression within adenomas. Most importantly, DCLK1 promoter driven diphtheria toxin receptor expression combined with treatment with diphtheria toxin in $APC^{Min/+}$ showed significant ablation of adenoma formation. These studies demonstrate that tumors of the intestine have a high likelihood of forming from the ISC and that DCLK1 positive cells may play a more significant role in tumorigenesis rather than normal intestinal function. Additional studies have implicated DCLK1 as a stem cell marker and potential marker for CSCs in pancreatic cancer, neuroblastoma and gastric cancer (May et al., 2010; Qing-Bin et al., 2013; Sureban et al., 2011; Verissimo et al., 2012).

While LGR5 and DCLK1 were discovered based upon functional aspects of the ISCs and then validated as markers for CSCs, there are numerous other markers that have been shown to mark colonic CSCs with variable reliability. The enzyme aldehyde dehydrogenase 1A1 (ALDH1A1) was a promising stem cell marker in numerous epithelial tissues. Strongly ALDH1A1 positive cells were seen in the putative ISC niche while the remaining colon crypt was weakly ALDH1 positive (Deng et al., 2010). Additionally, high levels of nuclear localized ALDH1A1 as measured by IHC has been shown to predict shortened overall survival while increased cytoplasmic staining showed no association with prognosis (Kahlert et al., 2012).

Another potential stem cell marker for neuronal stem cells was identified in 2000 by Uchida, *et al.* In this study it was shown that human neuronal cells expressing a phenotype of CD133+, CD34-, CD45- were capable of enhanced neurosphere formation, a property thought to be a characteristic of stem cells. Additionally, CD133+/CD34-/CD45- cells showed the capacity to differentiate into neurons or glia, and could self-renew producing secondary neurospheres (Uchida et al., 2000). The relevance of CD133 in colorectal cancer was elucidated with a study showing that CD133+ colon cancer cells, while only comprising a minority of the total cell population, were able to increase tumor initiation capacity from 1/57,000 to 1/262. The CD133+ cells were able to reconstitute a heterogeneous population of cells within tumor xenografts and were able to self-renew giving rise to secondary tumors (O'Brien et al., 2007). Additionally, it was recently shown that membrane expression levels of CD133 significantly correlated with chemoresistance and recurrence of colorectal cancer following surgical intervention (Takahashi et al., 2010). On the other hand, recent studies have also shown that CD133- cells taken from metastases are also capable of initiating tumor formation and sustaining long term tumors in a xenograft casting some doubt regarding the reliability of CD133 as a stem cell marker

(Shmelkov et al., 2008). There is currently some controversy regarding CD133 as a stem cell marker with some studies showing that CD133+ cells are required for tumor initiation and others claiming that tumor initiation can be accomplished by CD133- cells. It is possible that certain molecular mechanisms result in a CD133+ stem cell in specific cancers while other cancers contain CSCs that do not express CD133. However, the relevance of CD133 expression and CSCs is currently under debate.

Another stem cell marker, CD44 has shown significant promise as it marks cells that can be more aggressive and metastatic. In immortalized non-transformed breast epithelial cells, it was shown that cells expressing high levels of CD44 and low levels of CD24 ($CD44^{+}/CD24^{Lo}$) displayed increased mammosphere formation (Al-Hajj et al., 2003). Interestingly, these cells also showed a more mesenchymal phenotype (Mani et al., 2008). These studies indicated that the combination of $CD44^{+}/CD24^{Lo}$ phenotype would select for a more mesenchymal cell and that the mesenchymal cells are enriched for stem cells at least in breast cancers. In colorectal cancer, cells displaying a CD44+ phenotype also showed increased tumor initiating capacity, increased capacity for differentiation as observed by their capacity to regenerate a heterogenous tumor and increased self-renewal as shown by their capacity to generate long term tumor xenografts (Dalerba et al., 2007). However, the relative enrichment of CD44+ cells for stem cells and the relevance of CD44 or CD133 as stem cell markers has been questioned by a number of recent studies (Muraro et al., 2012; Wang et al., 2012).

Overall, there are a number of CSC markers for several different tissues. However, it should be noted that studies regarding stem cell markers are numerous and differing in their views of the reliability of said markers. Because of many of the robust *in vivo* studies demonstrating the effects of DCLK1 and LGR5 in ISCs, in the current study, we primarily investigate changes in

DCLK1 and LGR5 as markers of the stem cell phenotype. Additionally due to relations with the Wnt/β-catenin signaling pathway, we will also investigate utilize the CD44/CD24 phenotype to measure "stemness."

CSCs and resistance to treatment

The importance of the CSC cannot be emphasized enough. One of the major properties of the CSC is that it's relatively resistance to conventional chemotherapies. Often, chemotherapy regimens result in early tumor regression followed by late tumor relapse. These relapsed tumors can be composed of a chemoresistant population that is refractory to a second round of treatment. It is estimated that greater than 90% of chemotherapy failures in metastatic disease is due to the acquisition of chemoresistance (Longley and Johnston, 2005). Current evidence supports a few paradigms leading to chemoresistant recurrence of tumors (Meacham and Morrison, 2013). One possibility is that if the tumor contains enough genetic diversity, some existing mutation allows for the continued propagation of subclones of the tumor. This is evidenced by the fact that following chemotherapy of some acute myelocytic leukemias previously minor subclones become dominant implying a genetic advantage of this subclone either during or following therapy (Ding et al., 2012; Meacham and Morrison, 2013). Another possibility is that chemotherapies allow a subset of the heterogeneous tumor population to survive and given enough time, *de novo* mutations occur allowing for a subclone to escape from the cytostatic or cytotoxic effects of chemotherapy. For example, imatinib is a tyrosine kinase inhibitor that targets Bcr-Abl, a tyrosine kinase often observed in chronic myeloid leukemia. Imatinib

resistance can often be traced to secondary mutations in the *BCR-ABL* gene resulting in relapse (Bixby and Talpaz, 2011; Meacham and Morrison, 2013).

The model primarily investigated within this study is that that tumor relapse occurs through survival of the chemoresistant CSC population following the initial round of therapy. This CSC population could then later gives rise to a rapidly dividing pool of chemoresistant progeny (Figure 3). While this model cannot be generalized to all chemoresistant recurrences, there is evidence demonstrating that chemoresistant tumor recurrence can occur through this pathway. In a study by Saigusa, *et al.*, the levels of stem cell markers CD133, OCT4 and SOX2 were evaluated before and after combination radiation and chemotherapy in 33 patients with rectal cancer. This study demonstrated that patients with resistant recurrences showed higher levels of the stem cell markers and the elevation in stem cell markers were correlated to shorter disease free survival (Saigusa et al., 2009). This study further demonstrates the close association with resistant phenotypes and stem cells in colon cancer. Similar studies have shown that xenogeneic colorectal cancer cells show increased expression of ALDH1A1 which conferred the ability to detoxify cyclophosphamide, a classical chemotherapeutic agent (Dylla et al., 2008). In agreement with these findings, Yang, *et al.* developed a substrain of the colorectal cancer cell line HCT 116 which was resistant to oxaliplatin. It was observed that the oxaliplatin resistant strain was additionally resistant to treatment with paclitaxel implying a mode of resistance that was not mechanism specific to oxaliplatin. This cell line also showed a greater portion of G0/G1 arrest implying quiescence, higher spheroid formation capacity, higher expression of ABCG2 and enriched for stem cell markers (Yang et al., 2013). These studies demonstrate that the cells capable of surviving and following chemotherapy may have strong stem cell-like characteristics such as slowed cell cycle progression, increased stem cell marker expression and increased

Figure 3

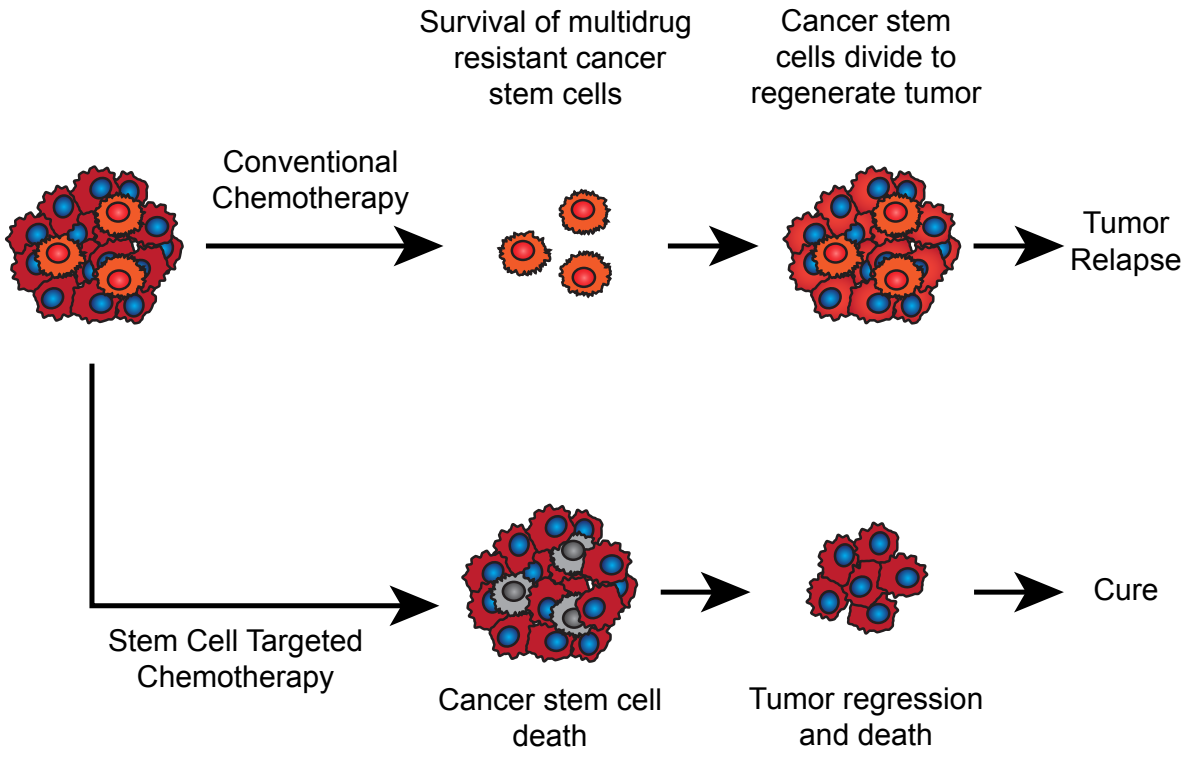
Survival of multidrug resistant cancer stem cells
Cancer stem cells divide to regenerate tumor
Conventional Chemotherapy
Tumor Relapse
Stem Cell Targeted Chemotherapy
Cancer stem cell death
Tumor regression and death
Cure

Figure 3: Diagram representing the hierarchical model of cancer in response to chemotherapy. Classical chemotherapies target rapidly proliferating progeny of cancer stem cells resulting in rapid shrinkage of the tumor leaving only CSCs as remaining malignant cells. Tumors relapse once CSCs being to regenerate progeny. Stem cell targeted therapies would theoretically inhibit pathways required for stem cell survival resulting in loss of self-renewal capacity in tumors leading to spontaneous tumor regression following death of proliferative progeny.

expression of ABC transporters. Additionally, in a recent study published by Merlos-Suarez, *et al*, gene signatures were established for physiologic ISCs and transit amplifying cells which were then used to show that only cells containing the gene signature of ISCs were the capable of generating a recurrent colorectal cancer (Merlos-Suarez et al., 2011). Similar studies validate these findings in other tissues such as ovaries, prostate, liver and lung (Bisson and Prowse, 2009; Chau et al., 2013; Kawabata et al., 2001; Noda et al., 2009; Yang et al., 2008b). Taken as a whole, these studies show that colorectal cancer originates from a population of dysregulated stem-like cells that resist initial rounds of chemotherapy and generate a chemoresistant recurrent tumor.

The range of mechanisms that cancer cells employ include suppression of the apoptotic response, acquisition of quiescence, upregulation of drug elimination pathways and mutation of the target of the chemotherapy. One of the primary mechanisms of chemoresistance in CSCs is overexpression of ATP binding cassette (ABC) transporters to attain multidrug resistance. ABC transporters are transmembrane transporters that utilize the hydrolysis of ATP to efflux a broad range of lipophilic xenobiotics in order to protecting the cell from the activity of many cytotoxic agents regardless of their mechanism of action. Similar to normal adult stem cells, CSCs are known to overexpress ABC transporters such as phospho-glycoprotein (Pgp), breast cancer resistance protein (BCRP) and multidrug resistance protein (MRP). These transporters confer CSCs the ability to actively efflux many conventional chemotherapies such as doxorubicin (ADM), paclitaxel, 5-fluoro-uracil (5-FU) and many others (Dean et al., 2005).

The association between multidrug resistance and stem cells was effectively established upon discovery of the “side population” (SP) of bone marrow cells (Goodell et al., 1996). A diagrammatic representation of the SP assay is shown (Figure 4). It was revealed that following

Figure 4

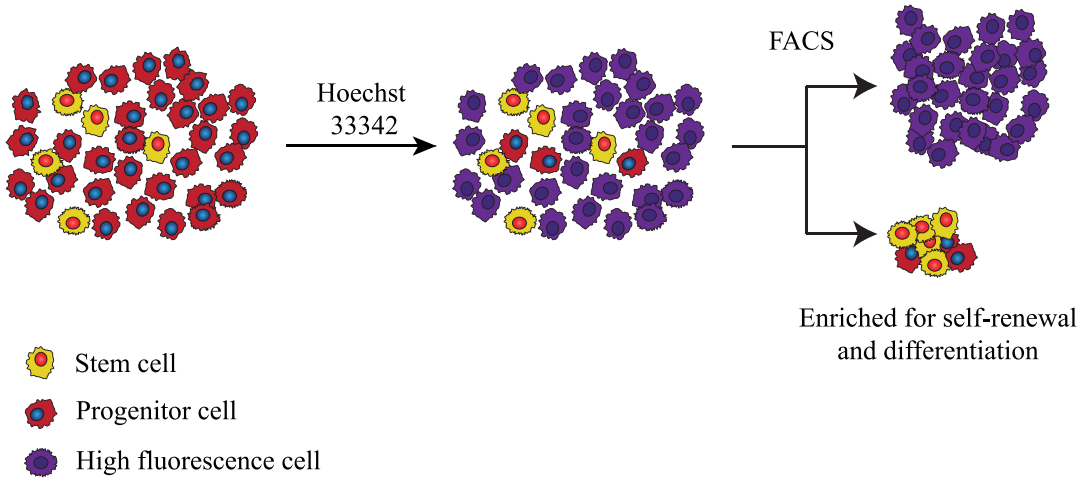
Hoechst
33342
FACS
Enriched for self-renewal
and differentiation
Stem cell
Progenitor cell
High fluorescence cell

Figure 4: Diagram of SP assay. The pooled population of cells are exposed to a cell permeable fluorescent marker (Hoechst 33342) resulting in the majority of cells showing high intracellular fluorescence. A minority of cells show low intracellular fluorescence presumably through high levels of efflux activity. Fluorescence activated cell sorting (FACS) is capable of separating cells of high fluorescence versus cells of low fluorescence (SP). The SP fraction from bone marrow has shown >1000-fold increase in differentiation and self-renewal capacity.

treatment with a cell permeable fluorescent dye, namely Hoechst 33342, a diminishingly small population (~0.1%) of mouse bone marrow cells maintained low intracellular fluorescence as measured by flow cytometry. Interestingly, these SP cells also displayed a significant enrichment in the capacity to self-renew and differentiate implying that the SP population was enriched for HSCs. By examining Hoechst 33342 efflux rates in cellular vesicles from cell lines known to be enriched for Pgp compared to cell lines known to be low in Pgp expression it was shown that the kinetics of Hoechst efflux could be significantly modulated by the expression levels of Pgp (Shapiro et al., 1997). This established that Hoechst 33342 was a substrate of Pgp and implied a possible causative link between SP cells and ABC transporters. Further confirmation that Pgp expression is a prominent feature of HSCs came, when Scharenberg, *et al.* demonstrated that the HSCs showed high levels of *Pgp* mRNA initially, but upon lineage commitment and differentiation, significantly downregulated transcript levels of *Pgp* (Scharenberg et al., 2002). SP cells have also been demonstrated in the gastrointestinal tract. Upon examination of 16 cell lines, fifteen showed the presence of the SP which also showed characteristics of stem cells (Haraguchi et al., 2006). The presence of SP cells and their link to stem cell characteristics have also been demonstrated in breast, ovarian and hepatocellular carcinoma as well (Chiba et al., 2006; Christgen et al., 2007; Szotek et al., 2006).

In conjunction with Pgp, BCRP and MRP are two additional ABC transporters important to the efflux based multidrug resistance phenotype in cancer. Overexpression of BCRP confers multidrug resistance with some overlap of multidrug resistance conferred by Pgp (Litman et al., 2000). Further studies demonstrated BCRP as a potential characteristic of stem cells when it was shown to be upregulated in stem cells of various tissues and downregulated upon terminal

differentiation (Zhou et al., 2001). Additionally, it was observed that following overexpression of BCRP, cells were more prone to retain a stem like state.

The MRP family of proteins contains MRP1 through 6 with MRP1 and MRP2 having shown significant roles in multidrug resistance of cancer. MRP1 is fairly ubiquitously expressed and MRP2 is localized more toward the liver, kidney and gut (Borst et al., 1999). Additionally, the MRP family of transporters have been shown to generate chemoresistance to several chemotherapeutic agents including ADM and paclitaxel (Szakacs et al., 2006). Important to note is that these transporters share some overlap in the xenobiotics they are capable of effluxing, however their kinetics differ granting cells varying cross resistance depending upon which panel of transporters it has upregulated (Litman et al., 2000; Szakacs et al., 2006).

These studies demonstrate that CSCs often acquire the capacity to efflux xenobiotics through the upregulation of a subset of ABC transporters such as Pgp, BCRP and MRP which can contribute to multidrug resistance. Additionally, these transporters are responsible for the formation of the SP fraction that also show significant enrichment for stem cell characteristics. Important to note however is that although many attempts have been made to inhibit efflux transporters to reestablish chemosensitivity, none have yet to be successful and progress is still slow-moving (Szakacs et al., 2006). Directly targeting the mechanisms that establish the CSC may be the viable alternative rather than attempting to subvert effects secondary to cancer "stemness."

Regulation of ISCs and CSCs by the Wnt/β-catenin signaling pathway

Due to the relative importance of CSCs, it is important to understand the cellular signaling pathways that can regulate the ISC and CSC compartments and factors that can modulate the

activity of these signaling pathways. One such pathway governing the maintenance of ISCs is the Wnt/β-catenin signaling pathway. A schematic representation of the canonical Wnt/β-catenin signaling pathway is shown for reference (Figure 5). Normally β-catenin exists in three primary pools. In most intestinal epithelial cells β-catenin is primarily observed at the membrane and acts as an anchoring protein linking the actin cytoskeleton to the extracellular adhesion molecule E-cadherin (Ozawa et al., 1990). Additionally, there is a minimal and transient pool of β-catenin in the cell cytoplasm. This pool of β-catenin experiences high turnover due to rapid degradation by a destruction complex composed of APC, Axin, and the two serine/threonine kinases glycogen synthase kinase 3β (GSK3β) and casein kinase 1 (CK1). This complex binds cytoplasmic β-catenin at which point CK1 primes β-catenin through phosphorylation of β-catenin at Ser45. This allows GSK3β to phosphorylate β-catenin at Ser33, Ser37 and Thr41 (Liu et al., 2002). Phosphorylation of β-catenin at these sites leads to binding of β-catenin to β transducing repeat containing protein (βTrCP) leading to polyubiquitinilation of β-catenin followed by proteasomal degradation.

Under specific exogenous conditions β-catenin degradation is inhibited. For example, the canonical Wnt/β-catenin involves the binding of the extracellular Wnt ligand to the transmembrane receptors low density lipoprotein related protein (LRP) 5/6 and Frizzled. Following ligand binding, the complex of LRP5/6 and Frizzled inhibit the destruction complex through a poorly understood mechanism. One prevailing theory regarding destruction complex inhibition is that Wnt ligand binding of LRP5/6 and Frizzled results in sequestration of the members of the destruction complex at the cell membrane limiting access to the cytoplasmic pool of β-catenin. It was shown that administration of Wnt ligand results in phosphorylation of the LRP5/6 receptor in a GSK3β and CK1 dependent fashion and that this phosphorylation is

Figure 5

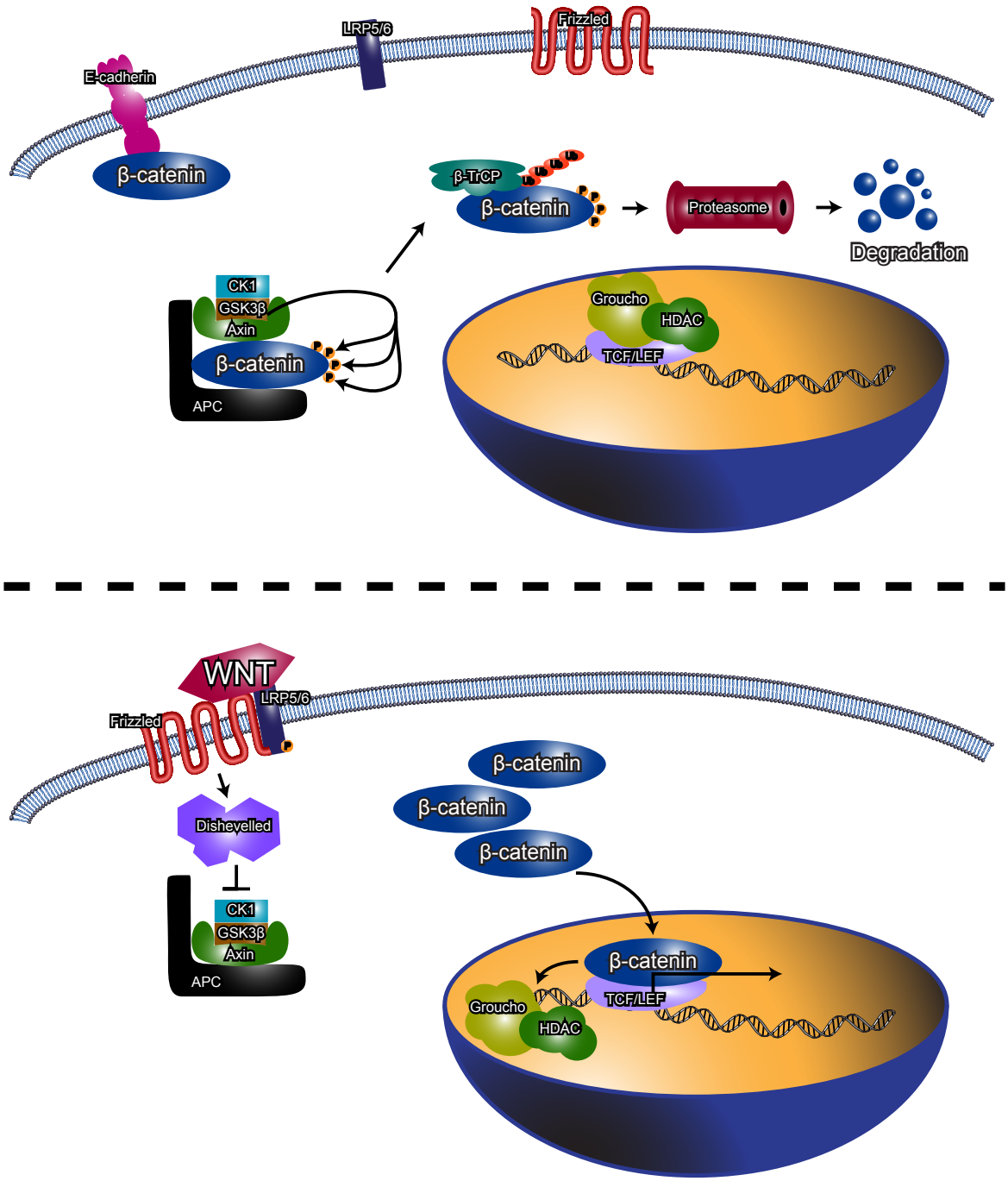
LRP5/6
Frizzled
E-cadherin
β-catenin
β-TrCP
Ub
P
Proteasome
Degradation
CK1
GSK3β
Axin
APC
Groucho
HDAC
TCF/LEF
WNT
Dishevelled

Figure 5: Schematic representation of the Wnt/β-catenin signaling pathway. In the absence of exogenous signal β-catenin exists at the membrane associated with E-cadherin. The cytoplasmic pool of β-catenin is rapidly degraded by association with the destruction complex. β-catenin is initially phosphorylated by CK1 then GSK3β tagging it for polyubiquitinylation by β-TrCP. It is then degraded by the proteasome. In the presence of Wnt signal, Frizzled and LRP5/6 bind the Wnt ligand inducing phosphorylation of LRP and recruitment of Disheveled. Disheveled inhibits the destruction complex resulting in accumulation of β-catenin in the cytoplasm. Cytoplasmic β-catenin then translocates to the nucleus, displacing transcriptional repressors such as Groucho and associates with TCF/LEF. β-catenin association with TCF/LEF drives transcription of a number of β-catenin target genes such as *COX-2, IL-8, Cyclin D1* and *c-MYC*.

required for association of LRP5/6 with Axin (Zeng et al., 2005). Phosphorylation of LRP5/6 results in recruitment of Disheveled to the plasma membrane where it associates with Frizzled and sequesters Axin to the cell membrane (Bilic et al., 2007; Yamamoto et al., 2006).

Inhibition of the destruction complex leads to accumulation of β-catenin in the cytoplasm allowing β-catenin to translocate to the nucleus. In the absence of nuclear β-catenin, transcriptional repressors such as Groucho bind transcription factor/lymphoid enhancer binding factor (TCF/LEF) (Cavallo et al., 1998). Upon translocation to the nucleus β-catenin displaces transcriptional repressors such as Groucho and histone de-acetylase (HDAC) and associates with TCF/LEF and initiates transcriptional changes within the cell. For a more comprehensive review of the Wnt/β-catenin signaling pathway as well as interplay between β-catenin signaling and other stem cell signaling pathway such as Notch, the reader is referred to the following sources (Fodde and Brabletz, 2007; Nakamura et al., 2007; Reya and Clevers, 2005; van der Flier and Clevers, 2009).

Importantly, β-catenin associated TCF/LEF transcriptional activity has been shown to be critical for maintenance of ISCs. In mice lacking Tcf-4, it was noted that intestinal endoderm developed normally into epithelium, however, the proliferative compartments within the crypts were absent and only terminally differentiated cells remained of the crypt epithelium, implying that the Tcf-4 transcriptional program is critical to maintaining epithelial stem cells (Korinek et al., 1998). Additionally, important mediators of cell cycle and proliferation such as *c-MYC* and *cyclin-D1* are Wnt target genes implicating the Wnt/β-catenin transcriptional program as being critical for promoting expansion of the transit amplifying compartment (He et al., 1998; Tetsu and McCormick, 1999).

It is important to note that canonical Wnt/β-catenin signaling is a major factor regulating stem cell homeostasis in other tissues. For example, HSCs show activity of a TCF/LEF luciferase reporter called TOPFlash, and overexpression of active β-catenin can expand the pool of HSCs. Additionally, inhibition of Wnt in HSCs using a decoy receptor or inhibition of β-catenin by overexpressing Axin results in a diminishing of the HSC pool implying that Wnt/β-catenin signaling is important for hematopoiesis at the level of the HSC (Reya et al., 2003).

If the β-catenin signaling cascade is a major regulator of the intestinal crypt stem cell compartment and ISC homeostasis, it would stand to reason that an unregulated overactivation of β-catenin transcriptional activity could result in malignant transformation. Indeed, this is the case in colon cancer as well as several other neoplasias. One of the major pieces of evidence linking the β-catenin signaling cascade to colon cancer tumorigenesis was the discovery that the majority of colorectal cancers (estimated to be >80%) contained a homozygous loss of function mutation in the *APC* gene (Fearon and Vogelstein, 1990). Subsequently, it was identified that a heterozygous mutation in the *APC* gene is the hereditary factor contributing to Familial Adenomatous Polyposis (FAP), one of two currently known genetic syndromes for colorectal cancer implying that loss of functional APC is a major contributing factor to not only sporadic but also hereditary colon cancers (Groden et al., 1991). As loss of functional APC is the initiating and rate limiting step of oncogenic transformation, it is thought that LOH in FAP patients is responsible for generation of multiple colonic adenomas (Kinzler and Vogelstein, 1997). Further evidence for the role of APC in intestinal tumorigenesis came from mouse studies using random mutagenesis to generate a mouse with multiple intestinal neoplasia (MIN) where the genetic lesion was found to be in the *Apc* gene (Moser et al., 1990). In fact, loss of functional APC is such a significant regulating step in tumorigenesis that the predominant genetic mouse

models for intestinal cancer utilize lesions of the *Apc* gene to induce spontaneous intestinal neoplasias; one of the most commonly used genetic mouse model for intestinal neoplasia is the *Apc* MIN ($Apc^{Min/-}$) model (Fodde et al., 1994; Moser et al., 1990).

While this evidence pointed toward APC as a tumor suppressor which upon loss of function causes the initiation of colonic neoplasia, evidence linking APC to the β-catenin transcriptional program was still lacking. Further studies demonstrated that tumors with loss of functional APC showed increased levels of β-catenin with the nuclear fraction of β-catenin associated with transcriptionally active TCF/LEF (Korinek et al., 1997). Additionally, reintroduction of functional APC transiently into APC deficient colorectal cancer cells showed a significant abrogation of nuclear β-catenin and loss of β-catenin transcriptional activity (Korinek et al., 1997; Munemitsu et al., 1995). Evidence further linking loss of β-catenin regulation as the initiating step of colonic tumorigenesis was that many of the tumors with intact APC showed mutations of the phosphorylation sites of β-catenin itself resulting in the inability of CK1 and subsequently GSK3β to phosphorylate β-catenin (Morin et al., 1997; Polakis, 2007). Taken together, this evidence points to the primary initiating factor of colonic tumorigenesis being the overstabilization of β-catenin, either through loss of APC or the inability of the destruction complex to target β-catenin itself. Subsequently TCF/LEF transcriptional activity is upregulated in response to overstabilization of β-catenin leading to a transcriptional state within the cell that generates hyperplasia and adenoma formation.

Another point to note is that although β-catenin signaling is not specifically established as the rate limiting step of oncogenesis, stabilized β-catenin is also a hallmark of several cancers such as breast cancer, ovarian cancer, neuroblastoma and hepatocellular carcinoma (Chau et al., 2013; Flahaut et al., 2009; Noda et al., 2009; Woodward et al., 2005). For example, it is estimated that

over half of breast cancers contain increased levels of β-catenin with increased levels of β-catenin being associated with a poor prognosis (Woodward et al., 2005).

While much of the evidence presented thus far implicates β-catenin as the driving force initiating adenoma formation, there is also evidence that points to β-catenin dysregulation contributing to the progression and increased aggressiveness of colon cancers. The overactivation of β-catenin transcription results in numerous changes to cellular biology that can result in a more aggressive neoplasia. For example, inactivation of APC or activation of β-catenin drives intestinal hyperplasia (Reya and Clevers, 2005). This is thought to be due in part to two major transcriptional targets of β-catenin, namely *c-MYC* and *cyclin-D1* both of which are potent stimulators of cell cycle progression (He et al., 1998; Tetsu and McCormick, 1999). Additionally, using a dominant negative TCF4 in colorectal cancer cell lines and examination of the global transcriptional changes through microarray analysis, it was revealed that the *APC* -/- transcriptional changes closely mirror the transcriptional programs observed at the crypt base where the crypt stem cells and progenitors are located (van de Wetering et al., 2002). This heavily suggests that the overactivation of β-catenin is the causative factor driving stem cell or progenitor cell expansion. An additional transcriptional change seen in overactivation of β-catenin is an increase in levels of survivin. Survivin expression is found to be increased at the crypt base compared to higher along the crypt axis and reconstitution of wild type *APC* in colon cancer cells results in decreased survivin expression (Zhang et al., 2001). Increased survivin expression serves to inhibit caspase activity and protect the cell from apoptotic pathways (Tamm et al., 1998). This is theorized to be a potential mechanism behind the apoptosis observed in colon cancer cells with reconstituted wild type *APC* and also implicates overactivation of β-catenin as a CSC inducer as CSCs tend to suppress apoptotic pathways.

Overactivation of the Wnt/β-catenin pathway has also been implicated in the acquisition of chemoresistance. A recent study has shown that human hepatocellular carcinomas refractory to 5-fluorouracil (5-FU) treatment show higher levels of β-catenin activity and that if cells are treated with 6-bromoindirubin-3'-oxime (BIO), an inhibitor of GSK3β, to upregulate β-catenin activity, cells show increased multidrug resistance (Noda et al., 2009). In agreement with this, it was also demonstrated that ADM resistant neuroblastomas had upregulated MRP1 which correlated with increased nuclear β-catenin staining. Upon inhibition of β-catenin, MRP1 levels decreased with significant sensitization to ADM (Flahaut et al., 2009). Additional studies have also correlated resistance to paclitaxel and cisplatin in ovarian cancers with activation of Wnt/β-catenin signaling as well as upregulation of BCRP (Chau et al., 2013). These studies reveal that β-catenin activity can contribute to the multidrug resistance phenotype associated with many aggressive neoplasms as discussed earlier.

Important to note also is that loss of functional APC and increased nuclear β-catenin does not solely result in transcriptional changes but also induces changes such as cell migration and intercellular adhesion. In cancer conditions, the association of β-catenin with E-cadherin remains intertwined and changes in the membrane associated β-catenin pool is mirrored by similar changes in E-cadherin (van der Wurff et al., 1997). Additionally, it has been noted that nuclear β-catenin is more prominently expressed at the migrating front of tumors compared to central regions of tumors (Brabletz et al., 1998). This is heavily suggestive that E-cadherin and β-catenin together have major effects on maintaining cell polarity and adhesion.

Additionally, Brabletz, *et al.* noted that nuclear β-catenin levels progressively increase as cancers progress from low grade adenomas to high grade adenomas demonstrating a dose dependence of β-catenin activity in colon cancer (Brabletz et al., 2000). To further elucidate this phenomenon,

studies were conducted to observe the dose dependent effects of β-catenin. By using a series of hypomorphic mutants of *APC*, it was observed that these different mutations in *APC* generated different degrees of β-catenin overactivation, and more importantly, the degree of β-catenin overactivation correlated with the number of polyps formed within the intestine (Gaspar and Fodde, 2004). This finding implies that a dosage dependence of β-catenin activity can confer the capacity to undergo different transcriptional programs and may account for the pleiotropic effects observed upon loss of APC and subsequent overactivation of β-catenin.

As tumors at the invasive front show higher levels of nuclear β-catenin it is presumable that they should show lower levels of E-cadherin and a more mesenchymal phenotype while also maintaining a high proliferative index. However, studies have shown that cells within these invasive fronts, while showing an epithelial-to-mesenchymal transition (EMT) with loss of E-cadherin and higher nuclear β-catenin, actually demonstrate a paradoxical lower rate of proliferation (Jung et al., 2001). In fact, Jung, *et al.* showed that compared to central regions of tumors showing a more differentiated phenotype with lower nuclear β-catenin, the invasive fronts generally showed low levels of the proliferative marker Ki-67. It is presumable, that based on context and the dose dependence of nuclear β-catenin that these cells experience an alternative transcriptional program generating a distinct phenotype. This transcriptional program may induce a more quiescent phenotype with more invasive characteristic for some CSCs.

Most important to note however, is that although the majority of colon cancers display a loss of APC function or inability of the destruction complex to target β-catenin, there is still heterogeneity of β-catenin signaling within the tumor. This implies that while the loss of the canonical mechanism of β-catenin regulation is important there are numerous other factors yet to

be discovered that regulate the activity of this pathway to potentially modulate the many phenotypic characteristics associated with Wnt/β-catenin signaling.

RBM3 and its physiologic roles

Recently, several reports have emerged on an RNA binding protein revealing a role in the initiation and progression of different solid tumors. Expression of the RNA binding motif containing protein 3 (RBM3) has been recently shown to be upregulated in several solid tumors to varying degrees with higher expression occurring with more aggressive or higher grade tumors. It has also been shown to serve as an oncogene when overexpressed implicating its role in tumor initiation. However, the exact mechanism responsible for RBM3 mediated oncogenesis and tumor progression is still poorly understood. Here we outline the current knowledge relating to RBM3 and its role in cellular physiology and cancer. Furthermore, we go on to describe the rationale linking previous studies to the hypothesis of RBM3 being a stem cell regulating factor.

RNA binding proteins known to affect stem cell phenotype

While the potential for RBM3 regulating stem cell behavior is fairly novel, it should be noted that it is not unprecedented that RNA binding proteins can alter stem cell behavior. Previous studies have elucidated the potential for Musashi1 (Msi1), Human antigen R (HuR) and Lin28 as some examples of RNA binding proteins capable of modulating stem cell behavior through various molecular mechanisms.

Lin28 could currently be one of the most prominent RNA binding proteins to affect stem cell regulation. It was first discovered in *C. elegans* under regulation of the let-7 miRNA (Ambros and Horvitz, 1984). It was subsequently shown that the mouse homolog is also regulated by let-7 implying a highly conserved mechanism of regulation. Furthermore, it is highly expressed in mouse embryonic cell and significantly downregulated following terminal differentiation (Moss and Tang, 2003). One of the primary pieces of evidence linking Lin28 to the regulation of stem cells was shown in work by Yu, *et al.* where it was demonstrated that Lin28 is one of four factors required to generate induced pluripotent stem cells (iPSCs) from mouse fibroblasts (Yu et al., 2007). The mechanism of Lin28 mediated stem cell induction was unclear until it was demonstrated that the molecular mechanism governing Lin28 action was based on its ability to suppress the maturation of let-7 miRNA (Viswanathan et al., 2008). It was further demonstrated that Lin28 could act upon cells to promote oncogenic transformation and aid in progression of malignancy (Viswanathan et al., 2009). This implies that in the developmental context, Lin28 is required for maintaining "stemness" and is soon downregulated in terminally differentiated tissues. It is also upregulated in cancers presumably to maintain self-renewal of CSCs. For a more comprehensive review, the reader is referred to the following source (Shyh-Chang and Daley, 2013).

Msi-1 is an RNA binding protein with a well-established mechanism for stem cell regulation. In order to discover its roles within the cell, the systematic evolution of ligands by exponential enrichment (SELEX) technique was used to determine the Msi-1 consensus binding sequence. Based on this information it was demonstrated that Msi-1 could bind the 3'-UTR of m-Numb mRNA and inhibit its translation. Additionally, Msi-1 overexpression resulted in suppression of m-Numb protein (Imai et al., 2001). As m-Numb is a primary repressor of the Notch signaling

cascade, a pathway critical for maintaining stem cells in various tissues, the established mechanism of action of Msi-1 is by suppressing the suppressor of Notch signaling. Importantly, Msi-1 also has significant effects on cancer as it was demonstrated that upon siRNA mediated knockdown of Msi-1 in tumor xenografts, cells underwent growth arrest with reduced tumor growth coupled with inhibition of Notch signaling (Sureban et al., 2008a).

HuR was initially discovered as a ubiquitously expressed RNA binding protein with affinity for AU-rich elements (Ma et al., 1996). Depletion of HuR in mice leads to degeneration of rapidly renewing tissues such as crypt epithelium and bone marrow (Ghosh et al., 2009). This implies that HuR is an important protein for maintaining proliferation of rapidly cycling organs at least at the level of the proliferative progeny of the stem cells. Interestingly, HuR has also been shown to associate with β-catenin protein (Kim et al., 2012b). The importance of this binding was further emphasized following a study showing HuR to be critical for maintaining stem-cell characteristics under conditions of hypoxia through binding of β-catenin and client mRNAs (D'Uva et al., 2013). HuR localization also appears to play an important role in stem cell function as undifferentiated myoblasts show accumulation of HuR within the nucleus but upon differentiation, HuR appears to transition to the cytoplasm (van der Giessen and Gallouzi, 2007). Importantly, HuR has been shown to be critical in the early progression of colon cancer through alteration of COX-2 expression (Young et al., 2009). While it is currently unclear the degree of regulation HuR imparts upon stem cells or the mechanism responsible for this regulation, HuR remains an important protein of interest in regards to stem cell regulation and cancer pathogenesis.

RBM3 discovery and regulation

RBM3 was originally discovered through cDNA selection in yeast artificial chromosomes of the Xp11.2 region. The longest open reading frame of *RBM3* yields a 157 amino acid long protein that has a putative RNA recognition motif. Due to homology to an RNA binding protein in maize it is presumed that RBM3 may serve a fundamental role in cellular biology that is carried over from plants to animals (Derry et al., 1995). The first factor discovered to modulate RBM3 expression was hypothermia. It was shown that while the cell lines that were examined maintained basal levels of RBM3 expression, exposure to mild cold shock (specifically 24 hours at 32°C) was capable of significantly upregulating RBM3 mRNA levels. Interestingly, transcript levels were also increased upon exposure to translation inhibition agents such as puromycin and cycloheximide (Danno et al., 1997). In accordance with these findings, it was shown that *Rbm3* expression was significantly increased in the Sertoli cells of mouse testes which reside in an environment of approximately 32°C. Interestingly, increasing temperature of the testes to 37°C resulted in abrogation of RBM3 expression (Danno et al., 2000).

As many cold shock response proteins serve roles in post-transcriptionally regulating mRNA, it was proposed that RBM3 may serve a role in regulating RNA by altering translation, stability or splicing of transcripts Cyclooxygenase 2 (COX-2) is a proinflammatory enzyme that is responsible for the rate-limiting conversion of arachadonic acid into inflammatory mediators. While COX-2 is expressed in low levels under normal conditions, it is induced to high levels following exposure to lipopolysaccharide (LPS) (Roshak et al., 1994). One major method of regulating COX-2 levels in the cell is with rapid turnover of the mRNA thereby maintaining very low levels of *COX-2* mRNA (Newton et al., 1997). Upon exogenous stimuli such as exposure to LPS, *COX-2* mRNA half-life is significantly increased (Barrios-Rodiles et al., 1999). In order to

identify potential proteins that could alter *COX-2* mRNA stability, the 3' untranslated region (UTR) was conjugated to biotin and incubated with nuclear proteins. The bound protein was then isolated, subjected to two dimensional Western analysis and mass spectrometry. Using this method, RBM3 was identified as a protein that could bind the *Cox-2* 3'UTR (Cok et al., 2004). Additional studies using actinomycin-D treatment, an inhibitor of *de novo* mRNA synthesis, established that RBM3 overexpression was capable of increasing the half-life of *COX-2* mRNA (Sureban et al., 2008b). This evidence points strongly toward RBM3 as a potential factor that can alter the progression of colon cancer as COX-2 overexpression is thought be an early event in its progression. Another major study to elucidate the cellular function of RBM3 came when it was revealed that RBM3 is upregulated by hypoxia. Exposure of Z-33 human leukemia cells and Hepa-1 mouse hepatoma cells to moderate and severe hypoxia (8% and 1% O_2 respectively) resulted in significant increases in protein levels of RBM3 (Wellmann et al., 2004). This increase was abrogated by the use of actinomycin D implying that hypoxia induced increases in RBM3 were at the transcriptional level. Interestingly, these cell lines are deficient for specific hypoxia inducible factors (HIFs). Z-33 cells are deficient in HIF-1α and Hepa-1 cells are deficient in HIF-1β implying that this upregulation of RBM3 was independent of HIF based transcription.

The first major piece of evidence of RBM3 being associated with stem cells came from a study investingating RBM3 levels within HSCs (Baghdoyan et al., 2000). Using a gene trap approach, it was shown that RBM3 was specifically upregulated during treatment with granulocyte monocyte colony stimulating factor (GM-CSF). Additionally, GM-CSF treatment increased the CD34+ HSC pool which showed a selective increase in the RBM3 transcript level (Baghdoyan et al., 2000). A second study also confirmed that in a mouse model for spontaneous hemolytic anemia, erythropoietic CD34+ stem cells showed increased RBM3 levels (Yang et al., 2008a).

This major finding was the first implication that RBM3 may have a significant role in regulating the proliferation of stem cells by showing that it is upregulated in proliferating HSCs.

RBM3 and cell survival under stress

While many studies show how RBM3 is regulated under specific conditions and its expression levels in certain disease states, there are few studies showing direct effects of altered RBM3 expression on the biology of cells. One of the earlier studies of RBM3 function was revealed using RBM3 overexpression in neuroblastoma cells. RBM3 overexpression in this context showed an increase in total protein synthesis under conditions of either euthermia or hypothermia. It was further shown that RBM3 overexpression showed global changes in microRNA (miRNA) levels implying that RBM3 can act as a global regulator of protein synthesis by modulating miRNA levels (Dresios et al., 2005). Further confirmation of this effect was demonstrated recently by showing that RBM3 overexpression does indeed alter miRNA levels on a global scale and that RBM3 appears to alter the processing of miRNAs within the cytoplasm at the processing step involving Dicer (Pilotte et al., 2011). These studies imply that RBM3 could affect cellular biology at a very fundamental and very global scale to induce widespread changes following certain stress conditions such as cold shock, hypoxia or serum deprivation.

The first studies to reveal that RBM3 may have some role in cell death and apoptosis came from Kita, *et al.* where apoptosis was induced by conditionally overexpressing the polyglutamine repeat responsible for neurodegeneration in Huntingon's disease. It was revealed that RBM3 was upregulated in the early stages of apoptosis, however, exogenous overexpression of RBM3

impaired polyglutamine repeat induced cell death in both neural and non-neural cells (Kita et al., 2002). In agreement with this study, it was also shown that exposure of the marine biotoxin dominoic acid induces upregulation of RBM3 in the early stages of apoptosis however this study did not specifically address if the upregulation of RBM3 was a part of the cell death process or a compensatory cytoprotective factor (Ryan et al., 2005). A recent study addressed this and showed that RBM3 is a necessary protein for cell survival. Overexpression of RBM3 in primary neurons under conditions of hypothermia showed significant abrogation of apoptosis whereas siRNA mediated RBM3 knockdown resulted in increased cell death under hypothermia (Chip et al., 2011). This study concluded that the clinical use of hypothermia to preserve brain function following injury could be mediated by RBM3. RBM3 overexpression, either exposure to cold shock or through vector transfection of an RBM3 overexpressing construct, also showed significant protection from apoptosis in C_2C_{12} myoblast cells. Treatment of cells with staurosporine or H_2O_2, both of which normally induce apoptosis, was not as effective in inducing apoptosis in cells exposed to cold shock or cells overexpressing RBM3 (Ferry et al., 2011). This implied that RBM3 may have a role in inducing cytoprotective effects on cells following exposure to the stressor conditions it is upregulated by, namely hypoxia and cold shock. Additionally, as RBM3 overexpression attenuated the apoptosis response following staurosporine and H_2O_2 treatment, it may serve as an inhibitor of apoptosis under many conditions.

RBM3 also appears to have effects on regulation of cell cycle progression and proliferation. siRNA mediated knockdown of RBM3 in colon cancer cells resulted in cells accumulating at the G2/M phase of cell cycle and subsequently undergo apoptosis (Sureban et al., 2008b). A study by Wellmann *et al.* further confirmed that RBM3 serves in this role. These studies revealed

several insights into the physiologic roles of RBM3. Primarily, it was observed that RBM3 mRNA transcript levels closely mirrored proliferation rates in human fibroblasts and HEK293 embryonic kidney cells. Inhibition of proliferation using serum deprivation or contact inhibition showed decreases in RBM3 levels while forced overexpression of RBM3 showed rescue of serum deprivation induced growth arrest. Additionally, siRNA-mediated RBM3 knockdown showed cells eventually losing proliferative capacity and undergoing cell death (Wellmann et al., 2010). Additionally, this study further confirmed by IHC that RBM3 was increased in colon and prostate adenomas compared to normal, terminally differentiated tissue.

RBM3 expression and cancer

One of the most prominent studies of the potential role that RBM3 may serve in colon cancer showed that RBM3 is capable of inducing oncogenic transformation (Sureban et al., 2008b). First, it was demonstrated that if RBM3 was overexpressed in NIH/3T3, non-transformed, immortalized mouse fibroblasts, the cells were capable of anchorage independent growth, a marker of malignant transformation. This is currently one of the strongest pieces of evidence suggesting that RBM3 overexpression can be oncogenic. Second, this study also was the first to reveal that RBM3 mRNA and protein levels are elevated in colon cancer in a stage dependent manner compared to normal adjacent tissue. Additionally, IHC of tumor microarrays revealed that RBM3 immunoreactivity was increased in breast, pancreatic, lung, ovarian and prostate cancers. Finally, it was also revealed that in addition to *COX-2* mRNA, interleukin-8 (*IL-8*) and vascular endothelial growth factor (*VEGF*) mRNA half-lives were increased following RBM3 overexpression revealing a more mechanistic role for RBM3 in oncogenic transformation and

potentially progression. Zeng, *et al.* demonstrated that using either heat shock or small interfering RNAs (siRNAs) to knock down expression of RBM3, prostate cancer cell lines were more susceptible to the chemotherapeutic agents cisplatin and ADM (Zeng et al., 2009). This further shows that RBM3 may play a role in progression of cancers by mediating an increase in the multi-drug resistance phenotype.

Following the finding that RBM3 is upregulated in colon cancer numerous studies have shown RBM3 expression levels in other cancers. In a subsequent study, RBM3 was measured in human astrocytoma using real-time RT-PCR, Western blot and IHC. RBM3 transcript levels were greater than 5-fold in grade III-IV astrocytomas (by World Health Organization grading criteria) and approximately 1.6-fold greater in grade I-II compared to adjacent normal tissue. The RBM3 positive staining rate by IHC was revealed to be 92.5% in grade IV astrocytomas falling to 37.5% in normal brain tissues. This data implies that RBM3 may have a role in both astrocytoma carcinogenesis as well as progression of astrocytoma (Zhang et al., 2013). In a study of RBM3 in prostate cancer, RBM3 levels were examined using IHC on tissue microarrays containing over 11,000 prostate cancer samples. Higher RBM3 expression was correlated to advanced tumor stage, Gleason score and metastasis to lymph nodes. 25.6% of tumors from the microarray showed strong staining of RBM3 which was correlated to deletions in PTEN. RBM3 expression was also correlated with recurrence. This study demonstrates that RBM3 serves as a strong independent prognostic marker of prostate cancers (Grupp et al., 2013). In agreement with this data, microarray analysis of human prostate cancer tissues showed that in poorly differentiated prostate cancer compared to moderately differentiated tumors or normal tissue, RBM3 transcript levels were elevated (Shaikhibrahim et al., 2013).

From the evidence presented by these studies, it would appear that RBM3 shares a loose correlation with stem cells. Primarily, RBM3 expression is upregulated in the CD34+ HSC population following GM-CSF treatment. Second, RBM3 is upregulated by hypoxia and CSCs are enriched within hypoxia. Third, CSCs are particularly resistant to apoptosis and chemotherapy and RBM3 is implicated in resistance to apoptosis and chemoresistance. Additionally, RBM3 overexpression has been shown to be oncogenic and upregulation of the stem cell compartment is thought to be an initiating event in oncogenesis. Finally, RBM3 expression seems to correlate with a poor prognosis in cancer. Importantly, the current evidence only implies a correlative link between RBM3 and the CSC. Currently any causative evidence is lacking.

In this study, we provide evidence that exogenous RBM3 overexpression is capable of increasing the population of stem cells. Furthermore, this increase in the stem cell population is correlated with an increase in chemoresistance further confirming that RBM3 overexpression can result in a functional change in cancer cells. These studies also show a novel link between RBM3 and the Wnt/β-catenin signaling pathway showing the mechanism driving the RBM3 induced stem cell phenotype. Taken together these data show a causative link between RBM3 and the stem cell phenotype as well as the stem cell signaling pathway that RBM3 modulates.

Chapter II: Overexpression of RBM3 increases stem cell characteristics and chemoresistance in colon cancer cells

Introduction

RBM3 expression levels as measured by protein and mRNA levels in solid tumors appear to increase as cancers become progressively more aggressive (Grupp et al., 2013; Lleonart, 2010; Shaikhibrahim et al., 2013; Sureban et al., 2008b; Zeng et al., 2009; Zhang et al., 2013). Additionally, most tumors even at earlier stages appear to have significantly elevated RBM3 levels compared to normal adjacent tissue. Finally, current evidence for the physiologic functions of RBM3 points toward a potential role in regulating stem cell populations (Lleonart, 2010; Yang et al., 2008a). Additional studies strongly point toward RBM3 being linked with both the initiation and progression of astrocytoma, colon and prostate cancer. Unfortunately, most of the current studies only show correlative data linking RBM3 to oncogenesis and tumor progression and fail to show any major causative evidence or mechanistic data. Here we demonstrate that RBM3 overexpression is capable of inducing a phenotypic change that results in an increase in the percentage of cells with stem-like properties. Additionally, we present evidence that RBM3 overexpression is capable of increasing the chemotherapy resistance phenotype through increase of ABC transporter activity. This evidence implies a strong correlative link between RBM3 and the initiation and progression of cancer.

Rationale

In order to discern a potential causative link between RBM3 expression levels and colon cancer progression, we exogenously modulate RBM3 expression using a doxycycline (Dox) inducible lentiviral RBM3 overexpression construct in both HCT 116 and DLD-1 cells. We presumed that because the physiologic functions of RBM3 share a significant amount of overlap with known

characteristics of stem cells, then if RBM3 plays a role within the biology of cancer cells, it would likely be in the regulation of the stem cell compartment. Also, as a dysregulation in the stem cell pool is thought to lead to the initiation of colon cancer, we hypothesize that if RBM3 is capable of altering stem cell homeostasis, this could be a potential explanation for its previously demonstrated role as an oncogene. Furthermore, as expansion of the CSC fraction correlates with increased aggressiveness of colorectal cancer, we also propose that increased RBM3 expression in advanced cancers causes an expansion of the CSC population that leads to poor prognosis associated with high RBM3 expression.

Stem cell population measurement

We measure the change in stem cell population using two functional assays for stem cell population as well as quantifying expression of the stem cell markers DCLK1, LGR5 and CD44.

As mentioned previously, studies have demonstrated that isolation of the SP fraction yields a population that is highly enriched for self-renewal and differentiation capacity (Goodell et al., 1996). SP cells have also been shown to be upregulated in many primary tumors and cancer cell lines (Chiba et al., 2006; Christgen et al., 2007; Haraguchi et al., 2006; Hirschmann-Jax et al., 2004; Szotek et al., 2006). This observation implies that alterations in the SP percentages could represent alterations in stem cell homeostasis as well as an increase in MDR. Additionally, in the context of cancer, SP fractions may be a method to measure and isolate the CSC population. On the other hand, global alteration in the intracellular fluorescence profile would indicate global changes in ABC transporter expression rather than increased expression in the discrete population of SP cells.

The second functional method of measuring stem cell characteristics is the spheroid formation assay. This assay is an *in vitro* culture system initially established in the culture of neurospheres where these cells were revealed to be highly enriched in stem cell characteristics (Reynolds and Weiss, 1996). The spheroid forming cells were shown to be capable of increased differentiation into neurons, astrocytes and oligodendrocytes. Additionally, spheroid forming cells were capable of sustained iterations of spheroid formation implying self-renewal capacity as well. Essentially, the assay relies on exposing the heterogeneous cell population to a combination of anchorage independent growth and serum deprivation resulting in an environment where only stem cells have the capacity to proliferation and other cells undergo apoptosis. Additionally, spheroid assays often take place over the course of seven to ten days allowing cells with self-renewal capacity to maintain spheroids. An elegant study by Dontu, *et al.* showed that cells cultured as spheroids have been shown to have significant increases in self-renewal and differentiation capacity for mammary epithelial culture establishing mammospheres as a culture method for expanding stem cells *in vitro* (Dontu et al., 2003). Interestingly, this study also revealed that the spheroid forming stem cell also resides within the SP fraction providing confirmation that both assays enrich for stem cells. Spheroid forming capacity has also been shown to be a valid *in vitro* culture method for expanding stem cells for colonic epithelial cells (Kanwar et al., 2010; Ricci-Vitiani et al., 2007). Here we use spheroid formation capacity in colonospheres as a method for measuring "stemness" within the RBM3 overexpressing colon cancer cell lines.

Finally, the expression of DCLK1, LGR5 and CD44 has been shown to mark colonic CSCs (Barker et al., 2009; Barker et al., 2007; Dalerba et al., 2007; May et al., 2008; Qing-Bin et al., 2013; Verissimo et al., 2012). We measured changes in the percentage of cells positive for stem cell marker expression. As previously discussed, a consensus has yet to be reached on a single

reliable stem cell marker for either ISCs or CSCs, so we confirm this data with the two mentioned functional assays to provide compelling evidence that RBM3 overexpression increases the percentage of stem cells in a given cancer cell population.

Materials and Methods

Cell culture

HCT 116 and DLD-1 cell lines were obtained from ATCC and cultured under conditions of 5% CO_2 in Dulbecco's Modified Eagle Medium (DMEM) (Corning) containing 10% fetal bovine serum (FBS) (Sigma-Aldrich) and 1% antibiotic/antimycotic solution (Corning). Following transduction of tGFP or tRBM3 plasmids, cells were cultured as mentioned above with additional 1 mg/mL G 418 (Santa Cruz Biotechnology) and 1μg/mL puromycin (Life Technologies).

Lentivirus propagation and infection

The Tet-On Advanced tetracycline inducible empty vector system (ClonTech Laboratories, Inc.) was used to generate an inducible RBM3 overexpressing system. Tetracycline inducible RBM3 plasmids were generated using the In-Fusion cloning system (ClonTech Laboratories, Inc.) to insert the human RBM3 gene into the multiple cloning site of the pLVX-Tight-Puro vector according to manufacturer recommendations. Using this approach, three plasmids were generated: pLVX-tRBM3, pLVX-tGFP and pLVX-tGFP-RBM3 where pLVX-tRBM3 is the Dox inducible human RBM3, pLVX-tGFP is Dox inducible enhanced green fluorescent protein

(eGFP) and pLVX-tGFP-RBM3 is a Dox inducible eGFP/RBM3 fusion protein. Lenti-X cells were obtained from Dr. Roy Jensen and were used to generate virus. Lenti-X cells were transfected with 7.5 μg of each of the pGIPZ packaging plasmids obtained from Dr. Roy Jensen as well as 24 μg of the cargo vector (either pLVX-TetOn, pLVX-tRBM3, pLVX-tGFP, or pLVX-tGFP-RBM3) using Lipofectamine 2000 (Life Technologies). Viral supernatant was collected at 48, 72 and 96 hours following lipofectamine transfection, pooled, clarified through a 0.45 μm syringe filter and concentrated using the Lenti-X concentrator (ClonTech Laboratories, Inc.). Virus was tittered through limiting dilution (10^{-6} dilution of 10 μL of concentrated virus) and colony formation against appropriate selection (1 mg/mL of G 418 for pLVX-TetOn virus or 1 μg/mL of puromycin for pLVX-tRBM3, pLVX-tGFP or pLVX-tGFP-RBM3 virus). Parental control cells were used to ensure no colony formation occurred in untransduced cells.

Following tittering, HCT 116 and DLD-1 cells were co-transduced in suspension with 4 μg/mL polybrene (Sigma Aldrich) using a mean of infection (MOI) of 5 for pLVX-tRBM3, pLVX-tGFP or pLVX-tGFP-RBM3 and an MOI of 10 for the pLVX-TetOn. 24 hours following transduction, fresh media was added and following 48 hours of transduction dual selection media was added. Parental cells were cultured alongside transduced cells for 1 week under similar selection antibiotics to ensure that no untransduced cells survived following the 1 week of selection under gross inspection by microscopy.

Following 1 week of selection, cells were evaluated for GFP or RBM3 overexpression by real time RT-PCR and western blot using both a dose dependence and time dependence of Dox treatment.

Western blotting

Western blot were performed using poly-acrylamide gel electrophoresis within a Miniprotean Tetracell apparatus (BioRad) followed by blotting onto 0.45 μm pore size Immobilon polyvinyl difluoride membrane (Millipore) using a mini Transblot module (BioRad). Antibodies for RBM3 were obtained from AbCam (AbCam) or custom generated through Fisher (Thermo Fisher Scientific). Antibodies for β-catenin and phospho-β-catenin were obtained from Cell Signaling (Cell Signaling Technology) or BD Biosciences (BD Biosciences). Antibodies for GSK3β and phosphor-GSK3β were obtained from Cell Signaling (Cell Signaling Technology).

Real time RT-PCR

Total cellular RNA was isolated using TRIzol reagent followed by reverse transcription using SuperScript II in the presence of random hexonucleotide primers (Life Technologies). cDNA was then analyzed by real-time RT-PCR using Jumpstart Taq polymerase (Sigma Aldrich) and SYBR Green nucleic acid stain (Life Technologies). Threshold crossing values for each gene were normalized to glyceraldehyde phosphate dehydrogenase (GAPDH) gene expression. mRNA expression was then normalized to fold change relative to uninduced controls. Primers used in this study are as follows:

RBM3: 5’-TGGGAGGGCTCAACTTTAAC-3’ / 5’-ATGCTCTGGGTTGGTGAAG-3’

GAPDH: 5’-CAGCCTCAAGATCATCAGCA-3’ / 5’-GTCTTCTGGGTGGCAGTGAT-3’

Pgp: 5’-TGCCTTCATCGAGTCACTGC-3' / 5’-TGACGTGGCTTCATCCAAAA-3'

MRP2: 5’-TGTGACCACAGATACCAGGA-3' / 5’-AAATATTTTGCCTGGGAACC-3'

IL-8: 5’-ATGACTTCCAAGCTGGCCGTGGCT-3’ / 5’-
TCTCAGCCCTCTTCAAAAACTTCTC-3’

SP assay

SP assay was performed as previously described with minor modifications (Mathew et al., 2009). In brief, cells were plated at 100,000 cells/mL into 6 well plates with relevant treatments. Following 72 hours of treatment cells were trypsinized and resuspended at 1 million cells/mL in DMEM and pre-warmed for 15 minutes at 37°C. Cells were then given 50 μM verapamil (Sigma Aldrich), as a pan efflux inhibitor, or vehicle for 30 minutes. Cells were then incubated with 10 μM Vybrant DyeCycle Violet (DCV) (Life Technologies) for 90 minutes at 37°C. Cells were then resuspended in ice cold SP buffer containing 2% FBS, 2 mM HEPES, 1 μg/mL 7-amino actinomycin D (7AAD) (Life Technologies) in Hank’s balanced salt solution and analyzed on a BD LSR II for SP. DCV was excited using a violet diode laser (408 nm) and emission was measured with a 450/50 nm bandpass filter (DCV Blue) and 630 nm longpass, 660/40 nm bandpass filter (DCV Red). Viability gating was established with 7AAD with excitation at 552 nm and emission monitored with a 630 nm longpass, 660/40 nm bandpass filter. Cells were initially gated for appropriate size using the side scatter (SSC) and forward scatter (FSC). Cells were then gated for viability using 7-AAD uptake to eliminate non-viable cells. Finally, the location of the SP gate was established using the verapamil treated sample.

Proliferation assay

Cells were induced with Dox for 72 hours. Following induction of RBM3 or GFP vector control, cells were plated at 50,000 cells per mL into 96 well plates and allowed to adhere overnight followed by treatment with paclitaxel or ADM at varying concentrations. Following 48 hours of treatment, cells were assayed for proliferation using the hexoseaminidase assay as previously described (Subramaniam et al., 2008). Briefly, cell culture medium was removed followed by addition of 75 μL hexoseaminidase substrate buffer (7.5 mM sodium citrate, pH 5.0, 3.75 mM 4-nitrophenyl-N-acetyl-β-D-glucosaminide, 0.25% Triton) per well and incubation at 37°C for 30 minutes. The reaction was quenched using 112.5 μL of hexoseaminidase developer solution (50 mM glycine, 5 mM EDTA, pH 10.4) and absorbance at 405 nm was read on a plate reader. Percentage proliferation was calculated as absorbance relative to untreated control and curves for inhibitory response were fit using GraphPad Prism software (GraphPad).

ADM uptake and efflux assay

Cells were plated at high concentration (350,000 cells/mL) for uptake assays into 6 well plates. Cells were induced with indicated concentrations of Dox for 72 hours. Cells were then treated with indicated concentrations of ADM (ADM) for 30 minutes followed aspiration of ADM containing media and addition of ice cold stop solution (200 mM KCl, 2 mM HEPES). Samples were washed additionally with stop solution to remove residual extracellular or bound ADM. Cells were then lysed with MDR lysis buffer (0.1% Triton-X in 0.3N sodium hydroxide) and fluorescence was read on a BioTEK plate reader. Lysates were then assayed for protein concentration using Bradford protein assay kit (BioRad) according to manufacturer

recommendations. Fluorescent measurements were normalized to protein content to establish normalized ADM uptake.

For efflux assays, cells were plated and induced similar to uptake assays. Following induction, cells were treated with 375 μM ADM for 2 hours, then washed with PBS twice and allowed to efflux into fresh PBS for varying time points. PBS fluorescence was measured and compared to standard curve of ADM fluorescence to establish ADM content effluxed. Cells were then lysed with MDR lysis buffer to calculate total protein content per well. Efflux capacity was calculated as total ADM effluxed per microgram of total protein.

Spheroid formation assay

Cells were appropriately treated in 2D culture, trypsinized followed by a wash in phosphate buffered saline (PBS) to remove residual serum. Cells were then resuspended in spheroid media containing 1x B27 supplement, 20 ng/mL basic recombinant fibroblast growth factor (bFGF) and 20 ng/mL recombinant epidermal growth factor (EGF) (Life Technologies) in DMEM. Cells were passed through a 35 μm sieve, counted and plated onto ultra-low attachment surface plates (Corning). Spheroid formation was allowed to proceed for 10-14 days followed by spheroid quantification and analysis using a Celigo Cyntellect embryoid body counter.

Stem cell marker flow cytometry

Cells were treated with Dox to induce expression of GFP or RBM3 for 72 hours. Cells were then trypsinized then resuspended at $1x10^6$ cells. For DCLK1 and LGR5, cells were stained with

Alexafluor 647 (AF647) conjugated LGR5 antibody (BD Biosciences) or PE conjugated DCLK1 antibody (AbCam) according to manufacturer recommendations. PE conjugation was performed using the Zenon PE labelling kit (Life Technologies) according to manufacturer recommendations. For the CD44/CD24 experiment, cells were stained using allophycocyanin (APCF) conjugated CD44 antibody and phycoerythrin (PE) conjugated CD24 antibody according to manufacturer recommendations with the exception of using half the recommended concentration of APCF-CD44 antibody (BD Biosciences). Compensation was performed using standardized fluorescent beads.

Results

We first developed HCT 116 and DLD-1 cell lines with stable Dox inducible RBM3, GFP and GFP-RBM3 (tRBM3, tGFP, tGFP-RBM3, respectively) expression. We initiated these studies by quantifying the time and dose dependence of Dox in these cells. There was a dose-dependent increase in RBM3 mRNA expression with maximal induction seen at a concentration of 500 ng/mL Dox (Figure 1). Importantly, even in the absence of Dox, HCT 116 tRBM3 cells still displayed 2.6-fold induction of *RBM3* mRNA levels compared to vector control implying that the Dox responsive promoter still generates slight overexpression inherently (Figure 2). Additionally, time dependence was investigated following treatment with 500 ng/mL Dox which reavealed that RBM3 mRNA levels reached maximal induction within 24 hours (Figure 3). We next quantified the induction in protein levels in both DLD-1 and HCT 116 tGFP and tRBM3 cells to validate that the Dox responsive dose and time dependence of mRNA induction correlated with protein expression. tGFP and tRBM3 protein expression mirrored mRNA levels with the exception of maximal induction of protein only appearing at 48 hours compared to 24

Figure 1

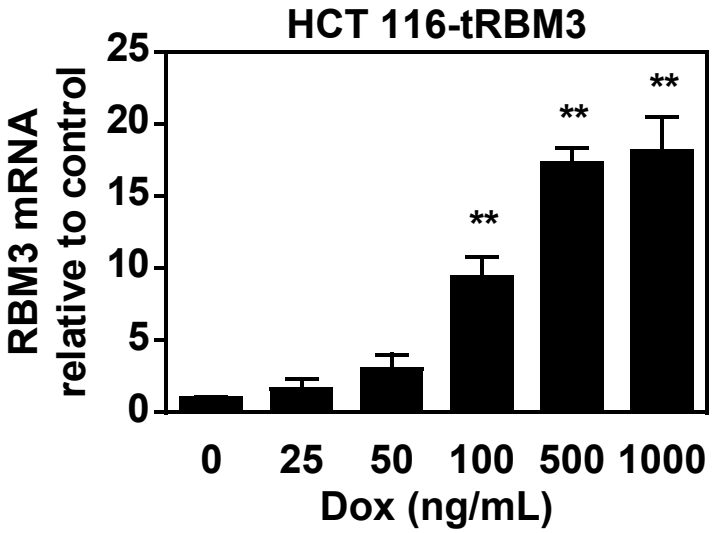
HCT 116-tRBM3
RBM3 mRNA relative to control
25
20
15
10
5
0
**
**
**
0
25
50
100
500
1000
Dox (ng/mL)

Figure 1: HCT 116-tRBM3 cells upregulate *RBM3* mRNA in a Dox dose responsive fashion. Real time RT-PCR analysis of RBM3 mRNA following 72 hour induction with indicated concentrations of Dox. mRNA fold change is normalized to uninduced control. Graphs show mean fold change with standard error of mean (SEM). *P < 0.05, **P < 0.01, ***P < 0.001 (Student's *t*-test).

Figure 2

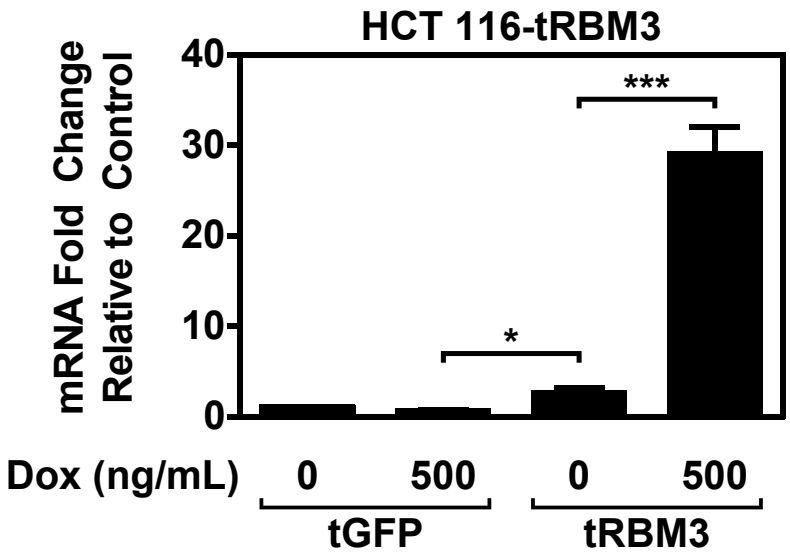
HCT 116-tRBM3
mRNA Fold Change Relative to Control
40
30
20
10
0
*
***
Dox (ng/mL)
0
500
0
500
tGFP
tRBM3

Figure 2: HCT 116-tRBM3 cells show minor increase in RBM3 expression in the absence of Dox induction. Real time RT-PCR analysis of RBM3 mRNA following 72 hour induction with indicated concentrations of Dox. mRNA fold change is normalized to uninduced control in HCT 116-tGFP cells. Graphs show mean fold change with SEM. *P < 0.05, **P < 0.01, ***P < 0.001 (Student's *t*-test).

Figure 3

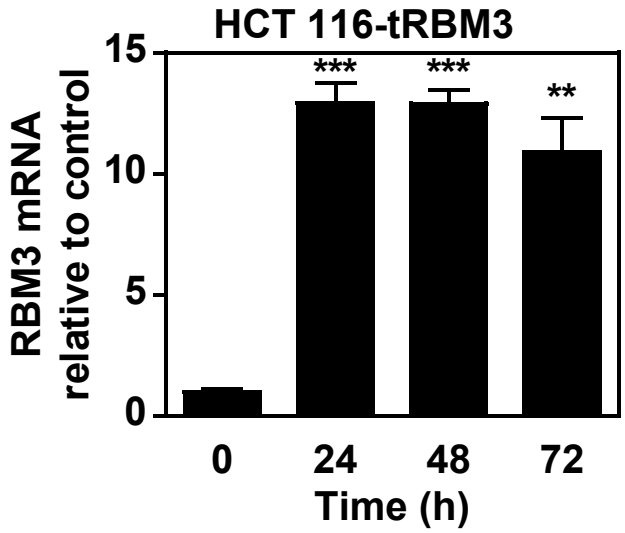
HCT 116-tRBM3
RBM3 mRNA relative to control
15
10
5
0
***
***
**
0
24
48
72
Time (h)

Figure 3: HCT 116-tRBM3 cells show upregulation of *RBM3* mRNA within 24 hours. Real time RT-PCR analysis of *RBM3* mRNA following 500 ng/mL Dox treatment for the specified amount of time. mRNA fold change is normalized to 0 hour control. Graphs show mean fold change with SEM. *P < 0.05, **P < 0.01, ***P < 0.001 (Student's *t*-test).

hours for mRNA (Figure 4). This lag is primarily attributed to the need to translate the high quantities of mRNA. DLD-1 and HCT 116 tGFP cells were also validated to have Dox induction of GFP (Figure 4). To validate that Dox induction generates functionally active RBM3 in HCT 116 tRBM3, we also validated that RBM3 expression generated an increase in *IL-8* expression as previously published (Baghdoyan et al., 2000; Sureban et al., 2008b) (Figure 5). Additionally, to further characterize dose dependence of Dox based induction we used fluorimetry to quantify overall GFP fluorescence following 48 hour treatment with serial dilutions of Dox. In both HCT 116 tGFP and tGFP-RBM3 cells we observed reliable, robust expression of GFP fluorescence (Figure 7). Finally using HCT 116 tGFP and HCT 116 tRBM3 cells we quantified localization of free GFP and the GFP-RBM3 fusion protein to validate that RBM3 localization was similar as that described in previous studies (Jogi et al., 2009). As expected, GFP expression was diffuse across the cell while GFP-RBM3 localization was primarily in the nucleus (Figure 7). Interestingly, we observed that GFP-RBM3 was expressed difflusely across the nucleus but showed focal localization in nucleolar regions which contrasts with previous reports stating that RBM3 localization is nuclear with exclusion from nucleolar regions (Figure 7).

To measure changes in the stem cell population, we first determined whether there was a change in SP percentages following RBM3 induction. SP population was originally described as a population of cells with the capacity to efflux Hoechst 33342 (Goodell et al., 1996). However, due to limitations with Hoescht 33342 requiring ultraviolet excitation, we opted to use DCV which can be excited using a lower energy available laser. The use of DCV in isolating the SP fraction has been previously described (Mathew et al., 2009). For these experiments we used an induction of 500 ng/mL of Dox for 72 hours. We used the pan-efflux inhibitor Verapamil to validate the location of the SP in both DLD-1 and HCT 116 cells (Figure 8). In DLD-1-tRBM3

Figure 4

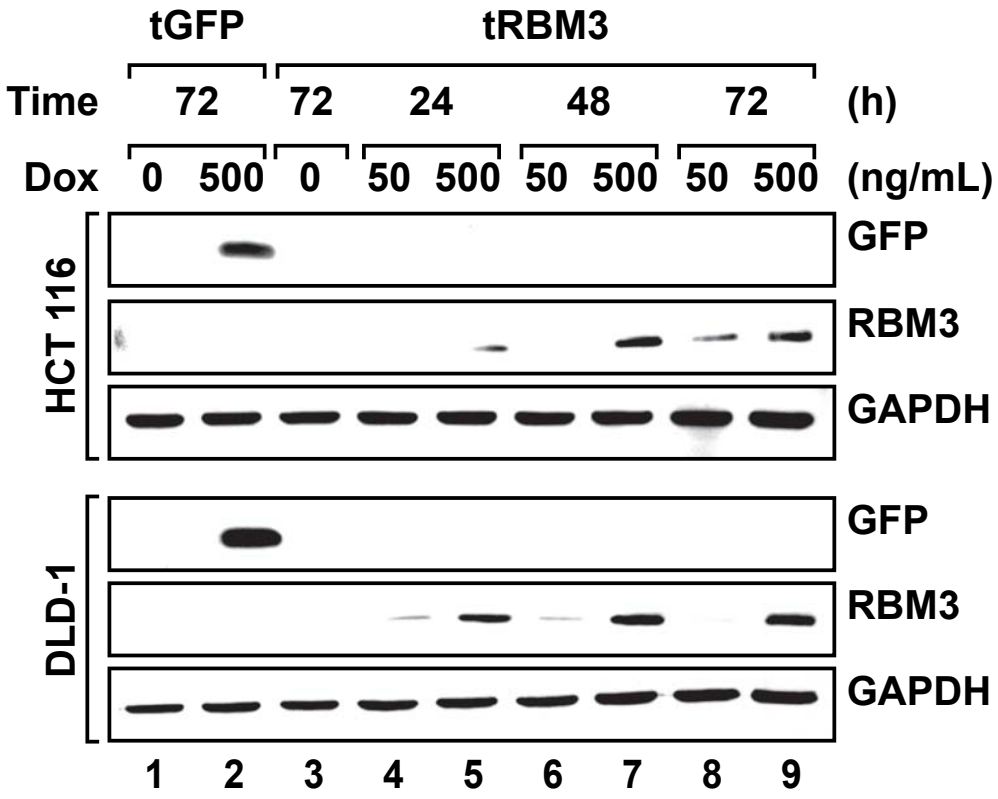
tGFP
tRBM3
Time
72
72
24
48
72
(h)
Dox
0
500
0
50
500
50
500
50
500
(ng/mL)
HCT 116
GFP
RBM3
GAPDH
DLD-1
GFP
RBM3
GAPDH
1
2
3
4
5
6
7
8
9

Figure 4: HCT116-tRBM3 and DLD-1-tRBM3 cells show upregulation of RBM3 protein in a time and dose dependent fashion. Western blot analysis of RBM3 or GFP overexpression in DLD-1 and HCT 116 tGFP or tRBM3 cells with indicated concentrations of and times of Dox treatment demonstrating the reliability of Dox induction in these cells.

Figure 5

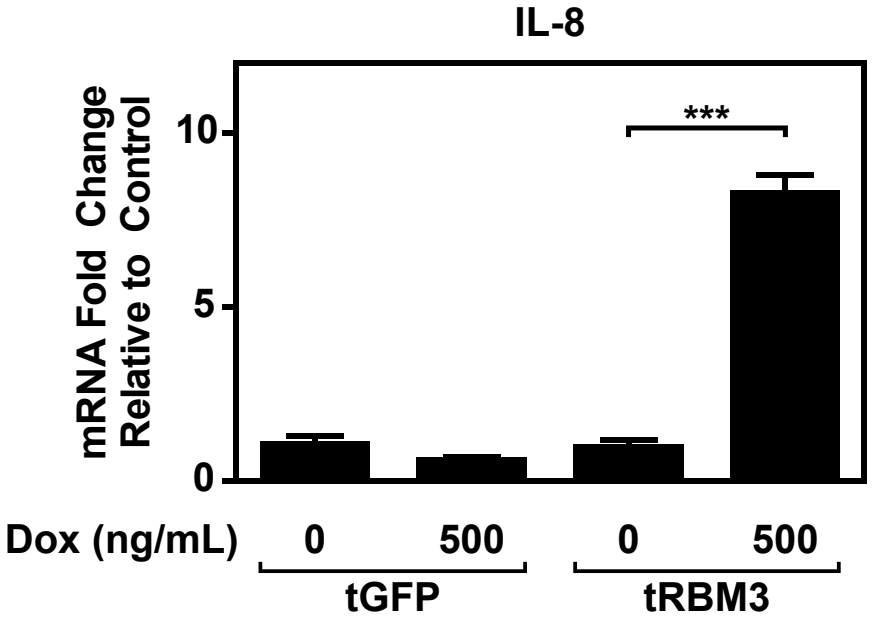
IL-8
mRNA Fold Change Relative to Control
10
5
0
***
Dox (ng/mL)
0
500
0
500
tGFP
tRBM3

Figure 5: RBM3 overexpression generates functional RBM3 protein that can induce increased *IL-8* expression. Real time RT-PCR analysis of *IL-8* mRNA following 72 hours of Dox treatment with indicated concentrations. mRNA fold change is normalized to uninduced HCT 116-tGFP control. Graphs show mean fold change with SEM. *P < 0.05, **P < 0.01, ***P < 0.001 (Student's *t*-test).

Figure 6

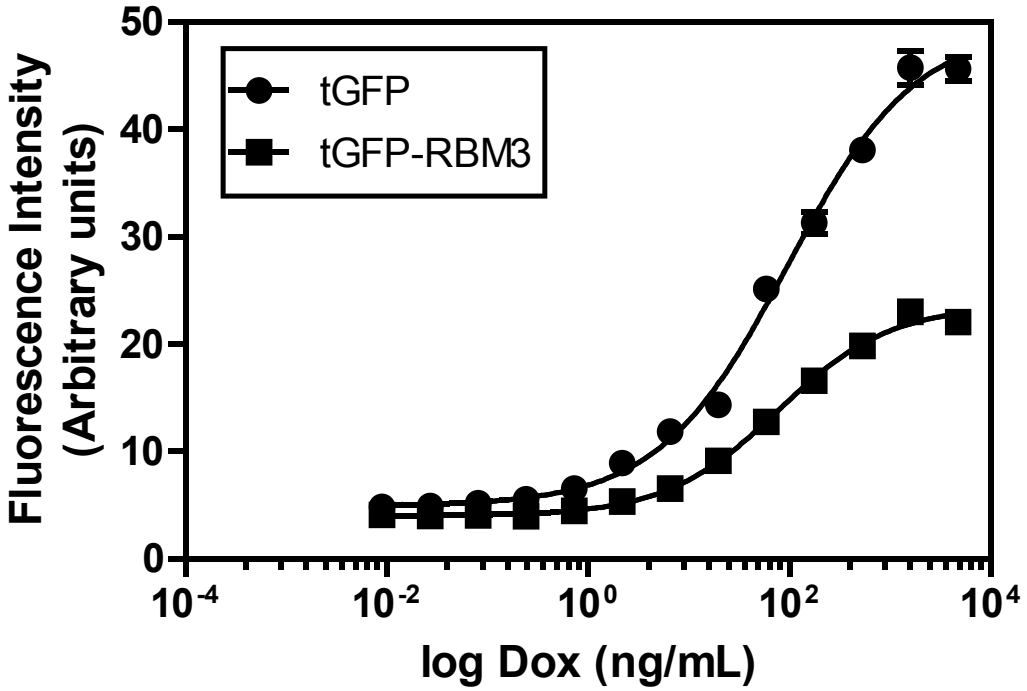
Fluorescence Intensity
(Arbitrary units)
50
40
30
20
10
0
tGFP
tGFP-RBM3
10-4
10-2
100
102
104
log Dox (ng/mL)

Figure 6: Induction characteristics of HCT 116-tGFP and HCT 116-tGFP-RBM3. Mean fluorescence intensity of GFP in HCT 116-tGFP and HCT 116-tGFP-RBM3 cells following 48 hours induction with indicated concentrations of Dox demonstrating appropriate induction characteristics of Dox treatment. Graph represents fluorescence intensity with error bars representing SEM.

Figure 7

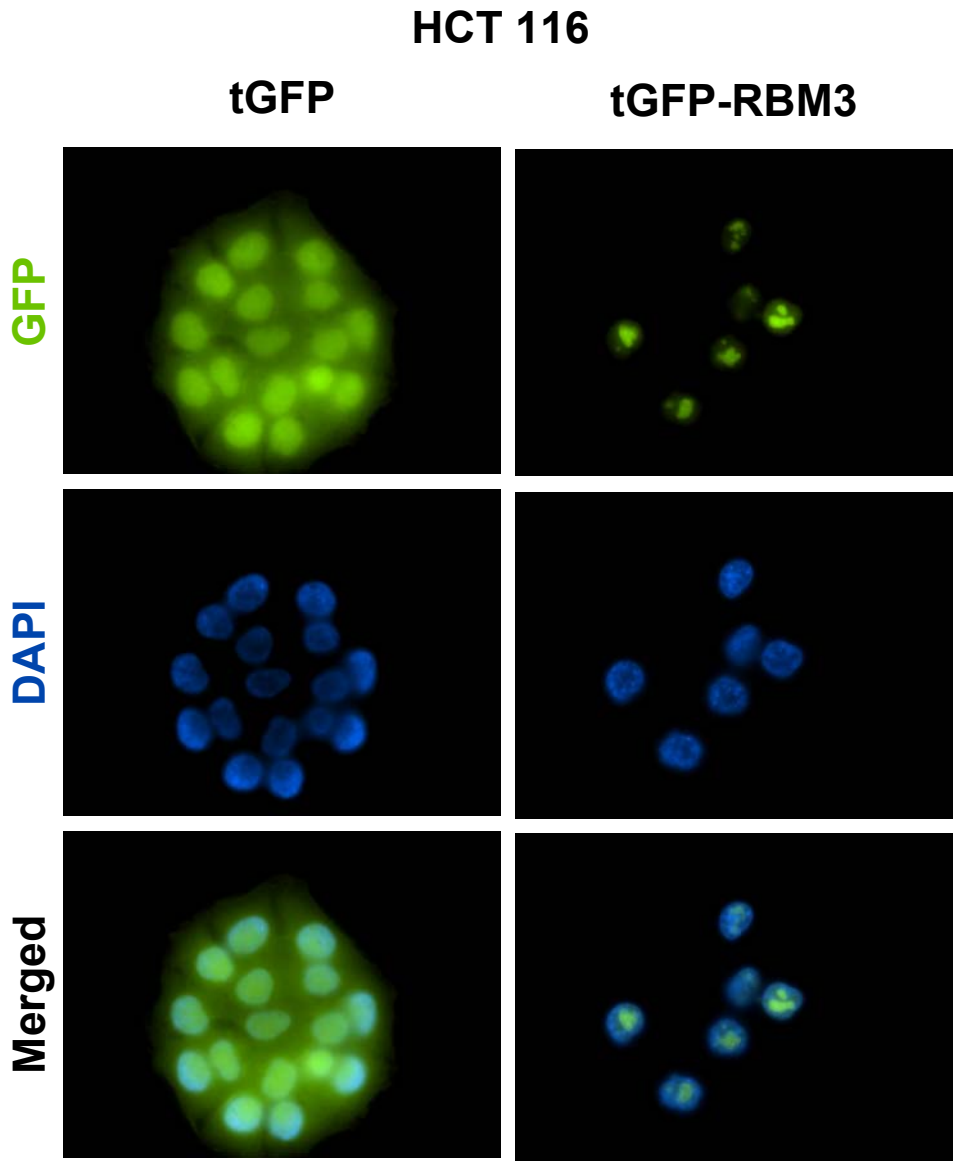

Figure 7: GFP-RBM3 is primarily localized within the nucleus with focal expression within the nucleolus. Fluorescence microscopy of HCT 116-tGFP and HCT 116-tGFP-RBM3 cells induced for 72 hours with 500 ng/mL Dox. Cell nuclei are stained with DAPI. Free GFP is observed to be diffuse across both cytoplasm and nucleus while GFP-RBM3 localizes primarily to nuclei with foci within nucleolar regions.

Figure 8

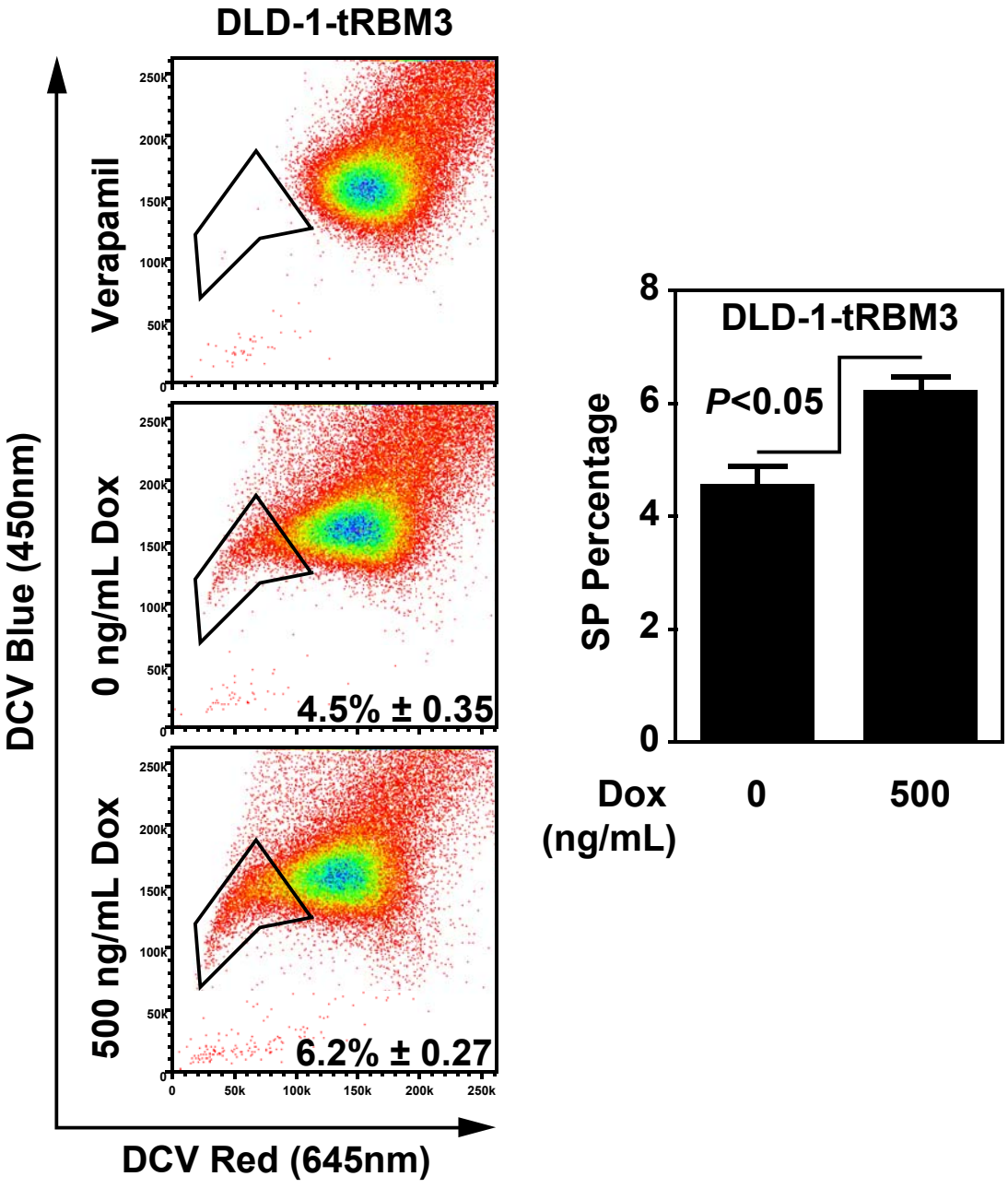
DLD-1-tRBM3
Verapamil
0 ng/mL Dox
500 ng/mL Dox
4.5% ± 0.35
6.2% ± 0.27
DCV Blue (450nm)
DCV Red (645nm)
0
50k
100k
150k
200k
250k
DLD-1-tRBM3
P<0.05
SP Percentage
0
2
4
6
8
Dox (ng/mL)
0
500

Figure 8: DLD-1-tRBM3 cells show increases in SP percentage following Dox induction of RBM3. Flow cytometry dot plots of DCV fluorescence in DLD-1-tRBM3 cells following 72 hours of induction with indicated concentration of Dox. Verapamil treatment was used as a pan efflux inhibitor to localize the SP. Percentages represent fraction of whole, single and viable cells within the side population region. Error bars represent SEM. P values shown are obtained with Student's *t*-test.

cells we observed a fairly high basal SP fraction by comparing verapamil treatment to untreated cells. Induction of RBM3 in these cells showed a robust increase in SP percentages (Figure 8). HCT 116 cells while showing nearly no basal SP fraction compared to verapamil treated control showed a significant induction of SP percentage following RBM3 induction (Figure 9). SP cells have the increased capacity to efflux chemotherapeutic agents. In confirmation of this we treated HCT 116 tRBM3 with various concentrations of ADM for 30 minutes and measured intracellular ADM fluorescence relative to total protein content to measure uptake of ADM. This revealed slightly lower ADM uptake in RBM3 induced HCT 116 tRBM3 cells compared to control at 75 μM ADM (Figure 10). Next, we treated cells with 325 μM ADM for 2 hours and allowed the cells to efflux ADM into fresh PBS for varying times. Here we noted that cells overexpressing RBM3 were capable of increased ADM efflux over the measured course (Figure 11). Interestingly, if we measure intracellular ADM fluorescence by flow cytometry we observe that RBM3 overexpressing cells show a distinct population of cells with low intracellular ADM while the overall histogram of the ADM positive cells remains largely unchanged (Figure 12). These data further implies that a subset of cells is capable of increased efflux, rather than a global shift in the efflux capacity of all cells within the heterogeneous cell pool. Finally, we measured changes in mRNA levels of the ABC transporters *Pgp* and *MRP2* in HCT 116-tRBM3 cells, and we observe that following RBM3 induction there is a time dependent increase in *Pgp* and *MRP2* (Figure 13). This observation confirms the increase in SP and efflux capacity due to an increase in Pgp and MRP2 expression. We next postulated that with a higher SP, RBM3 expression should also confer increased resistance to chemotherapies that are substrates of efflux mechanisms. To test this hypothesis, we measured cell proliferation following treatment with paclitaxel and ADM, both of which are substrates for ABC transporters (Szakacs et al., 2006).

Figure 9

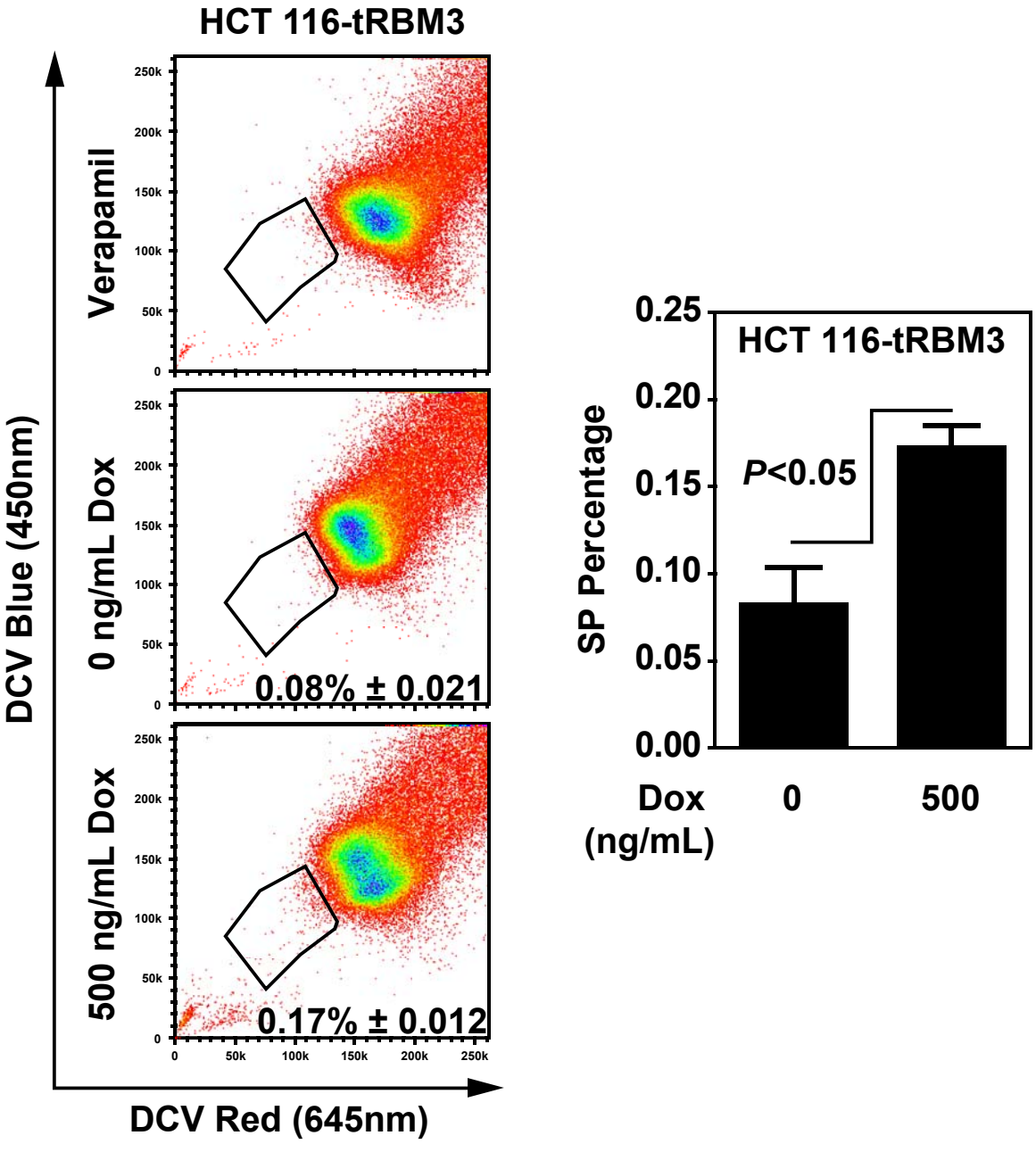
HCT 116-tRBM3
Verapamil
0 ng/mL Dox
500 ng/mL Dox
0.08% ± 0.021
0.17% ± 0.012
DCV Blue (450nm)
DCV Red (645nm)
250k
200k
150k
100k
50k
0
HCT 116-tRBM3
P<0.05
SP Percentage
0.25
0.20
0.15
0.10
0.05
0.00
Dox (ng/mL)
0
500

Figure 9: HCT 116-tRBM3 cells show increases in SP percentage following Dox induction of RBM3. Flow cytometry dot plots of DCV fluorescence in HCT 116-tRBM3 cells following 72 hours of induction with indicated concentration of Dox. Verapamil treatment was used as a pan efflux inhibitor to localize side population. Percentages represent fraction of whole, single and viable cells within the side population region. Error bars represent SEM. P values shown are obtained with Student's *t*-test.

Figure 10

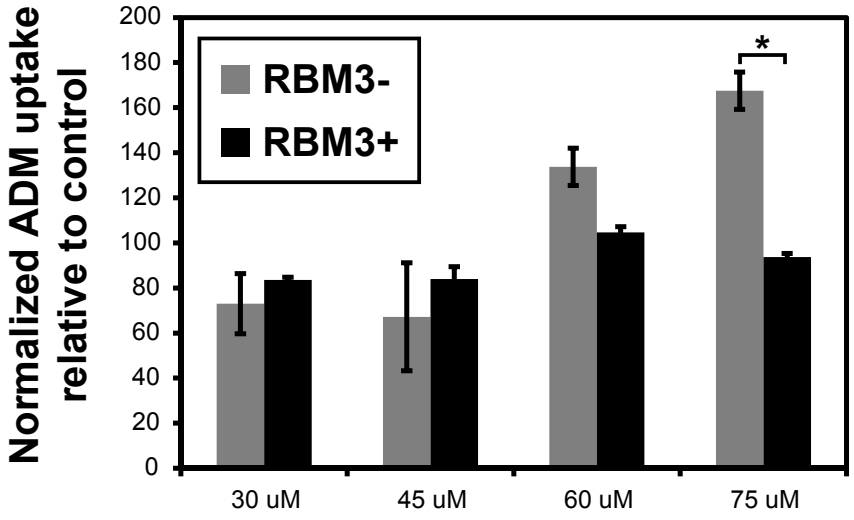
Normalized ADM uptake relative to control
200
180
160
140
120
100
80
60
40
20
0
RBM3-
RBM3+
*
30 uM
45 uM
60 uM
75 uM

Figure 10: HCT 116-tRBM3 cells show decreased ADM uptake upon RBM3 overexpression. Intracellular fluorescence following 30 minutes of treatment with indicated concentrations of ADM normalized to total sample protein. RBM3 induction was generated with 500 ng/mL Dox for 72 hours. Graphs show mean with SEM. *P < 0.05, **P < 0.01, ***P < 0.001 (Student's t-test).

Figure 11

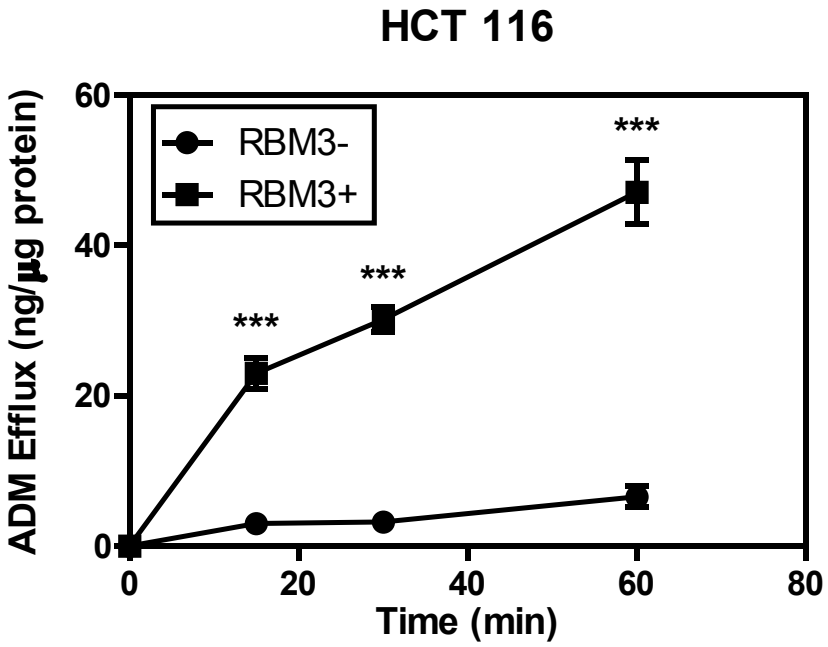
HCT 116
ADM Efflux (ng/µg protein)
60
40
20
0
RBM3-
RBM3+
***
***
***
0
20
40
60
80
Time (min)

Figure 11: HCT 116-tRBM3 cells show increased ADM efflux upon RBM3 overexpression. Extracellular fluorescence following 325 μM ADM treatment for 2 hours then efflux into fresh PBS for the indicated time. PBS fluorescence was measured for ADM concentration and normalized to total sample protein. RBM3 induction was generated with 500 ng/mL Dox for 72 hours. Graphs show mean with SEM. *P < 0.05, **P < 0.01, ***P < 0.001 (Student's *t*-test).

Figure 12

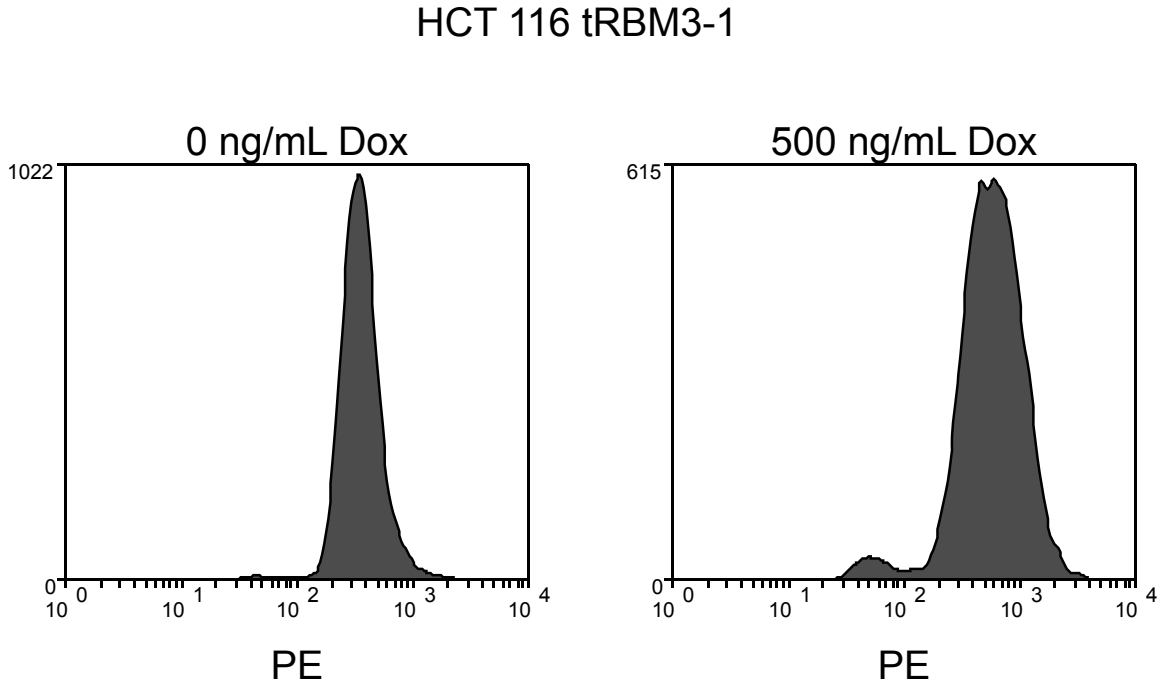
HCT 116 tRBM3-1
0 ng/mL Dox
1022
0
10 0 10 1 10 2 10 3 10 4
PE
500 ng/mL Dox
615
0
10 0 10 1 10 2 10 3 10 4
PE

Figure 12: HCT 116-tRBM3-1 overexpressing RBM3 show a distinct population of ADM low cell after allowing for efflux. Cells were treated with Dox at the indicated concentrations for 72 hours. Histogram represents intracellular ADM fluorescence in whole, single cells following treatment with 40 μM ADM and 2 hours of efflux into fresh DMEM.

Figure 13

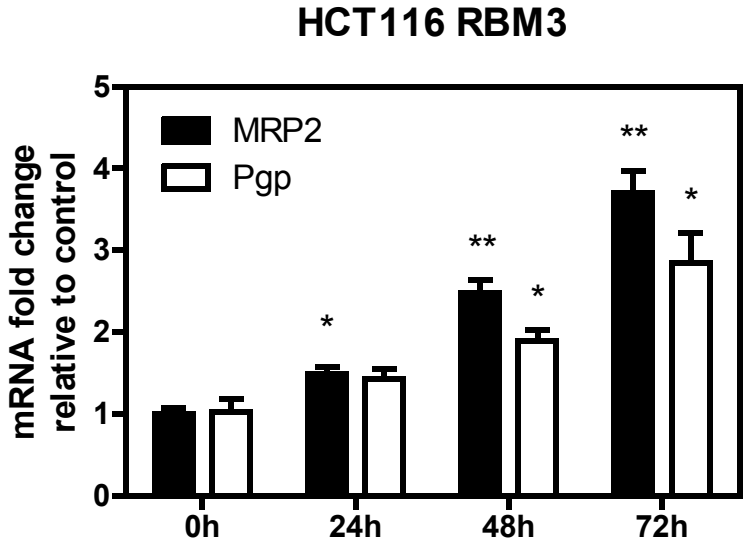
HCT116 RBM3
mRNA fold change relative to control
MRP2
Pgp
0
1
2
3
4
5
0h
24h
48h
72h
*
**
*
**
*

Figure 13: RBM3 overexpression generates an increase in *MRP2* and *Pgp* mRNA levels. Real time RT-PCR analysis of *Pgp* and *MRP2* mRNA following 500 ng/mL Dox treatment for the specified amount of time. mRNA fold change is normalized to 0 hour control. Graphs show mean fold change with SEM. *P < 0.05, **P < 0.01, ***P < 0.001 (Student's *t*-test).

HCT 116 Tet-RBM3 clones were induced for 72 hours with 500 ng/mL Dox and then treated with increasing concentrations of the two compounds. There was significantly higher level of survival of RBM3 overexpressing cells, especially at higher concentrations of paclitaxel (Figure 14). HCT 116 Tet-RBM3 clones were induced for 72 hours with 500 ng/mL Dox and then treated with increasing concentrations of the two compounds. There was significantly higher level of survival of RBM3 overexpressing cells, especially at higher concentrations of paclitaxel (Figure 14).

We also observe that the RBM3 induction is a dose depenent effect as induction of RBM3 using 100 ng/mL of Dox shows a moderate increase in resistance. There was also a small portion of cells that appeared resistant to ADM treatment (Figure 15). As expected, uninduced RBM3 cells showed no appreciable difference between GFP vector controls or parental cells in either paclitaxel or ADM treatment (Figures 14 - 16). These data suggest that RBM3 overexpression increases stem cells within colon cancer cells and alters sensitivity to chemotherapies. The studies are further confirmation of previous studies that correlated RBM3 knockdown with loss of resistance to ADM and cisplatin (Zeng et al., 2009).

We next characterized the relationship between RBM3 and spheroid formation. Interestingly, we observed that expresion of RBM3 protein within spheroids is higher than levels within monolayer cell cultures (Figure 17). This was observed in both DLD-1 and HCT 116 cells. This implies a correlative relationship between RBM3 expression and spheroid formation. We next determined whether RBM3 expression in monolayer culture could alter spheroid formation capacity. Following 72-h Dox induction in both DLD-1 and HCT 116 cells expressing vector control or RBM3, cells were plated into ultra-low attachment conditions and allowed to form spheroids. Both DLD-1 RBM3 and HCT 116 RBM3 overexpressing cells showed increased

Figure 14

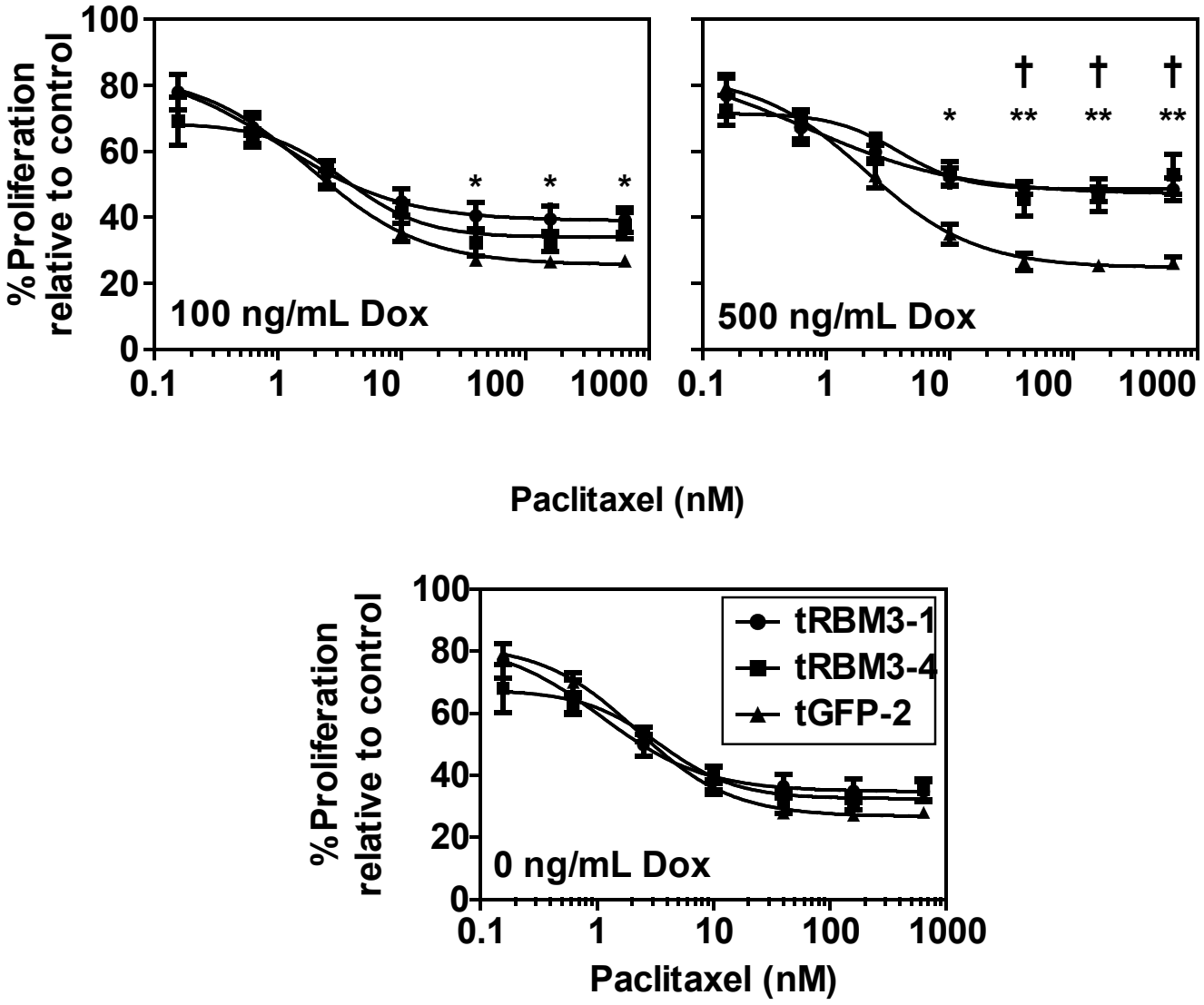
% Proliferation relative to control
100 ng/mL Dox
500 ng/mL Dox
0 ng/mL Dox
tRBM3-1
tRBM3-4
tGFP-2
Paclitaxel (nM)
0.1
1
10
100
1000
0
20
40
60
80
100
*
**
†

Figure 14: RBM3 overexpression generates resistance to paclitaxel treatment. Hexoseaminidase assay following 72 hour induction with 100 or 500 ng/mL Dox followed by 48 hour treatment with paclitaxel in GFP or RBM3 overexpressing cells. Error bars represent SEM. *P < 0.05, **P < 0.01, ***P < 0.001 for RBM3-1, † P < 0.05, ††P < 0.01, †††P < 0.001 for RBM3-4 (Student's t-test)

Figure 15

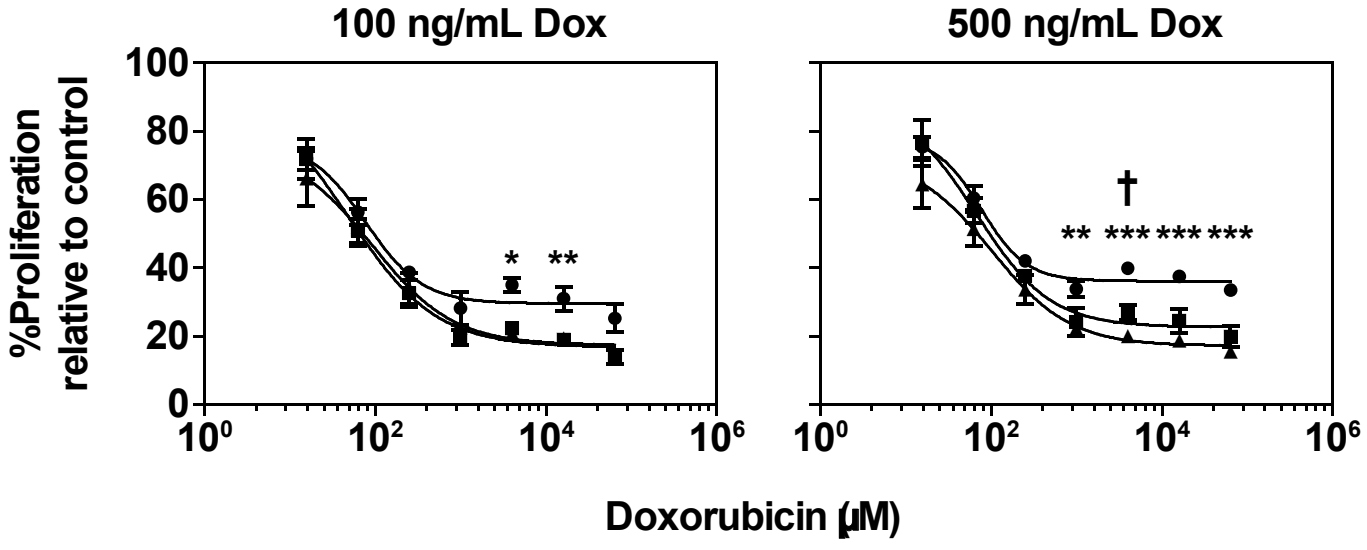
100 ng/mL Dox
500 ng/mL Dox
%Proliferation relative to control
100
80
60
40
20
0
10^0
10^2
10^4
10^6
*
**
†
** *** *** ***
Doxorubicin (μM)

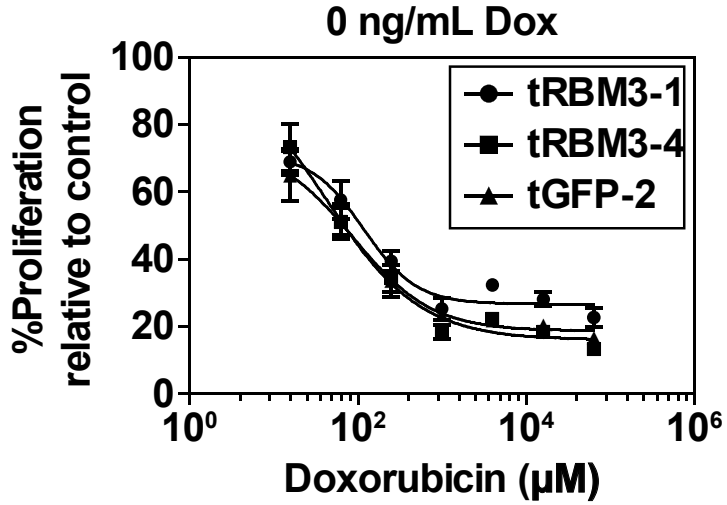
0 ng/mL Dox
%Proliferation relative to control
100
80
60
40
20
0
10^0
10^2
10^4
10^6
tRBM3-1
tRBM3-4
tGFP-2
Doxorubicin (μM)

Figure 15: RBM3 overexpression generates resistance to ADM treatment. Hexoseaminidase assay following 72 hour induction with 100 or 500 ng/mL Dox followed by 48 hour treatment with ADM in GFP or RBM3 overexpressing cells. Error bars represent SEM. *P < 0.05, **P < 0.01, ***P < 0.001 for RBM3-1, † P < 0.05, ††P < 0.01, †††P < 0.001 for RBM3-4 (Student's t-test)

Figure 16

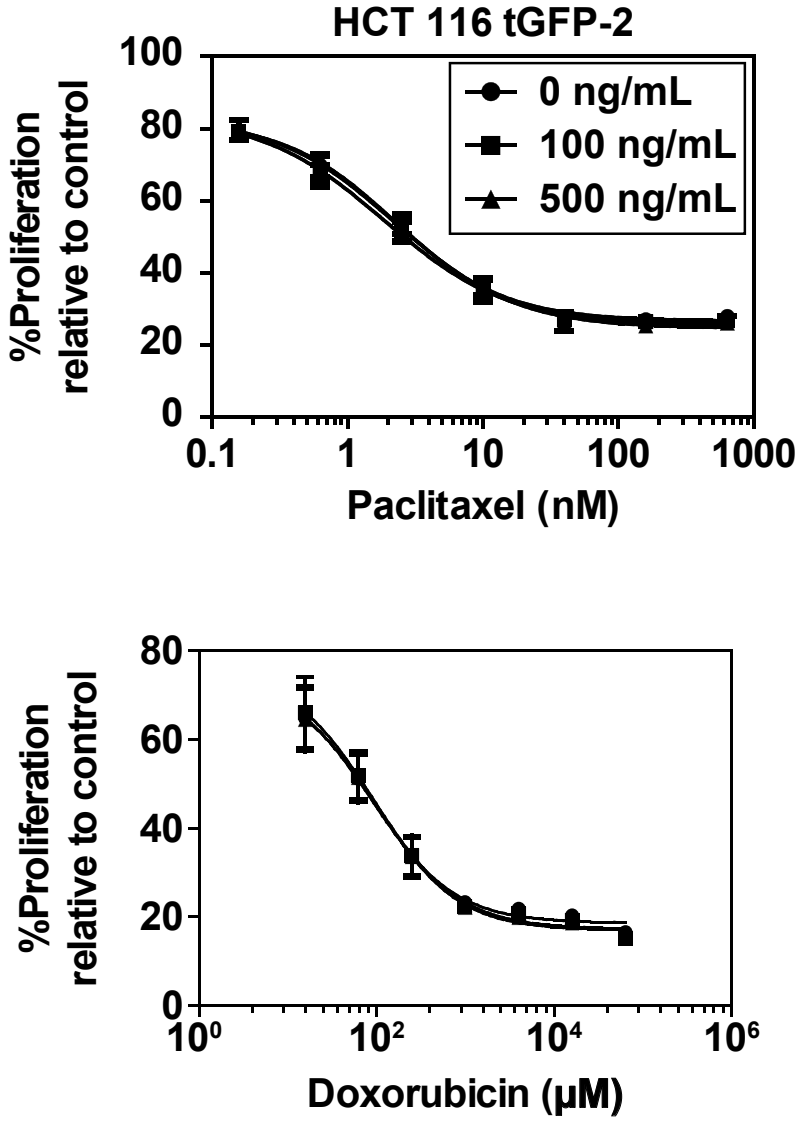
HCT 116 tGFP-2
0 ng/mL
100 ng/mL
500 ng/mL
%Proliferation relative to control
Paclitaxel (nM)
Doxorubicin (µM)

Figure 16: Uninduced RBM3 cells or GFP overexpressing cells show no significant resistance to either paclitaxel or ADM compared to parental controls. Hexoseaminidase assay following 72 hour induction with 100 or 500 ng/mL Dox followed by 48 hour treatment with ADM in GFP or RBM3 overexpressing cells. Error bars represent SEM. *P < 0.05, **P < 0.01, ***P < 0.001 for RBM3-1, † P < 0.05, ††P < 0.01, †††P < 0.001 for RBM3-4 (Student's t-test)

Figure 17

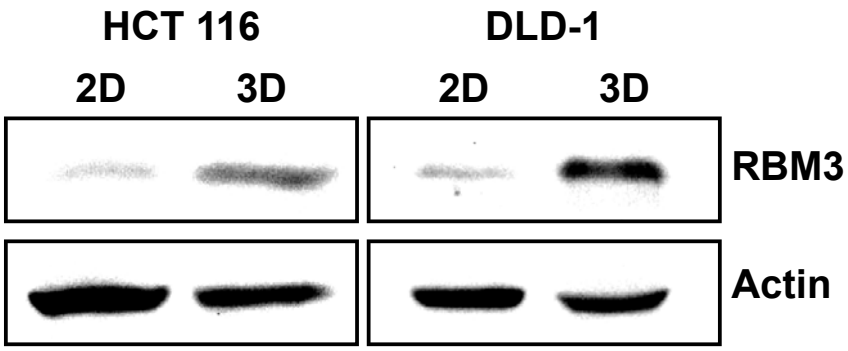

Figure 17: Spheroid formation induces RBM3 expression in DLD-1 and HCT 116 cells. Western blot analysis of RBM3 expression in monolayer culture of HCT 116 and DLD-1 cells compared to cells cultured in spheroid conditions for 14 days.

spheroid formation compared to vector or RBM3 uninduced controls (Figure 18). These data demonstrate that colorectal cancer cells increase RBM3 expression in the process of spheroid formation and that RBM3 is capable of enhancing spheroid formation capacity. Taken together, these data suggest that RBM3 overexpression enhances "stemness" in cancer cells.

To further validate the model of RBM3 induced colon CSCs, we next studied the expression of both DCLK1 and LGR5 both HCT 116 and DLD-1 cells. As previously described DCLK1 and LGR5 are important markers for both ISCs and CSCs (Barker et al., 2009; Barker et al., 2007; May et al., 2008; Nakanishi et al., 2013). Following maximal induction of RBM3 with 500 ng/mL Dox for 72 hours, we measured significant increases in the DCLK1+, LGR5+ and double positive populations in HCT 116 compared to uninduced control (Figure 19). Additionally, we measured increases in the LGR5+ and double positive populations with only a modest increase in DCLK1+ (P=.08) in DLD-1 cells compared to uninduced controls (Figure 20). We propose that the modest increase in DCLK1 expression in DLD-1 cells is due to DCLK1+ cells co-expressing LGR5 leading to most of the increase in DCLK1 expression being counted in the double positive population.

As an additional marker of the stem cell population, we next measured changes in the $CD44^{Hi}/CD24^{Lo}$ population. Previous studies have demonstrated that $CD44^{Hi}/CD24^{Lo}$ population of cells display characteristics of CSCs (Mani et al., 2008). Following RBM3 induction, HCT 116 Tet-RBM3 cells showed an increase in $CD44^{Hi}/CD24^{Lo}$ compared to uninduced controls (Figure 21). GFP vector controls showed no appreciable difference following Dox induction (Figure 22). Previous reports have also shown that RBM3 overexpression induces alternative splicing of CD44 increasing the tumor suppressing variant of CD44 (CD44s) while suppressing levels of the pro-oncogenic CD44 variants (CD44v) in prostate cancer cells (Zeng et al., 2013).

Figure 18

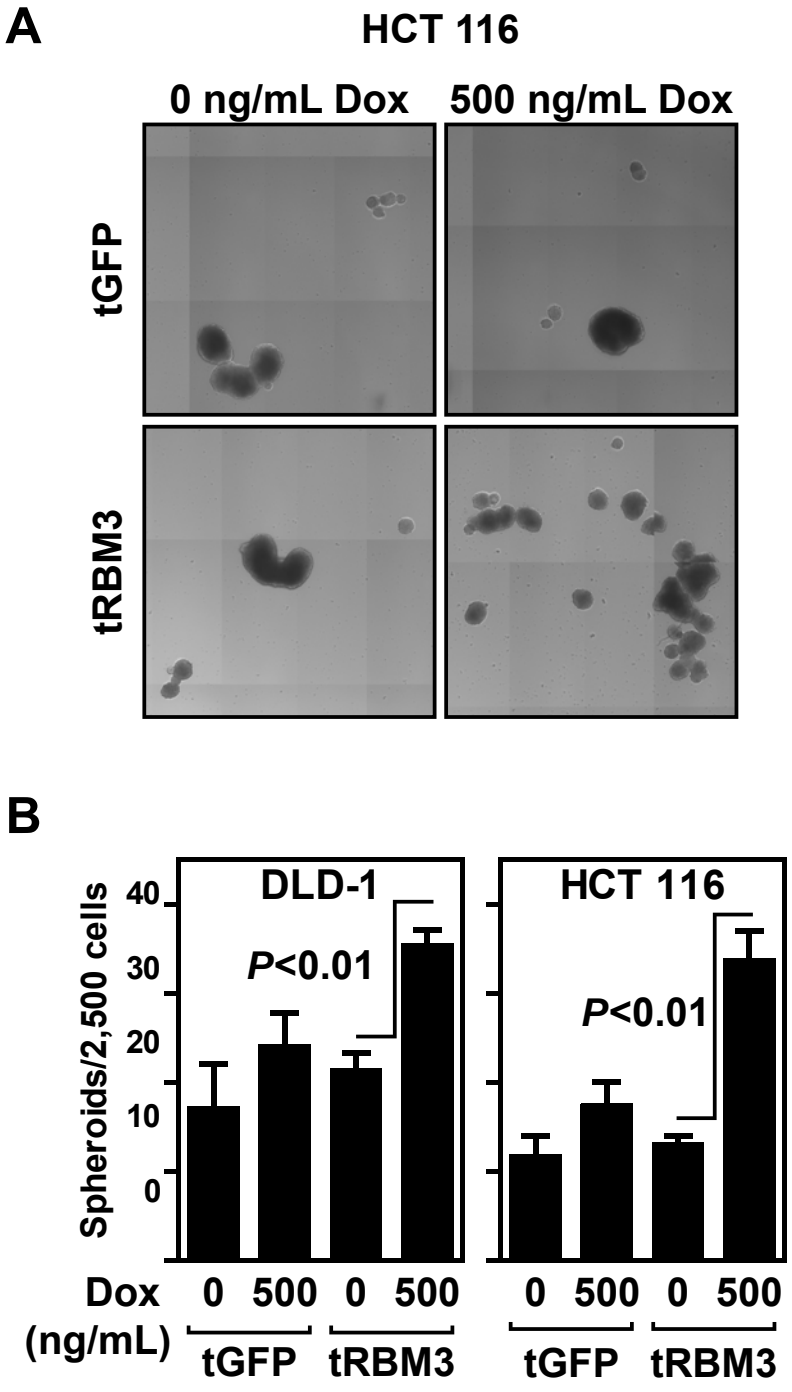
A
HCT 116
0 ng/mL Dox
500 ng/mL Dox
tGFP
tRBM3
B
DLD-1
HCT 116
P<0.01
P<0.01
Spheroids/2,500 cells
40
30
20
10
0
Dox (ng/mL)
0 500 0 500
0 500 0 500
tGFP tRBM3
tGFP tRBM3

Figure 18: RBM3 overexpression generates increased spheroid formation capacity in HCT 116 and DLD-1 cells. **(A)** Representative composite image of HCT 116 GFP or RBM3 inducible cells induced for 72 hours with 0 or 500 ng/mL of Dox then plated in ultra-low attachment plates with colonosphere media and allowed to form spheroids for 14 days. **(B)** Quantification of spheroid assay as performed by Celligo embryoid body counting system. Bar graph shows spheroid number from 2,500 seeded cells. Error bars represent SEM. P values shown are obtained with Student's t-test. *P < 0.05, **P < 0.01, ***P < 0.001 (Student's t-test).

Figure 19

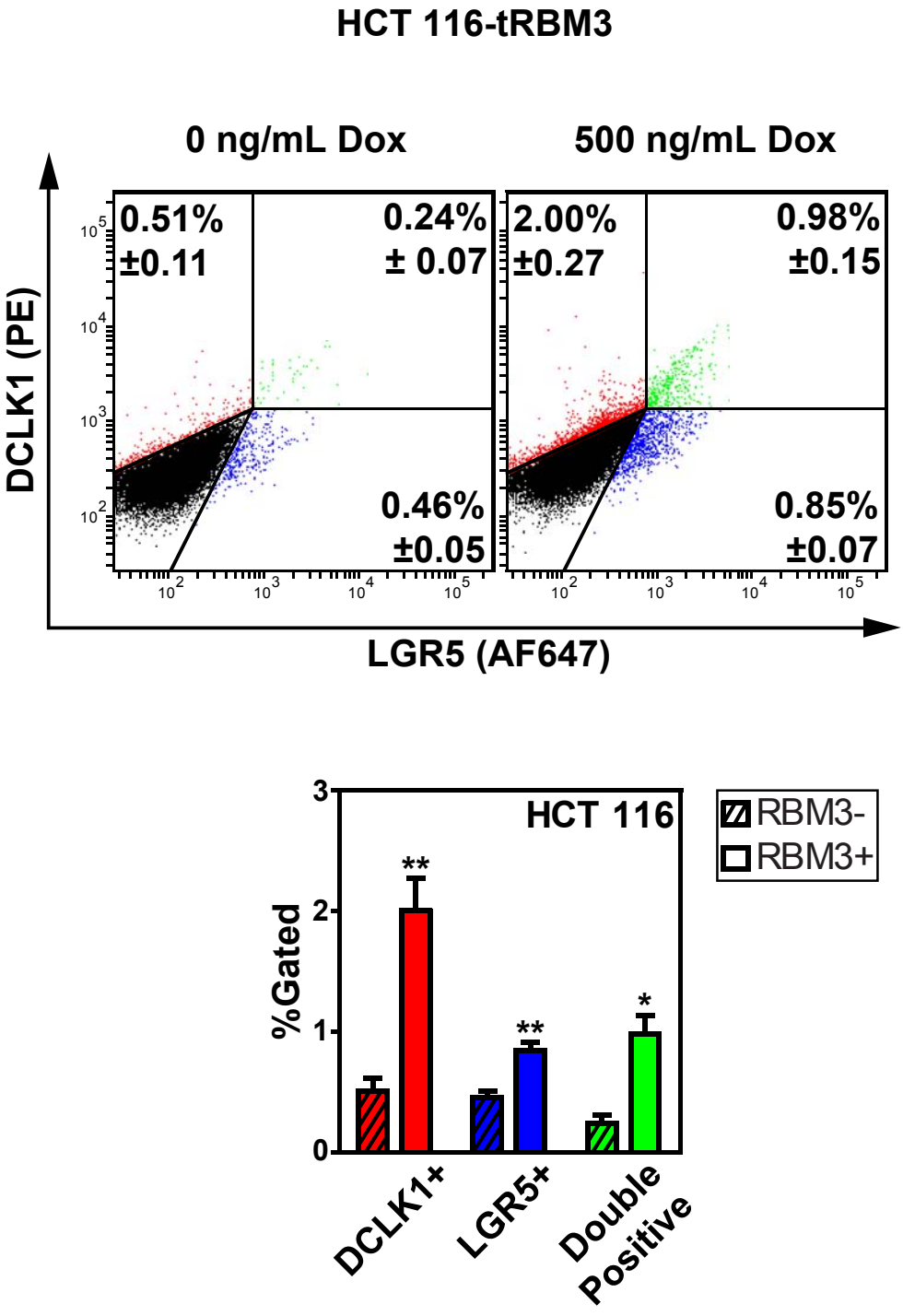
HCT 116-tRBM3
0 ng/mL Dox
500 ng/mL Dox
0.51%
±0.11
0.24%
± 0.07
0.46%
±0.05
2.00%
±0.27
0.98%
±0.15
0.85%
±0.07
DCLK1 (PE)
LGR5 (AF647)
HCT 116
RBM3-
RBM3+
%Gated
DCLK1+
LGR5+
Double Positive

Figure 19: RBM3 overexpression in HCT 116 cells increases the percentage of DCLK1+, LGR5+ and double positive cells. Representative flow cytometry dot plot of HCT 116-tRBM3 cells stained for DCLK1 (PE) and LGR5 (AF647) following induction with 500 ng/mL Dox for 72 hours. Bar graphs below represent percentage of DCLK1 positive, LGR5 positive and DCLK1+/LGR5+ double positive populations. Error bars represent SEM. P values shown are obtained with Student's *t*-test. *P < 0.05, **P < 0.01, ***P < 0.001 (Student's *t*-test).

Figure 20

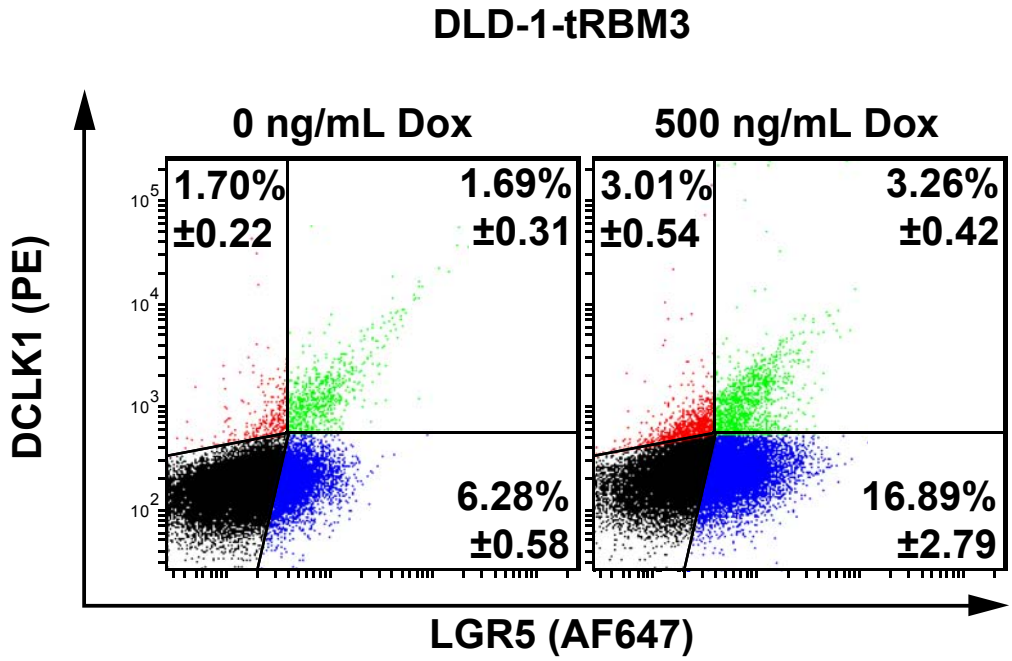
DLD-1-tRBM3
0 ng/mL Dox
500 ng/mL Dox
1.70%
±0.22
1.69%
±0.31
3.01%
±0.54
3.26%
±0.42
6.28%
±0.58
16.89%
±2.79
DCLK1 (PE)
LGR5 (AF647)

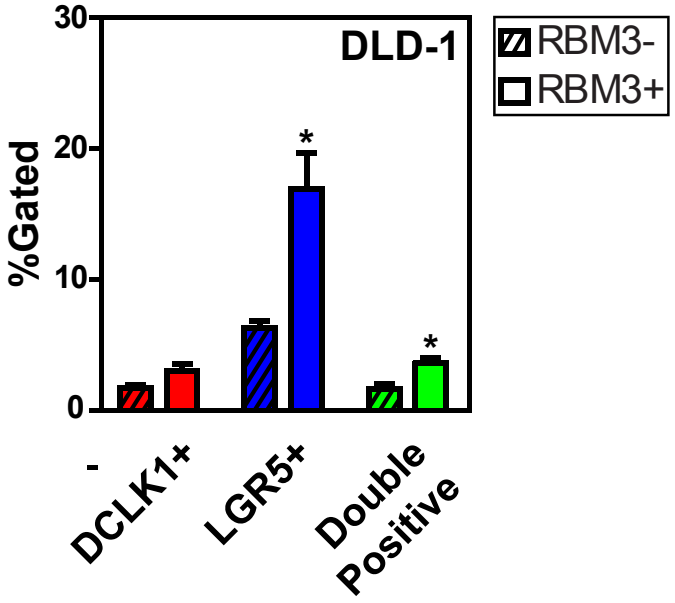
DLD-1
RBM3-
RBM3+
%Gated
30
20
10
0
*
*
-
DCLK1+
LGR5+
Double Positive

Figure 20: RBM3 overexpression in DLD-1 cells increases the percentage of LGR5+ and DCLK1/LGR5 double positive cells. Representative flow cytometry dot plot of DLD-1-tRBM3 cells stained for DCLK1 (PE) and LGR5 (AF647) following induction with 500 ng/mL Dox for 72 hours. Bar graphs below represent percentage of DCLK1 positive, LGR5 positive and DCLK1+/LGR5+ double positive populations. Error bars represent SEM. P values shown are obtained with Student's *t*-test. *P < 0.05, **P < 0.01, ***P < 0.001 (Student's *t*-test).

Figure 21

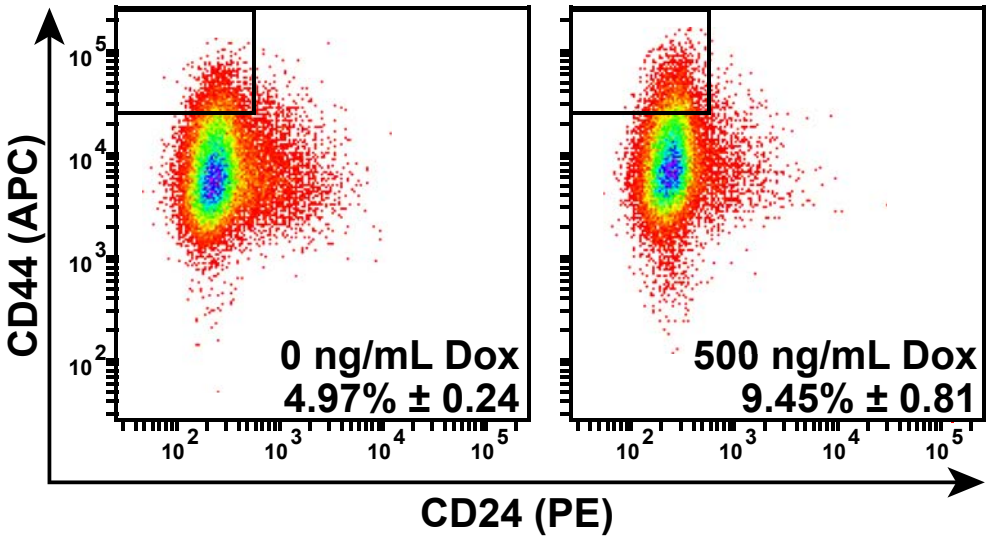
CD44 (APC)
CD24 (PE)
0 ng/mL Dox
4.97% ± 0.24
500 ng/mL Dox
9.45% ± 0.81

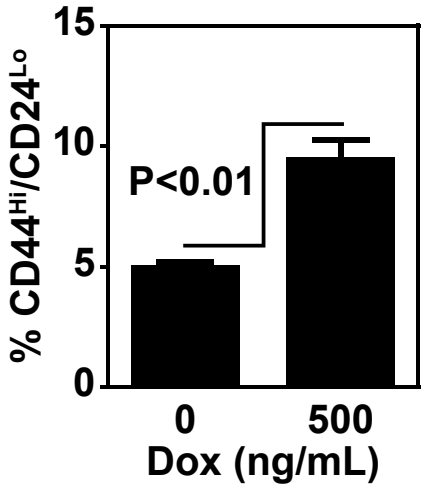
% CD44Hi/CD24Lo
P<0.01
Dox (ng/mL)

Figure 21: RBM3 overexpression in HCT 116 cells increases the percentage of $CD44^{Hi}/CD24^{Lo}$ cells. Representative flow cytometry dot plot of HCT 116-tRBM3 cells stained for CD24 (PE) and CD44 (APCF) following induction with 500 ng/mL Dox for 72 hours. Bar graphs below represent percentage of $CD44^{Hi}/CD24^{Lo}$ cells populations. Error bars represent SEM. P values shown are obtained with Student's *t*-test.

Figure 22

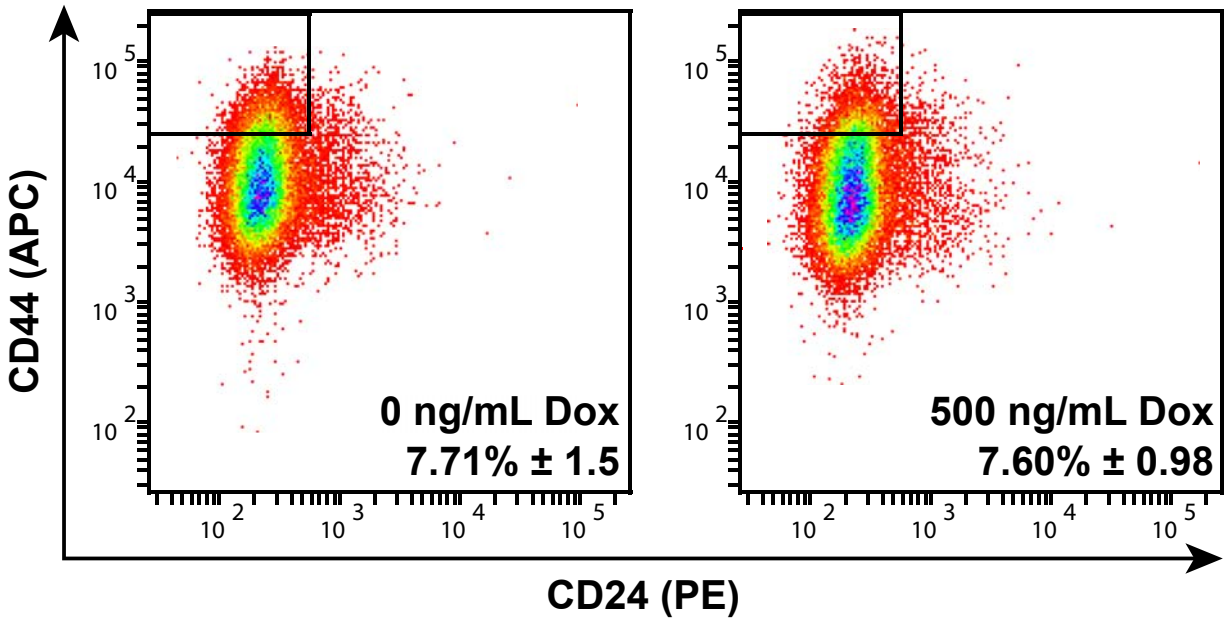
CD44 (APC)
CD24 (PE)
0 ng/mL Dox
7.71% ± 1.5
500 ng/mL Dox
7.60% ± 0.98

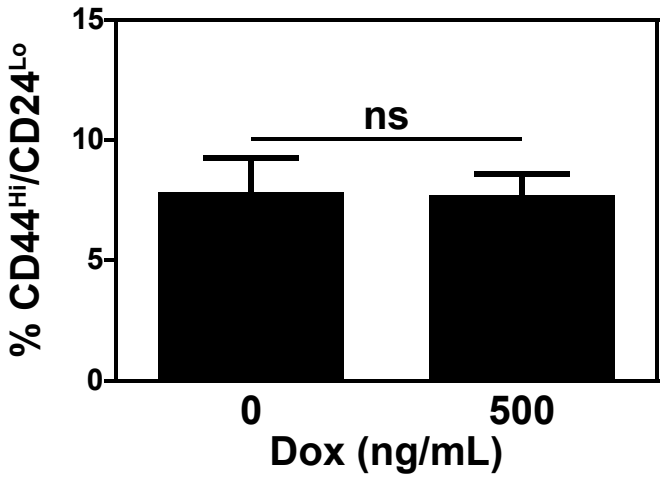
% CD44Hi/CD24Lo
ns
0
500
Dox (ng/mL)

Figure 22: GFP overexpression in HCT 116 cells generates no significant change in the percentage of $CD44^{Hi}/CD24^{Lo}$ cells. Representative flow cytometry dot plot of HCT 116-tGFP cells stained for CD24 (PE) and CD44 (APCF) following induction with 500 ng/mL Dox for 72 hours. Bar graphs below represent percentage of $CD44^{Hi}/CD24^{Lo}$ cells populations. Error bars represent SEM. P values shown are obtained with Student's *t*-test.

In HCT 116 Tet-RBM3 cells, RBM3 induction showed significant increases in both major isoforms of CD44 with no significant changes in GFP vector controls (Figure 23). This implicates RBM3 overexpression as inducing CD44 expression at the level of transcriptional changes. Additional studies are required to determine whether the $CD44^{Hi}/CD24^{Lo}$ also overexpress DCLK1 and LGR5. Also additional studies may also be necessary for validating the DCLK1 and LGR5 positive population correlate with the spheroid forming and SP cells. Nevertheless, taken together, these data provide evidence that RBM3 overexpression is capable of increasing the CSC population as measured by multiple methods.

Discussion

Following the characterization of the Dox inducible RBM3 induction, we observed that HCT 116 cells seemingly show less overall GFP fluorescence in GFP-RBM3 cells compared to GFP as read on a fluorimeter. This observation raises the possibilities that either RBM3 induction is less easily facilitated upon Dox treatment compared to GFP, RBM3 undergoes more rapid degradation than GFP resulting in lower steady-state levels or the focal localization of RBM3 results in less overall fluorescence read. Furthermore, it appears that RBM3 expression, as visualized by the GFP-RBM3 fusion protein, is not as previously described by antibody reactivity based localization (Jogi et al., 2009). This finding implies that there may be exogenous factors that affect the localization of RBM3 and thereby affects its overall cellular function. One previous study has shown that RBM3 can undergo alternative splicing to exclude a single exon from the open reading frame resulting in more cytoplasmic localization (Smart et al., 2007). As this inducible fusion protein has such well controlled dosage and time dependence with Dox, it

Figure 23

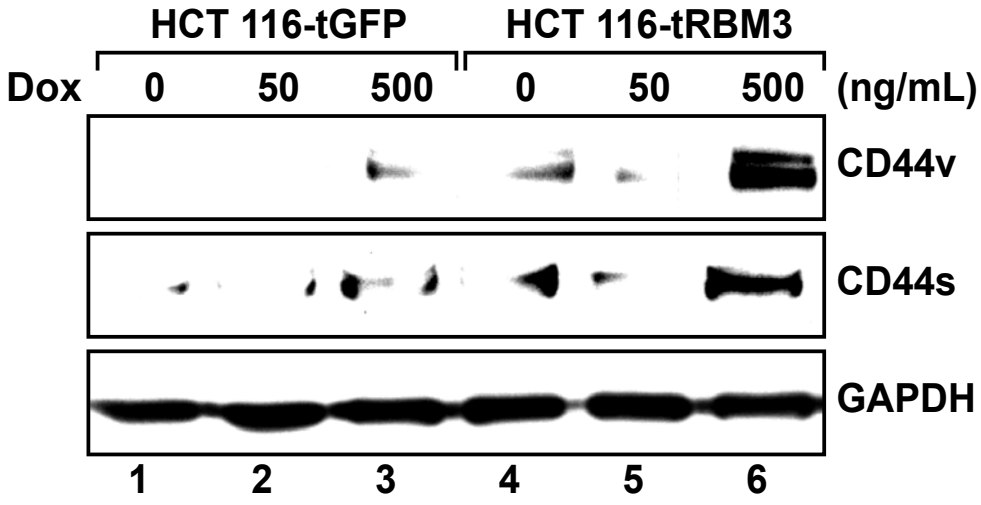
HCT 116-tGFP
HCT 116-tRBM3
Dox
0
50
500
0
50
500
(ng/mL)
CD44v
CD44s
GAPDH
1
2
3
4
5
6

Figure 23: RBM3 overexpression generates increases in both standard and variant isoforms of CD44 in HCT 116 cells. Western blot analysis for CD44 following 72 hours of induction with 500 ng/mL Dox in HCT 116-tGFP or HCT 116-tRBM3 cells.

may prove an ideal tool to pursue additional studies of RBM3 such as steady state levels, dose dependent pleiotropic effects and nuclear-cytoplasmic shuttling.

These studies also show numerous pieces of evidence implicating RBM3 as being capable of inducing stem cell characteristics in colon cancer cells. Previous studies have shown that RBM3 is upregulated within HSCs following treatment with GM-CSF; however, no evidence was presenting implicating RBM3 as the causative factor. Additionally, RBM3 has been previously demonstrated to confer resistance to classical chemotherapeutic agents cisplatin and ADM (Zeng et al., 2009). However, no clear mechanism was demonstrated regarding this chemoresistance. Our current study further confirms RBM3-induced chemoresistance to these agents and to paclitaxel. Our study also reveals a potential mechanism by which RBM3 is capable of increasing chemoresistance by inducing a SP of cells with high xenobiotic efflux capacity. It is interesting to note that while ADM and paclitaxel are both substrates of the ATP-binding cassette transporters, which are upregulated in the SP, cisplatin is not, but could be effluxed as a glutathione-cisplatin complex that may explain the fact that RBM3 knockdown sensitizes to cisplatin in prostate cancer (Ishikawa and Ali-Osman, 1993; Zeng et al., 2013).

It is also important to note that in all cases of quantification of stem cell induction, the DLD-1 cell line showed much higher endogenous stem cell activity. For example, SP assays demonstrated that DLD-1 cells show 4.5% SP cells compared to 0.08% in HCT 116. Spheroid formation for DLD-1 cells is approximately 14 spheres per 1,250 cells compared to approximately 10 spheres in HCT 116. Finally, DLD-1 cells showed higher populations of endogenous DCLK1+, LGR5+ and double positive populations. However, following RBM3 induction, the magnitude of difference was significantly higher in all three assays for HCT 116. It is possible that DLD-1 cells show higher endogenous stem cell signaling activity through some

mechanism inherent mutational status while HCT 116 cells lack that similar genotype. It is also possible that this mechanism is the route by which RBM3 induction causes "stemness" thereby generating rather large changes in HCT 116 cells following RBM3 induction compared to changes induced in DLD-1.

Furthermore, a significant question arises regarding stem cell marker expression in RBM3 overexpressing cells. It appears that RBM3 overexpression in both DLD-1 and HCT 116 induces an increase in the DCLK1/LGR5 double positive population. While previous studies have shown that DCLK1+ and LGR5+ cells occupy separate niches within normal intestinal epithelium, there is currently very little evidence investigating the co-expression of DCLK1 and LGR5 in colonic CSCs (Barker et al., 2007; May et al., 2008). Additionally, LGR5 expression has been shown to be driven primarily by Wnt/β-catenin signaling; however, no current studies have elucidated a regulatory factor promoting the expression of DCLK1 in the intestine. If RBM3 is inducing "stemness" correlated with DCLK1 expression, further studies of the RBM3 induced stem cell model may elucidate a signaling mechanism that regulates the expression of DCLK1 at the transcriptional level.

Here we propose a model where tumor formation and RBM3 expression are intertwined. Additionally, we show a potential mechanism through which RBM3 overexpression can lead to initiation of colorectal cancer through expansion of the stem cell compartment. Finally, while it is clear that RBM3 induction creates a significant increase in the stem cell population further studies are required to elucidate if the increased stem cell population arises through an increase in self-renewal of the existing stem cell population or through inducing an increase in plasticity of the proliferative progeny generating a de-differentiated cell.

Chapter III: RBM3 overexpression generates an increase in β-catenin signaling

Introduction

The β-catenin signaling cascade is one of the most critical factors driving the self-renewal of the ISC compartment in the intestinal epithelium (Korinek et al., 1998). Overactivation of β-catenin transcription is also the driving force for intestinal tumorigenesis and tumor progression in colorectal cancers. This is best exemplified by the fact that the majority of colorectal cancers contain an inactivating mutation of the APC tumor suppressor or activating mutations of β-catenin itself (Fearon and Vogelstein, 1990; Morin et al., 1997). These mutations lead to loss of appropriate regulation and overstabilization of β-catenin leading to increased nuclear β-catenin accumulation and subsequently transcription of genes that drive various programs resulting in increased proliferation and multidrug resistance (Flahaut et al., 2009; Noda et al., 2009; Reya and Clevers, 2005). While the majority of cancers show dysregulation of β-catenin signaling, there is heterogeneity in the level of nuclear β-catenin implying intratumoral variation in β-catenin transcriptional activity. It is theorized that the pleotropic effects of β-catenin signaling can be related to the fact that β-catenin activated transcriptional programs show dosage dependence to nuclear β-catenin (Gaspar and Fodde, 2004). As many of the clinically relevant characteristics of colorectal cancers are so heavily dependent upon β-catenin signaling, it becomes important to identify novel factors that modulate the activity of this pathway.

Our previous studies have revealed a role for RBM3 in inducing the stem cell phenotype within colorectal cancers. In order to elucidate a molecular signaling pathway for the RBM3 induced stem cell phenotype, here we investigate the β-catenin signaling pathway following RBM3 overexpression. We focused our studies on the Wnt/β-catenin pathway because both CD44 and LGR5 have been identified as β-catenin transcriptional targets (Barker et al., 2007; Kanwar et al., 2010; Wielenga et al., 1999). Moreover, β-catenin signaling activity has been shown to be

essential for SP cells and spheroid formation (Chikazawa et al., 2010; Kanwar et al., 2010). We demonstrate that RBM3 is capable of increasing the levels of nuclear β-catenin correlating with an overall increase in β-catenin transcriptional activity. Additionally, we show that RBM3 induction also increases AKT activity to inhibit the activity of the destruction complex member, GSK3β. We also show that this decreased GSK3β activity is correlated with a decrease in phosphorylation in β-catenin activity following RBM3 overexpression. Additionally, pharmacologic inhibition of GSK3β using BIO phenocopies the RBM3 induced β-catenin signaling phenotype. We demonstrate that RBM3 is a novel factor for the induction of the β-catenin signaling cascade in colorectal cancer cells which implies a mechanism for the RBM3 induced stem cell phenotype.

Materials and Methods

Cell culture

HCT 116 and DLD-1 cell lines were obtained from ATCC and cultured under conditions of 5% CO_2 in DMEM (Corning) containing 10% FBS (Sigma-Aldrich) and 1% antibiotic/antimycotic solution (Corning). Following transduction of viruses cells were continually cultured in 1 mg/mL G 418 (Santa Cruz Biotechnology) and/or 1μg/mL puromycin (Life Technologies) as relevant.

Lentivirus propagation and infection

DLD-1 and HCT 116 tGFP and tRBM3 cells were generated as described in Chapter II. Additionally, DLD-1 and HCT 116 CMV-Gus and CMV-RBM3 plasmids were generated using the Gateway cloning system according to manufacturer recommendations (Life Technologies). The plasmids were recombined into lentiviral overexpression plasmids obtained from Addgene (Campeau et al., 2009).

Lenti-X cells were obtained from Dr. Roy Jensen and were used to generate virus. Lenti-X cells were transfected with 7.5 μg of each of the pGIPZ packaging plasmids obtained from Dr. Roy Jensen as well as 24 μg of the cargo vector using Lipofectamine 2000 (Life Technologies). Viral supernatant was collected at 48, 72 and 96 hours following lipofectamine transfection, pooled, clarified through a 0.45 μm syringe filter and concentrated using the Lenti-X concentrator (ClonTech Laboratories, Inc.).

HCT 116 and DLD-1 cells were transduced in suspension with 4 μg/mL polybrene (Sigma Aldrich). 24 hours following transduction, fresh media was added and following 48 hours of transduction puromycin selection media was added. Parental cells were cultured alongside transduced cells for 1 week under similar selection antibiotics to ensure that no untransduced cells survived following the 1 week of selection under gross inspection by microscopy.

Western blotting

Western blot were performed using poly-acrylamide gel electrophoresis within a Miniprotean Tetracell apparatus (BioRad) followed by blotting onto 0.45 μm pore size Immobilon polyvinyl difluoride membrane (Millipore) using a mini Transblot module (BioRad). Antibodies for RBM3 were obtained from AbCam (AbCam) or custom generated through Fisher (Thermo Fisher

Scientific). Antibodies for β-catenin and phospho-β-catenin were obtained from Cell Signaling (Cell Signaling Technology) or BD Biosciences (BD Biosciences). Antibodies for GSK3β and phospho-GSK3β were obtained from Cell Signaling (Cell Signaling Technology).

Nuclear fractionation

Nuclear cytoplasmic extraction was generated through NE-PER kit (Thermo Fisher Scientific, Rockford, IL, USA) according to manufacturer recommendations. GAPDH antibody (Cell Signaling Technology) was used for cytoplasmic loading control and Lamin A/C antibody (Cell Signaling Technology) was used for nuclear loading control. Both loading controls were evaluated for each fraction to validate minimal cross-contamination of each compartment.

Immunofluorescence and immunohistochemistry

For immunofluorescence (IF), cells were plated on sterile glass cover slips with appropriate treatments. Cells were then fixed using neutral buffered formalin then permeablized using 0.1% Triton. Antigen blocking was achieved using 1% bovine serum albumin in PBS. Cells were incubated with primary antibody overnight at 4°C followed by staining with fluorophore conjugated secondary antibody for 1 hour at room temperature. Coverslips were mounted using Prolong Gold with DAPI (Life Technologies, Grand Island, NY, USA). For IHC, spheroids were embedded in paraffin blocks and slides were obtained with 5μm sections. Slides were deparaffinized then boiled for 20 minutes in antigen retrieval buffer (10 mM sodium citrate, pH 6, 0.05% Tween-20) followed by peroxidase quenching using Peroxabolish (Biocare Medical,

Concord, CA, USA). Slides were then stained using Histostain SP kit (Life Technologies) as per manufacturer recommendations. Antibodies used were the same as those used for western blots.

Wound healing assay

Cells were plated and allowed to reach confluency so that Dox induction was present for the indicated amount of time. Confluent cells were scratched and images were taken. Images were taken at the same spot at each indicated time point for each sample. Images were processed by ImageJ software (National Institutes of Health) to quantify number of total pixels in the wound area. Migration at each time point was calculated as the difference in the number of pixels of wound area at time 0 to the number of pixels at that time point.

Real time RT-PCR

Total cellular RNA was isolated using TRIzol reagent followed by reverse transcription using SuperScript II in the presence of random hexonucleotide primers (Life Technologies, Grand Island, NY, USA). cDNA was then analyzed by real-time RT-PCR using Jumpstart Taq polymerase (Sigma Aldrich, St. Louis, MO, USA) and SYBR Green nucleic acid stain (Life Technologies, Grand Island, NY, USA). Threshold crossing values for each gene were normalized to GAPDH gene expression. mRNA expression was then normalized to fold change relative to uninduced controls. Primers used in this study are as follows:

CD44: 5'- AACAGTCCTGTGACTCAACTCAAG-3' / 5'-
TTAGAGACATGGGACAAATGCCAC-3'

c-MYC: 5’-CACACATCAGCACAACTACGCA-3’ / 5’-TTGACCCTCTTGGCAGCAG-3’

GAPDH: 5’-CAGCCTCAAGATCATCAGCA-3’ / 5’-GTCTTCTGGGTGGCAGTGAT-3’

LGR5: 5’-TGGCACCCGCTATGTCCAG -3’ / 5’-GTAGCAGGGATTCTGTCTG -3’

TOPFlash assay

TOPFlash and FOPFlash β-catenin luciferase reporter plasmids were generously provided by Dr. Shahid Umar. Cells were plated in 24 well plates in antibiotic/antimycotic free medium and without selection antibiotics. Each well was transfected using 2 μL of Lipofectamine 2000 (Life Technologies) complexed with 900 ng of TOPFlash luciferase plasmid and 100 ng of CMV renilla luciferase plasmid. 8 hours following transfection, the media was replaced with normal growth medium containing selection antibiotics and appropriate treatments. Luciferase activity was then read using the dual-luciferase reporter assay system (Promega, Madison, WI, USA) on a plate reader. TOPFlash luciferase activity was normalized to CMV renilla luciferase activity.

siRNA transfection

siRNA for CTNNB1 (siCTNNB1) and scrambled siRNA (siSCR) were purchased from Life Technologies. Cells were plated in 6-well plates and allowed to adhere overnight. Cells were then transfected with either siCTNNB1 or siSCR using Lipofectamine RNAiMAX (Life Technologies) according to manufacturer specifications. 25 pmol of siRNA was added per well. Cells were treated with appropriate concentrations of Dox and were assayed 72 hours following transfection.

SP assay

SP assay was performed as previously described with minor modifications (Mathew et al., 2009). In brief, cells were plated at 100,000 cells/mL into 6 well plates with relevant treatments. Following 72 hours of treatment cells were trypsinized and resuspended at 1 million cells/mL in DMEM and pre-warmed for 15 minutes at 37°C. Cells were then given 50 μM verapamil (Sigma Aldrich), as a pan efflux inhibitor, or vehicle for 30 minutes. Cells were then incubated with 10 μM Vybrant DyeCycle Violet (DCV) (Life Technologies) for 90 minutes at 37°C. Cells were then resuspended in ice cold SP buffer containing 2% FBS, 2 mM HEPES, 1 μg/mL 7-amino actinomycin D (7AAD) (Life Technologies) in Hank's balanced salt solution and analyzed on a BD LSR II for SP. DCV was excited using a violet diode laser (408 nm) and emission was measured with a 450/50 nm bandpass filter (DCV Blue) and 630 nm longpass, 660/40 nm bandpass filter (DCV Red). Viability gating was established with 7AAD with excitation at 552 nm and emission monitored with a 630 nm longpass, 660/40 nm bandpass filter. Cells were initially gated for appropriate size using the side scatter (SSC) and forward scatter (FSC). Cells were then gated for viability using 7-AAD uptake to eliminate non-viable cells. Finally, the location of the SP gate was established using the verapamil treated sample.

Stem cell marker flow cytometry

Cells were treated with Dox to induce expression of GFP or RBM3 for 72 hours. Cells were then trypsinized then resuspended at $1x10^6$ cells. For DCLK1 and LGR5, cells were stained with Alexafluor 647 (AF647) conjugated LGR5 antibody (BD Biosciences) or PE conjugated DCLK1 antibody (AbCam) according to manufacturer recommendations. PE conjugation was performed

using the Zenon PE labelling kit (Life Technologies) according to manufacturer recommendations.

Treatments

(2'Z,3'E)-6-Bromoindirubin-3′-oxime (BIO) and N-[N-(3,5-Difluorophenacetyl)-L-alanyl]-S-phenylglycine t-butyl ester (DAPT) were purchased from Sigma-Aldrich. N-[2-(Cyclohexyloxy)-4-nitrophenyl]methanesulfonamide (NS-398) was generously donated by Dr. Dan Dixon.

Results

We initiated these studies by examining levels of total and nuclear β-catenin in RBM3 overexpressing cells. Following RBM3 induction in DLD-1 and HCT 116 cells, a moderate increase in total β-catenin levels was observed after 72 hours of 500 ng/mL Dox induction (Figure 1). Interestingly, analysis of multiple clones constitutively overexpressing RBM3 in HCT 116 and DLD-1 cells showed a more prominent increase in total β-catenin (4.12-fold vs 1.60-fold increase in HCT 116 and 2.05-fold vs 1.44-fold in DLD-1) compared to inducible RBM3 expression (Figure 2). One possibility to account for this comparative increase is that the time frame of RBM3 overexpression lends to a more prominent induction of β-catenin levels. However, as most previous studies have been carried out in RBM3 inducible heterogeneous populations, we chose to continue these studies in the same cell lines to maintain consistency.

As β-catenin transcriptional activity depends upon its localization to the nucleus, we next examined changes in β-catenin levels in the cytoplasm and nucleus following 72 hour Dox

Figure 1

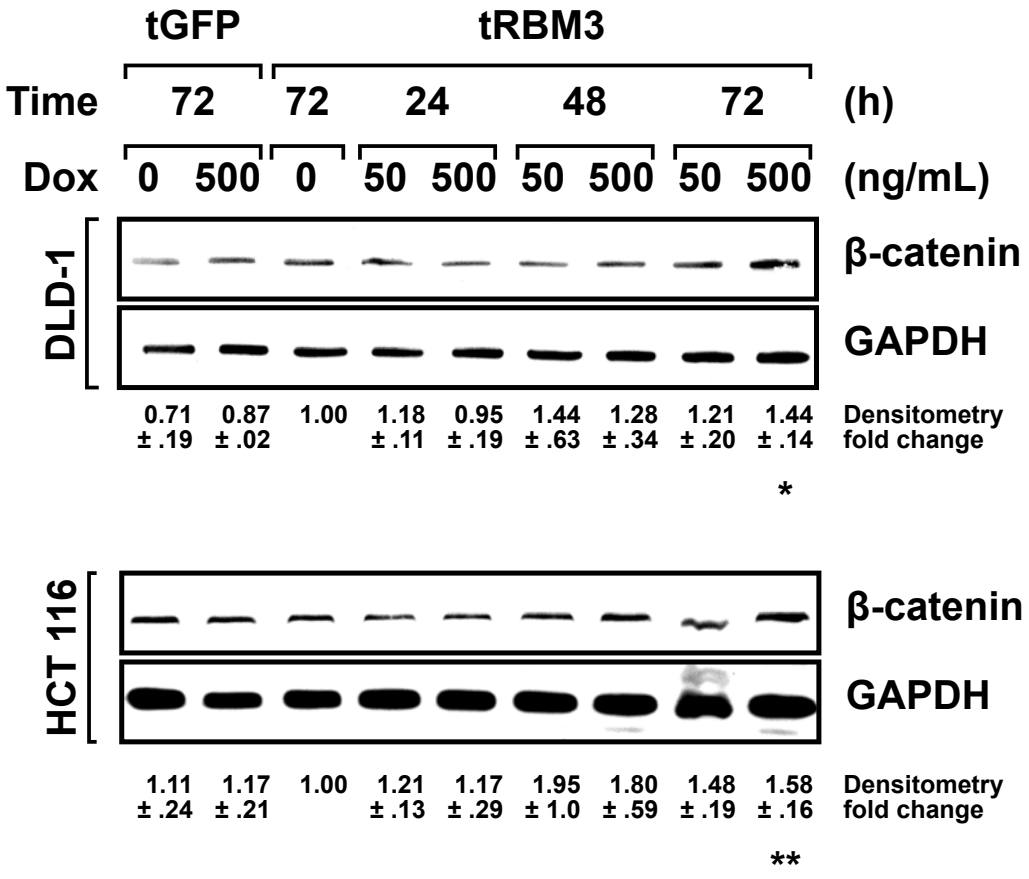
tGFP
tRBM3
Time
72
72
24
48
72
(h)
Dox
0
500
0
50
500
50
500
50
500
(ng/mL)
DLD-1
β-catenin
GAPDH
0.71 ± .19
0.87 ± .02
1.00
1.18 ± .11
0.95 ± .19
1.44 ± .63
1.28 ± .34
1.21 ± .20
1.44 ± .14
Densitometry fold change
*
HCT 116
β-catenin
GAPDH
1.11 ± .24
1.17 ± .21
1.00
1.21 ± .13
1.17 ± .29
1.95 ± 1.0
1.80 ± .59
1.48 ± .19
1.58 ± .16
Densitometry fold change
**

Figure 1: DLD-1 and HCT 116-tRBM3 cells show increases in total β-catenin following RBM3 induction. Western blot analysis of β-catenin in DLD-1 and HCT 116 tGFP or tRBM3 cells with indicated concentrations of and times of Dox induction. β-catenin levels show significant elevation at 500 ng/mL Dox for 72 hours. Densitometry represents fold change of total β-catenin relative to uninduced tRBM3 cells normalized to GAPDH. Error represents SEM. *P < 0.05, **P < 0.01, ***P < 0.001 (Student's *t*-test).

Figure 2

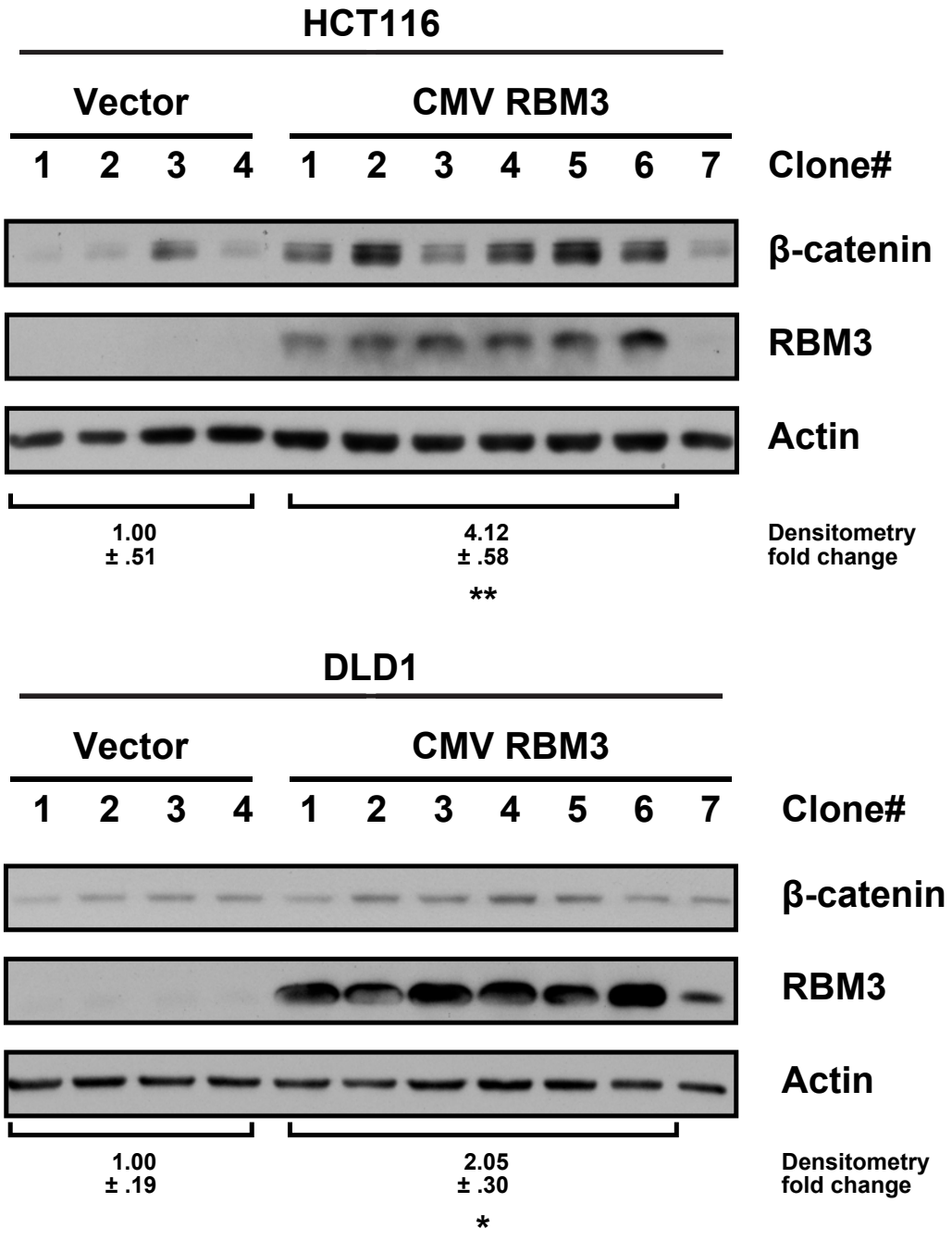
HCT116
Vector
CMV RBM3
1 2 3 4 1 2 3 4 5 6 7
Clone#
β-catenin
RBM3
Actin
1.00
± .51
4.12
± .58
**
Densitometry
fold change
DLD1
Vector
CMV RBM3
1 2 3 4 1 2 3 4 5 6 7
Clone#
β-catenin
RBM3
Actin
1.00
± .19
2.05
± .30
*
Densitometry
fold change

Figure 2: Constitutive RBM3 overexpression significantly increases β-catenin levels. Western blot analysis of β-catenin in DLD-1 and HCT 116 CMV-RBM3 cells or vector control following clonal selection. HCT 116 CMV-RBM3 and DLD-1 CMV-RBM3 clones show significant upregulation of total β-catenin following RBM3 overexpression for greater than one week. Densitometry represents fold change of total β-catenin relative to vector control group normalized to Actin. Error represents SEM. *P < 0.05, **P < 0.01, ***P < 0.001 (Student's *t*-test).

induction. RBM3 overexpression did not significantly affect cytoplasmic levels of β-catenin (Figure 3). However, nuclear levels of β-catenin were increased upon RBM3 overexpression in both DLD-1 and HCT 116 compared to uninduced or vector controls (Figure 3). Interestingly, levels of nuclear β-catenin were elevated in uninduced RBM3 cells compared to uninduced GFP vector control implying that due to the slight leakiness of the Tet-ON system, the mild induction of RBM3 may also elevate nuclear β-catenin. Additionally, IF labeling revealed nuclear accumulation of β-catenin in RBM3 overexpressing cells, while membrane localization of β-catenin showed no significant difference (Figure 4). This effect was further replicated with IHC of spheroids (Figure 5). Here we also note that observed localization of GFP-RBM3 is similar to RBM3 alone and that this was not an effect of the GFP tag on RBM3. IF staining of RBM3 in tRBM3 cells confirms that untagged RBM3 also primarily localizes at the nucleolus in DLD-1 and HCT 116 cells.

Since increased nuclear β-catenin is associated with loss of E-cadherin and EMT, we also determined whether RBM3 overexpression induces a similar change in colon cancer cells (Brabletz et al., 1998; van der Wurff et al., 1997). Our initial induction of RBM3 for 72 hours showed no significant changes in EMT as measured by wound healing. As other studies suggest that the molecular programming to induce EMT could take up to 2 weeks, we decided to continually induce RBM3 for a similar time period and measure wound healing capacity (Mani et al., 2008). We observed significant increases in wound healing following 12 days of Dox induction; however, no significant differences were observed at 9 days or less of Dox induction (Figure 6). This also raises the possibility that many phenotypic effects exerted by RBM3 could require extended periods of expression to see an effect. This is similarly validated by the

Figure 3

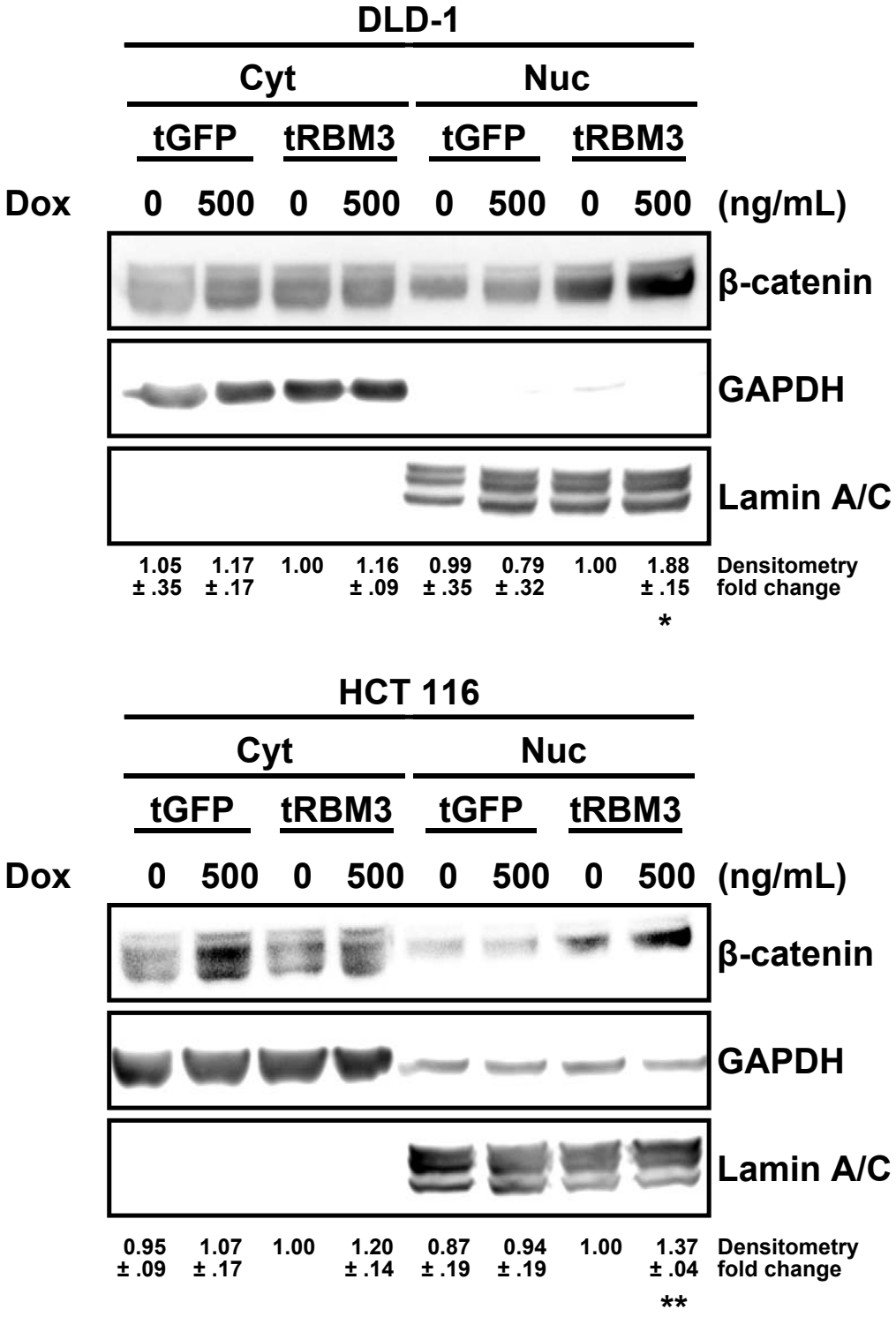
DLD-1
Cyt
Nuc
tGFP
tRBM3
tGFP
tRBM3
Dox
0 500 0 500 0 500 0 500 (ng/mL)
β-catenin
GAPDH
Lamin A/C
1.05 ± .35
1.17 ± .17
1.00
1.16 ± .09
0.99 ± .35
0.79 ± .32
1.00
1.88 ± .15
Densitometry fold change
*
HCT 116
Cyt
Nuc
tGFP
tRBM3
tGFP
tRBM3
Dox
0 500 0 500 0 500 0 500 (ng/mL)
β-catenin
GAPDH
Lamin A/C
0.95 ± .09
1.07 ± .17
1.00
1.20 ± .14
0.87 ± .19
0.94 ± .19
1.00
1.37 ± .04
Densitometry fold change
**

Figure 3: RBM3 overexpression significantly increases levels of nuclear β-catenin. Western blot analysis of nuclear and cytoplasmic extracts of HCT 116 and DLD-1 tGFP and tRBM3 cells. GAPDH and Lamin A/C are used as a loading controls for the cytoplasmic and nuclear fractions, respectively. β-catenin was primarily increased in the nuclear fraction upon RBM3 overexpression using 500 ng/mL Dox for 72 hours. Densitometry represents fold change of β-catenin relative to uninduced tRBM3 cells normalized to GAPDH for cytoplasmic extracts and Lamin A/C for nuclear extracts. Error represents SEM. *P < 0.05, **P < 0.01, ***P < 0.001 (Student's *t*-test).

Figure 4

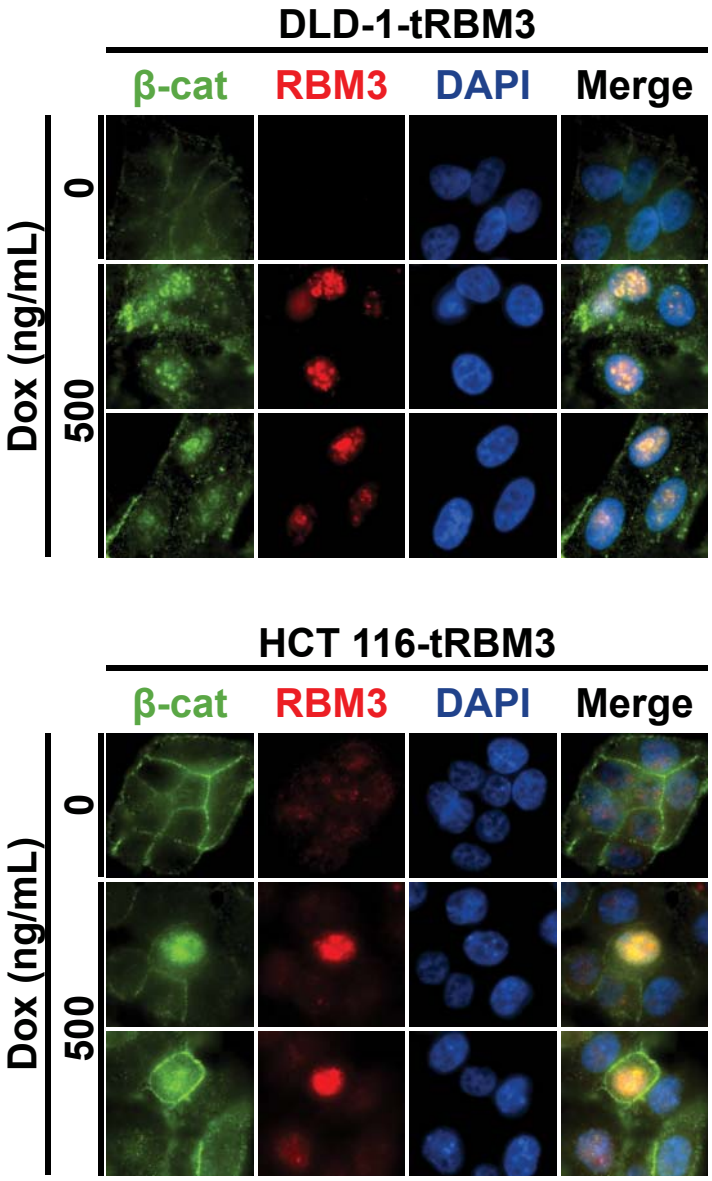
DLD-1-tRBM3
β-cat
RBM3
DAPI
Merge
Dox (ng/mL)
0
500
HCT 116-tRBM3
β-cat
RBM3
DAPI
Merge
Dox (ng/mL)
0
500

Figure 4: Cells with high levels of RBM3 show increased nuclear localization of β-catenin. Immunofluorescent microscopy of DLD-1 and HCT 116 tRBM3 cells following 72 hours of induction with indicated concentrations of Dox. Cells with high RBM3 also appear to contain increased levels of nuclear β-catenin. Regardless of RBM3 expression, levels of membrane associated β-catenin appear unchanged.

Figure 5

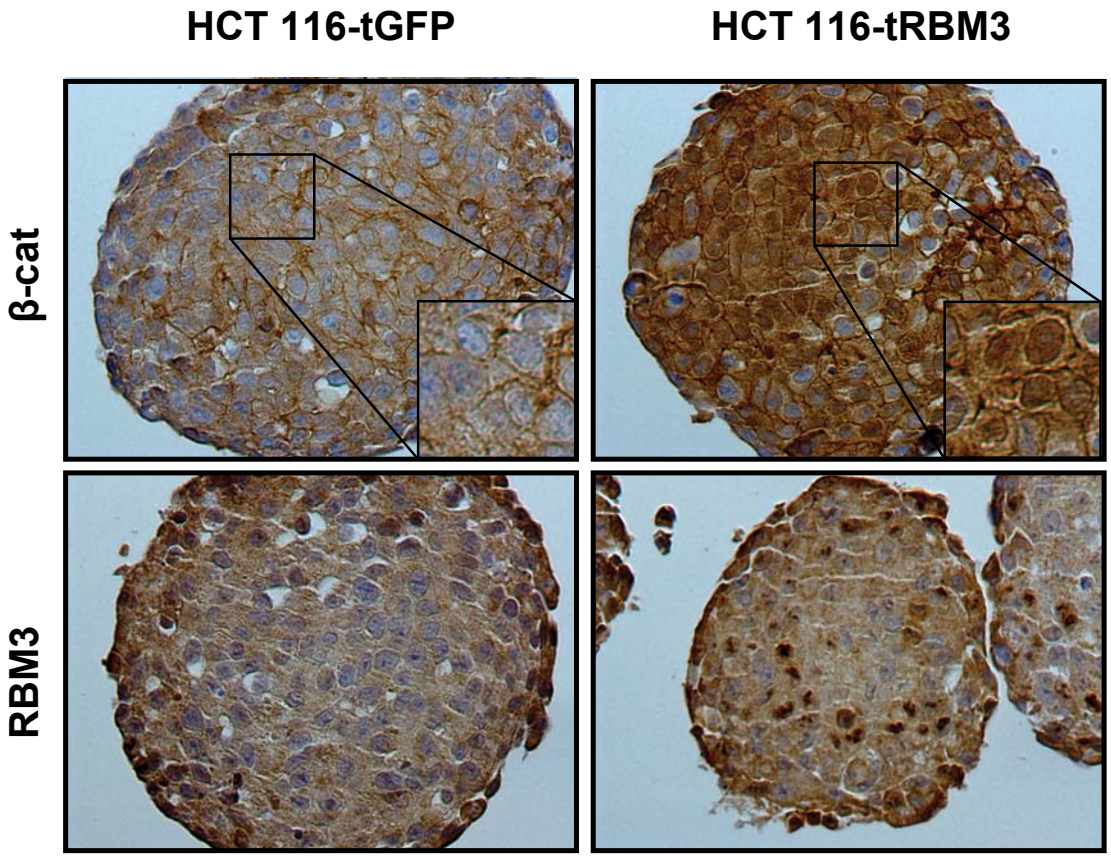

Figure 5: RBM3 overexpression enhances β-catenin nuclear localization in spheroids. IHC of β-catenin and RBM3 in HCT 116 tGFP or tRBM3 spheroids. Spheroids were grown for 14 days with 500 ng/mL Dox to induce GFP or RBM3 overexpression, then fixed and sectioned.

Figure 6

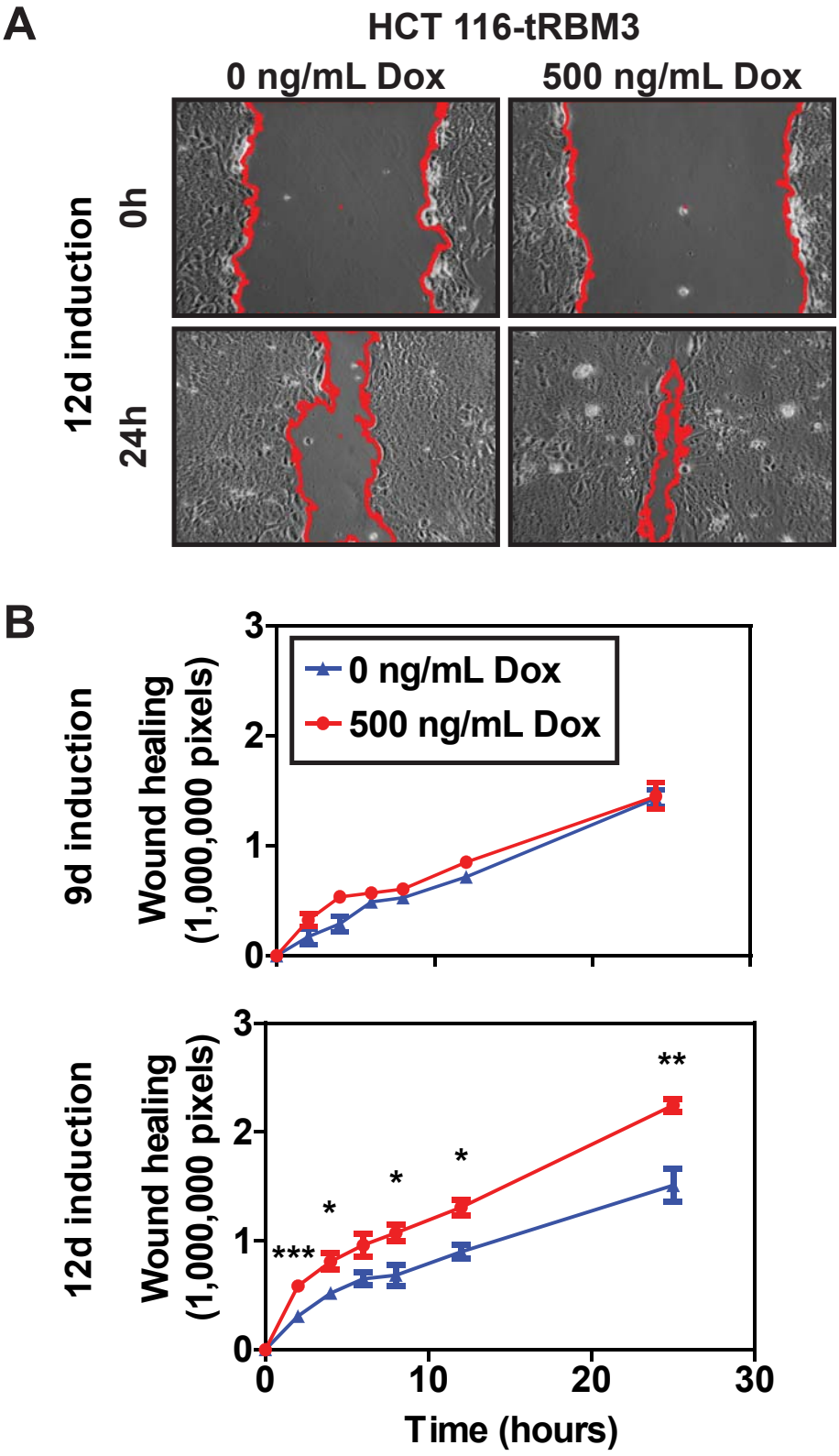
A
HCT 116-tRBM3
0 ng/mL Dox
500 ng/mL Dox
12d induction
0h
24h
B
9d induction
Wound healing (1,000,000 pixels)
0 ng/mL Dox
500 ng/mL Dox
12d induction
Wound healing (1,000,000 pixels)
***
*
*
*
**
Time (hours)

Figure 6: RBM3 overexpression generates increases in wound healing. **(A)** Cells were treated with indicated concentration of Dox for 10 days. Cells were then plated into 6 well plates with indicated concentrations of Dox and reached confluency at 12 days. Figure representsphase contrast microscopy of wound healing at 0 hours and 24 hours following after creation of wound. Red outline represents wound area in pixels as calculated by ImageJ software. **(B)** Line graph of time dependent wound healing following 500 ng/mL induction with Dox for indicated time. Wound healing is calculated as difference in number of pixels of wound at time compared to 0 hours. Error bars show SEM. *P < 0.05, **P < 0.01, ***P < 0.001 (Student's *t*-test).

observation that RBM3 overexpression for multiple weeks using constitutive overexpression generates much higher increases in β-catenin levels (Figure 2).

To validate that the increase in nuclear β-catenin levels correlates with increased transcriptional activity, we examined TOPFlash luciferase assay. The TOPFlash reporter plasmid encodes multiple copies of the TCF-1 consensus sequence driving a firefly luciferase gene and is a widely used reporter of β-catenin/TCF transcriptional activity (Korinek et al., 1997; van de Wetering et al., 1991). Following 48 hour RBM3 induction, TOPFlash luciferase activity, normalized to CMV/Renilla luciferase was significantly increased in both cell lines (Figure 7). Further confirmation of increased β-catenin transcriptional activity was observed through elevated levels of its target genes *c-MYC*, *LGR5* and *CD44* as well as c-MYC protein. (Barker et al., 2007; He et al., 1998; Wielenga et al., 1999) (Figure 8).

We have previously shown that RBM3 overexpression increases SP fraction and LGR5+ cells in HCT 116-tRBM3 and DLD-1-tRBM3 cells (Chapter 2, Figures 8, 9, 19 & 20). Furthermore, previous studies have shown that LGR5 expression and the SP fraction are dependent on β-catenin signaling (Barker et al., 2007; Chikazawa et al., 2010). Accordingly, we next wanted to investigate the dependence of RBM3 induced stem cell characteristics on β-catenin transcriptional activity. We first validated that siRNA to *CTNNB1* (siCTNNB1) would reliably decrease β-catenin expression (Figure 9). Next we measured changes in the percentage of LGR5+ and DCLK1+ in DLD-1-tRBM3 cells in the context of RBM3 overexpression and β-catenin knockdown. We observe that scrambled siRNA (siSCR) appears to have no effect on RBM3 induced LGR5 expression (Figure 10). However, following knockdown of β-catenin we observe an abrogation of the LGR5+ population which cannot be rescued with RBM3 overexpression (Figure 10). siCTNNB1 shows a similar effect on the SP fraction which also

Figure 7

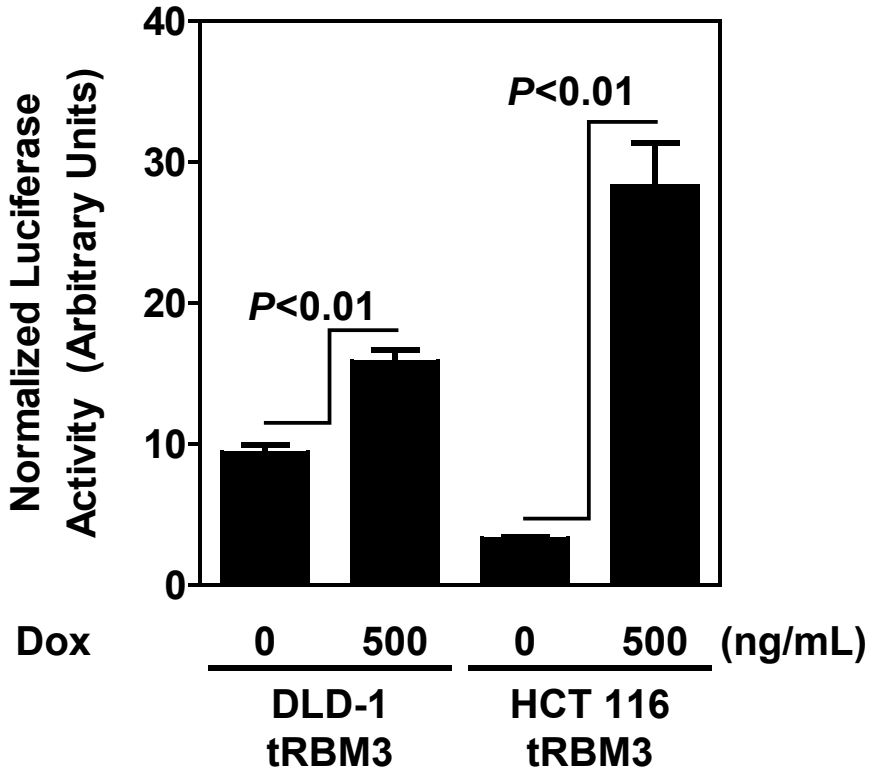
Normalized Luciferase Activity (Arbitrary Units)
40
30
20
10
0
P<0.01
P<0.01
Dox
0
500
0
500
(ng/mL)
DLD-1 tRBM3
HCT 116 tRBM3

Figure 7: RBM3 overexpression generates increased β-catenin transcriptional activity. DLD-1 and HCT 116 tRBM3 cells induced for 48 hours at 500 ng/mL Dox with transient transfection of TOPFlash firefly luciferase and CMV renilla luciferase plasmids. Bar graphs represent firefly luciferase luminescence normalized to renilla luciferase luminescence. Error bars represent SEM. P values shown are obtained with Student's *t*-test.

Figure 8

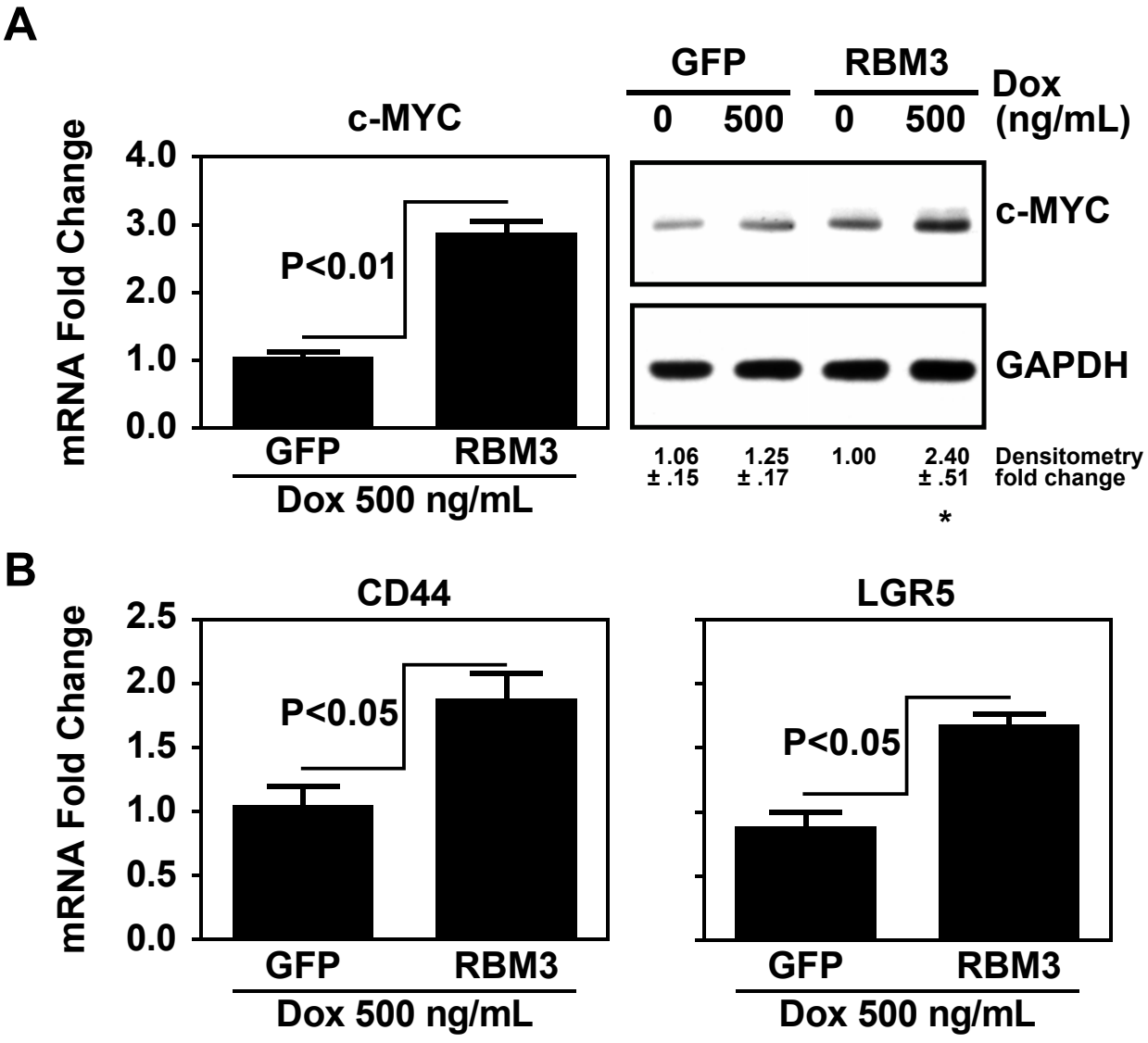
A
c-MYC
mRNA Fold Change
4.0
3.0
2.0
1.0
0.0
P<0.01
GFP
RBM3
Dox 500 ng/mL
GFP
RBM3
Dox
0
500
0
500
(ng/mL)
c-MYC
GAPDH
1.06
± .15
1.25
± .17
1.00
2.40
± .51
Densitometry
fold change
*
B
CD44
mRNA Fold Change
2.5
2.0
1.5
1.0
0.5
0.0
P<0.05
GFP
RBM3
Dox 500 ng/mL
LGR5
P<0.05
GFP
RBM3
Dox 500 ng/mL

Figure 8: RBM3 overexpression generates increases in β-catenin transcriptional targets. **(A)** Real time RT-PCR and western blot analysis of c-MYC showing following Dox induction for 72 hours. **(B)** Real time RT-PCR of CD44 and LGR5 following Dox induction for 72 hours. Bar graphs represent fold change relative to control. Error bars represent SEM. P values shown are obtained with Student's t-test. Densitometry represents fold change of c-MYC relative to uninduced tRBM3 cells normalized to GAPDH. Error represents SEM. *P < 0.05, **P < 0.01, ***P < 0.001 (Student's *t*-test).

Figure 9

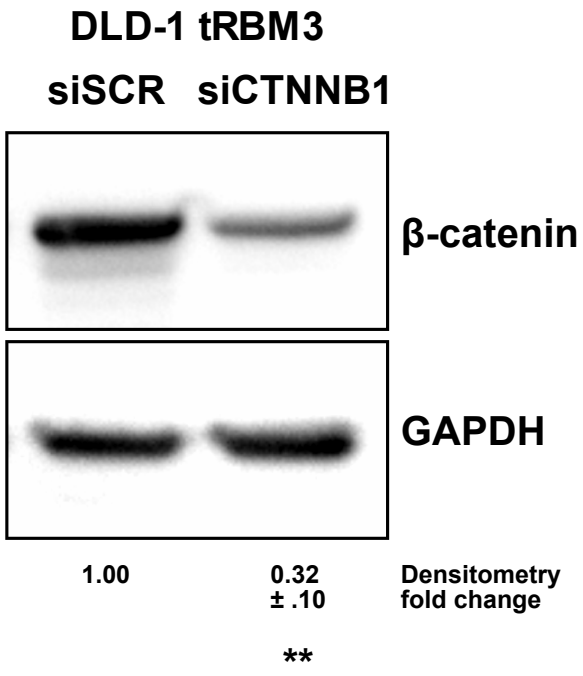
DLD-1 tRBM3
siSCR siCTNNB1
β-catenin
GAPDH
1.00
0.32
± .10
Densitometry
fold change
**

Figure 9: siCTNNB1 reliably knocks down β-catenin levels. Western blot analysis for total β-catenin in DLD-1-tRBM3 cells. Cells were transfected with either siSCR or siCTNNB1 for 72 hours then collected and analyzed. Densitometry represents fold change of β-catenin relative to siSCR transfected cells normalized to GAPDH. Error represents SEM. *P < 0.05, **P < 0.01, ***P < 0.001 (Student's *t*-test).

Figure 10

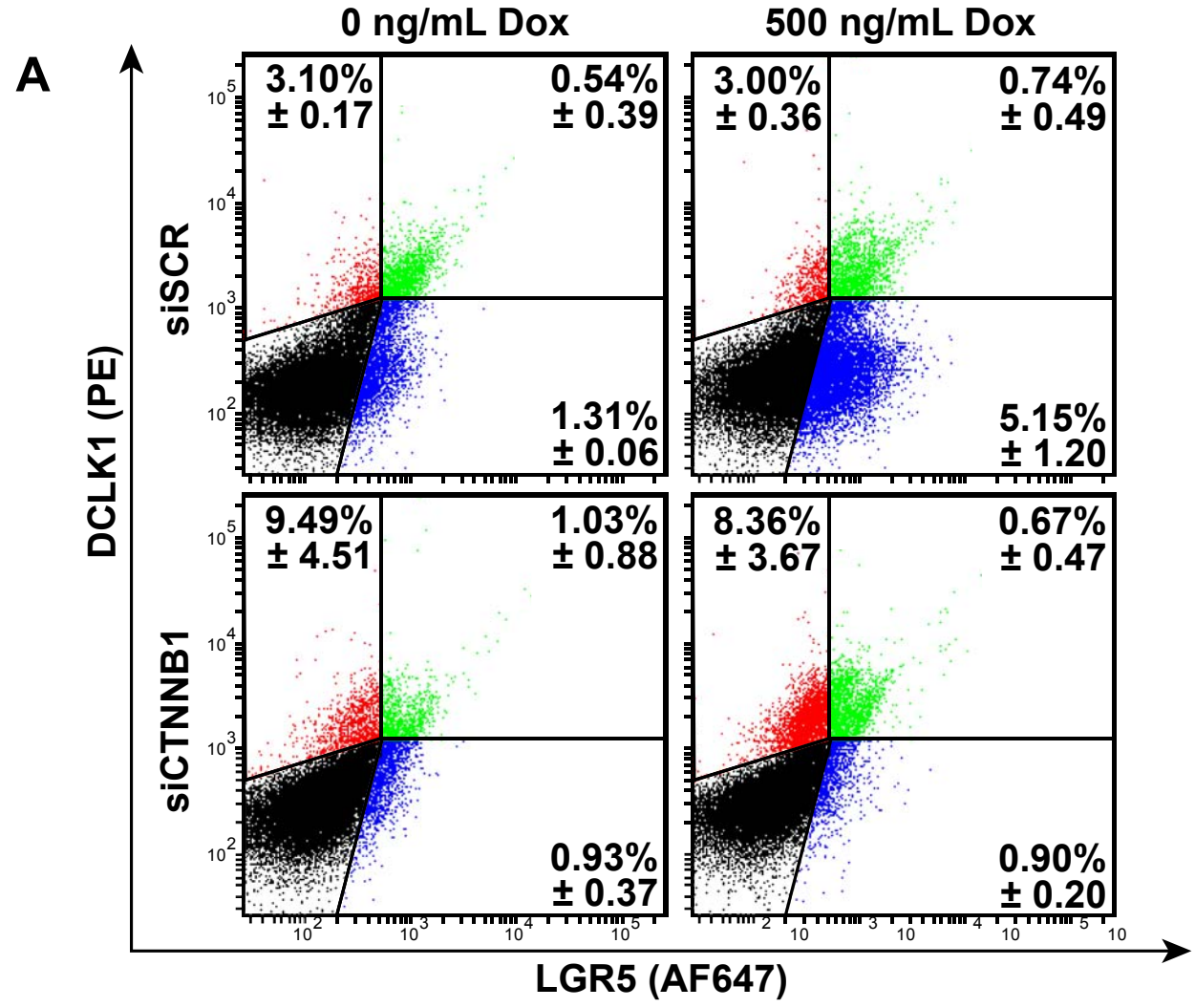
A
0 ng/mL Dox
500 ng/mL Dox
siSCR
siCTNNB1
DCLK1 (PE)
LGR5 (AF647)
3.10% ± 0.17
0.54% ± 0.39
1.31% ± 0.06
3.00% ± 0.36
0.74% ± 0.49
5.15% ± 1.20
9.49% ± 4.51
1.03% ± 0.88
0.93% ± 0.37
8.36% ± 3.67
0.67% ± 0.47
0.90% ± 0.20

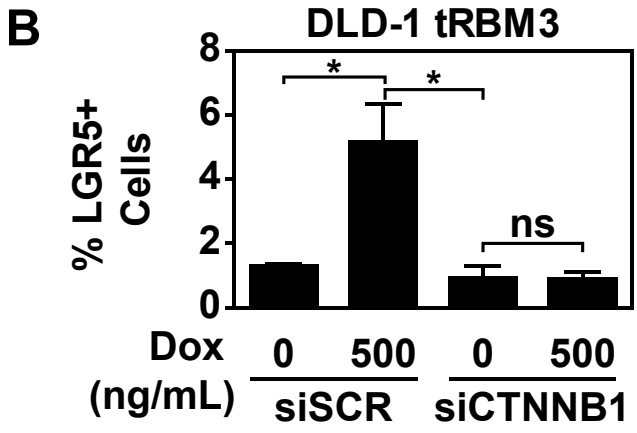
B
DLD-1 tRBM3
% LGR5+ Cells
ns
Dox (ng/mL)
0
500
0
500
siSCR
siCTNNB1

Figure 10: RBM3 mediated increases in LGR5 expression are dependent upon β-catenin. Representative flow cytometry dot plot of DLD-1-tRBM3 cells stained for DCLK1 (PE) and LGR5 (AF647) following induction with indicated concentrations of Dox and transfection with indicated siRNA for 72 hours. Bar graphs below represent percentage of LGR5 positive populations. Error bars represent SEM. P values shown are obtained with Student's *t*-test. *P < 0.05, **P < 0.01, ***P < 0.001 (Student's *t*-test).

cannot be rescued with RBM3 overexpression (Figure 11). This implies that the increases measured in SP fraction and LGR5 expression following RBM3 overexpression are dependent on an RBM3 mediated increase in β-catenin signaling.

Interesting to note is that, DLD-1 cells show a higher basal TOPFlash activity with a more modest increase following RBM3 overexpression compared to HCT 116. HCT 116 cells showing an average of 28.3 ± 3.1 compared to 3.3 ± 0.13 in uninduced controls and DLD-1 showing an average of 15.9 ± 0.79 compared to an average of 9.4 ± 0.52 in uninduced controls (Figure 7). We attribute this observation as well as the similar changes in SP population, spheroid formation and stem cell marker expression to the fact that DLD-1 cells encode a mutated *APC* whereas HCT 116 cells maintain intact wild type *APC* and at least one wild type β-catenin allele (Yang et al., 2006). Based on these data, we propose that RBM3 increases β-catenin transcriptional activity resulting in increased DCLK1+ and LGR5+ stem cell population thereby enhancing SP, spheroid formation and increasing β-catenin signaling activity.

The relative difference in the increases in β-catenin activity in HCT 116 RBM3 cells compared to DLD-1 RBM3 cells implies the mechanism of RBM3 mediated β-catenin signaling may act at the level of β-catenin degradation. This result would suggest that a member of the destruction complex could be affected. We chose to investigate GSK3β as a target for RBM3 mediated β-catenin activity because previous reports show that GSK3β is inactivated during hypoxia, and RBM3 expression is also induced following hypoxia (Mottet et al., 2003; Wellmann et al., 2004). We observed significant increases in inhibitory phosphorylation at serine position 9 in GSK3β (pS9 GSK3β) at 48 and 72 hours of RBM3 induction with 500 ng/mL Dox in HCT 116-tRBM3 cells (Figure 12A). DLD-1-tRBM3 cells also showed a trend to increase levels of pS9 GSK3β ($p=0.08$) at 48 hours with 500 ng/mL Dox induction (Figure 12A). As expected, GFP vector

Figure 11

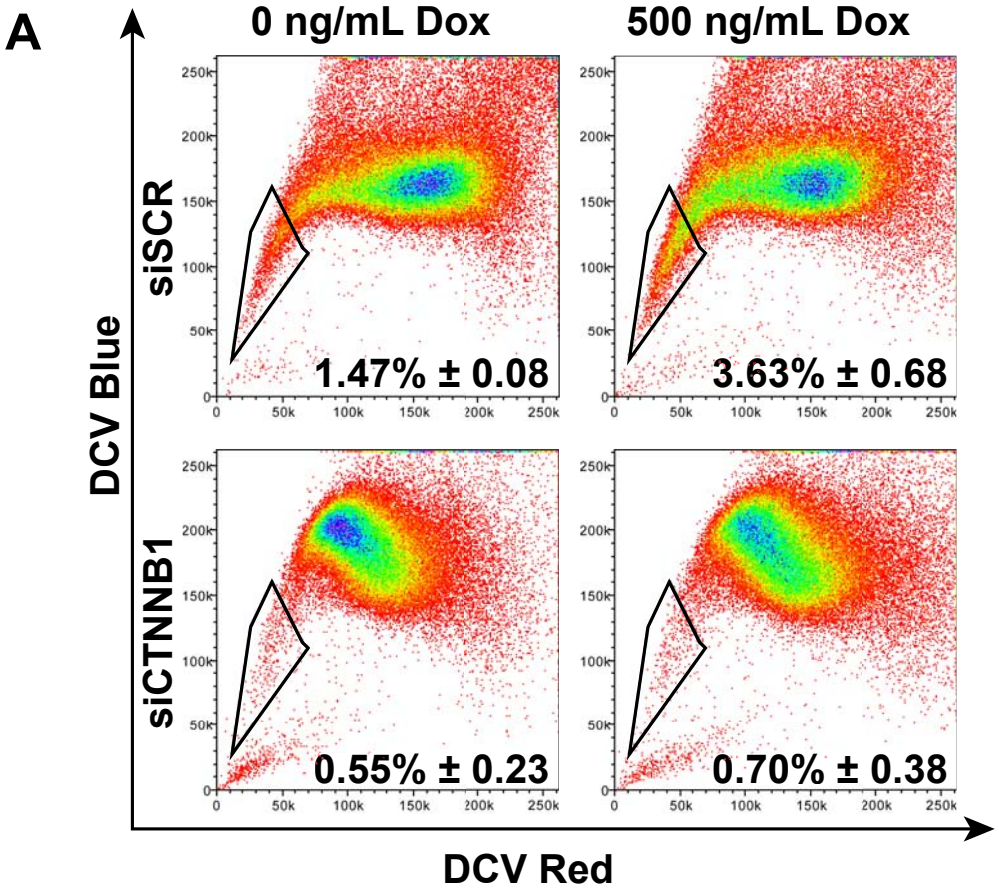
A
0 ng/mL Dox
500 ng/mL Dox
siSCR
siCTNNB1
DCV Blue
DCV Red
1.47% ± 0.08
3.63% ± 0.68
0.55% ± 0.23
0.70% ± 0.38

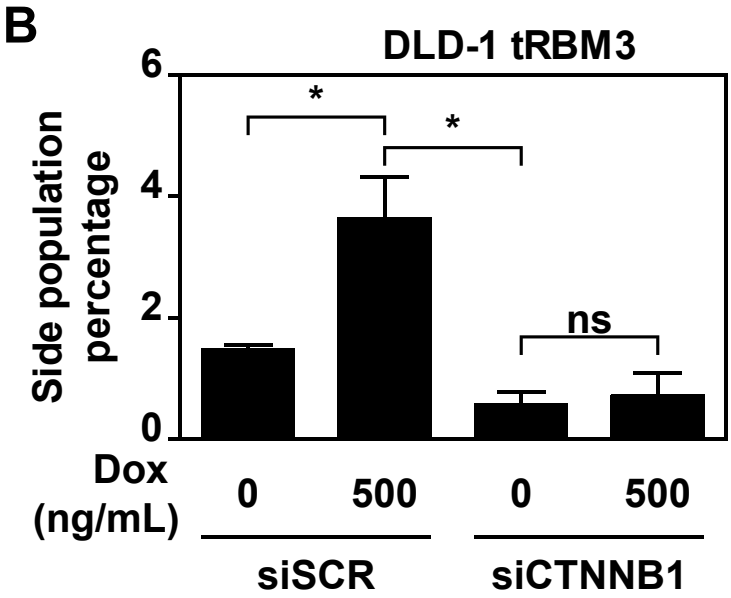
B
DLD-1 tRBM3
Side population percentage
Dox (ng/mL)
0
500
0
500
siSCR
siCTNNB1
*
*
ns

Figure 11: RBM3 mediated increases in SP fraction are dependent upon β-catenin. **(A)** Real time RT-PCR and western blot analysis of c-MYC showing following Dox induction for 72 hours. **(B)** Real time RT-PCR of CD44 and LGR5 following Dox induction for 72 hours. Bar graphs represent fold change relative to control. Error bars represent SEM. P values shown are obtained with Student's t-test. Densitometry represents fold change of c-MYC relative to uninduced tRBM3 cells normalized to GAPDH. Error represents SEM. *P < 0.05, **P < 0.01, ***P < 0.001 (Student's *t*-test).

Figure 12

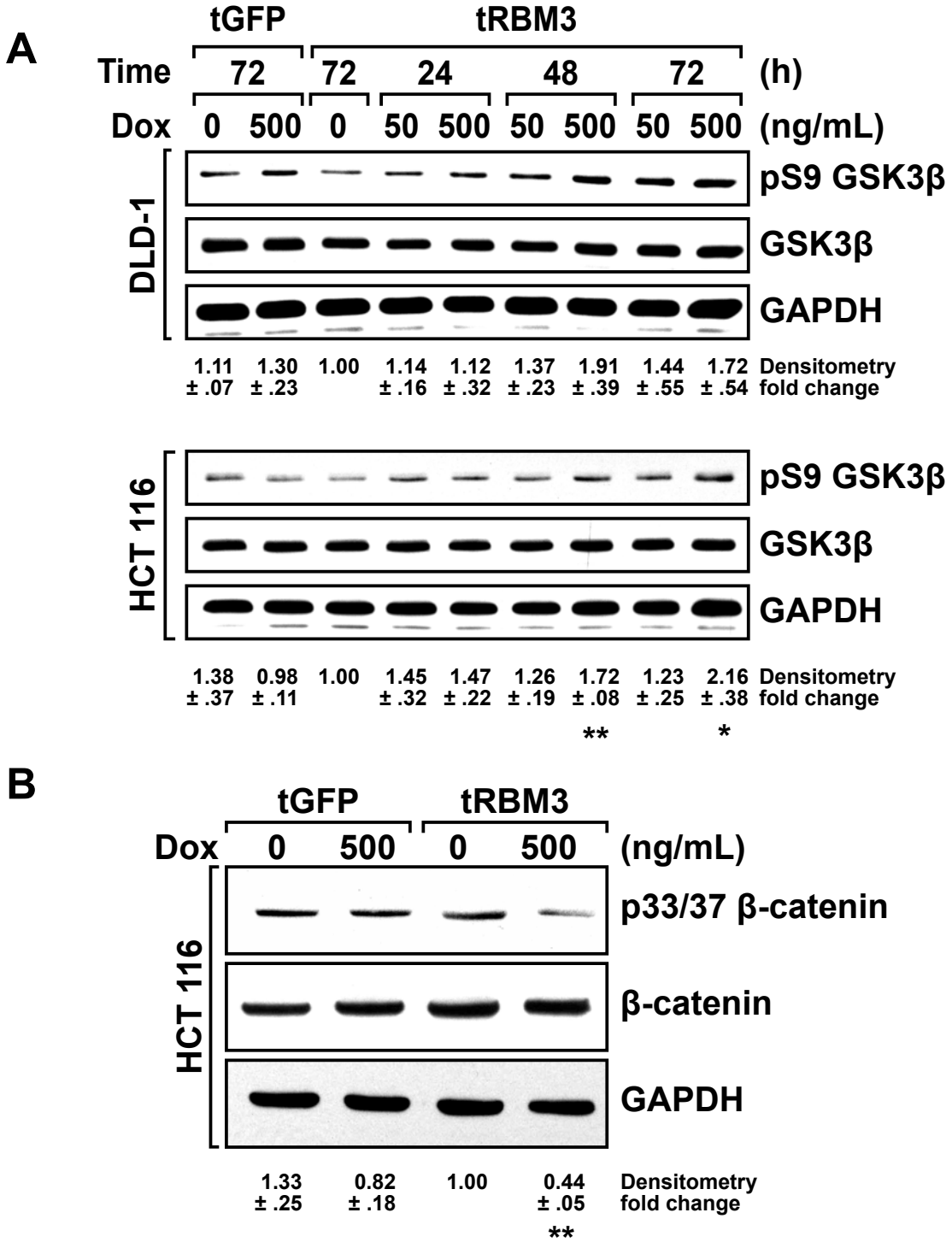
A
tGFP
tRBM3
Time
72
72
24
48
72
(h)
Dox
0
500
0
50
500
50
500
50
500
(ng/mL)
DLD-1
pS9 GSK3β
GSK3β
GAPDH
1.11 ± .07
1.30 ± .23
1.00
1.14 ± .16
1.12 ± .32
1.37 ± .23
1.91 ± .39
1.44 ± .55
1.72 ± .54
Densitometry fold change
HCT 116
pS9 GSK3β
GSK3β
GAPDH
1.38 ± .37
0.98 ± .11
1.00
1.45 ± .32
1.47 ± .22
1.26 ± .19
1.72 ± .08
1.23 ± .25
2.16 ± .38
Densitometry fold change
**
*
B
tGFP
tRBM3
Dox
0
500
0
500
(ng/mL)
HCT 116
p33/37 β-catenin
β-catenin
GAPDH
1.33 ± .25
0.82 ± .18
1.00
0.44 ± .05
Densitometry fold change
**

Figure 12: DLD-1 and HCT 116-tRBM3 cells show decreased GSK3β activity. **(A)** Western blot analysis of pSer9-GSK3β and GSK3β in DLD-1 and HCT 116 tGFP or tRBM3 cells with indicated concentrations of and times of Dox induction. Cells show significant increases in levels of pSer9-GSK3β at 500 ng/mL Dox induction for 72 hours. **(B)** Western blot analysis of p33/37/41-β-catenin following 6 hour treatment with 5μM MG 132 showing decreased pβ-catenin relative to total β-catenin following 500 ng/mL Dox induction for 72 hours. Densitometry represents fold change of pS9 GSK3β or p33/37 β-catenin relative to uninduced tRBM3 cells normalized to total GSK3β or total β-catenin, respectively. Error represents SEM. *P < 0.05, **P < 0.01, ***P < 0.001 (Student's *t*-test).

control showed no appreciable difference in GSK3β phosphorylation in either cell line (Figure 12A). We next validated this increase in GSK3β phosphorylation by determining phosphorylation at serines 33 and 37, and threonine at position 41 in β-catenin. There was reduced phosphorylation in β-catenin in HCT 116 cells (Figure 12B) suggesting that GSK3β is inactivated. GSK3β phosphorylation can occur through either induction of Wnt signaling or through the action of activated AKT kinase (Dorsam and Gutkind, 2007) (Figure 13). In previous studies, we have demonstrated that RBM3 induces *IL-8* mRNA and prostaglandin E2 (PGE2), both of which result in a phosphorylating activation of AKT (Chapter 2, Figure 5) (Sureban et al., 2008b). Accordingly, we determined whether AKT activity may explain attenuated GSK3β activity. RBM3 overexpression showed significant increases in AKT phosphorylation at serine 473, whereas no appreciable increase was observed in vector controls or uninduced RBM3 cells (Figure 14). These data imply that RBM3 overexpression increases β-catenin activity by inhibiting GSK3β through the actions of activated AKT kinase. Interestingly, inhibition of COX-2 using NS-398 did not significantly affect RBM3 induced β-catenin activity as measured by TOPFlash luciferase activity (Figure 15). This lack of change could be potentially explained by RBM3 induction of IL-8, as well as other currently unknown mRNA clients, which can act through similar mechanisms to induce AKT activation. This implies a potential need to validate this pathway using a dual inhibition of IL-8 and COX-2.

Finally, the GSK3β inhibitor (2'Z,3'E)-6-Bromoindirubin-3'-oxime (BIO) has been shown to upregulate β-catenin signaling and increase the expression of ABC proteins (Liu et al., 2012; Meijer et al., 2003). BIO shows high specificity towards GSK3 kinase activity with an IC_{50} measured at 5 nM compared to an IC_{50} of greater than 5 μM for other kinases such as protein kinase C family members, mitogen activated protein kinases, and cyclic-AMP dependent protein

Figure 13

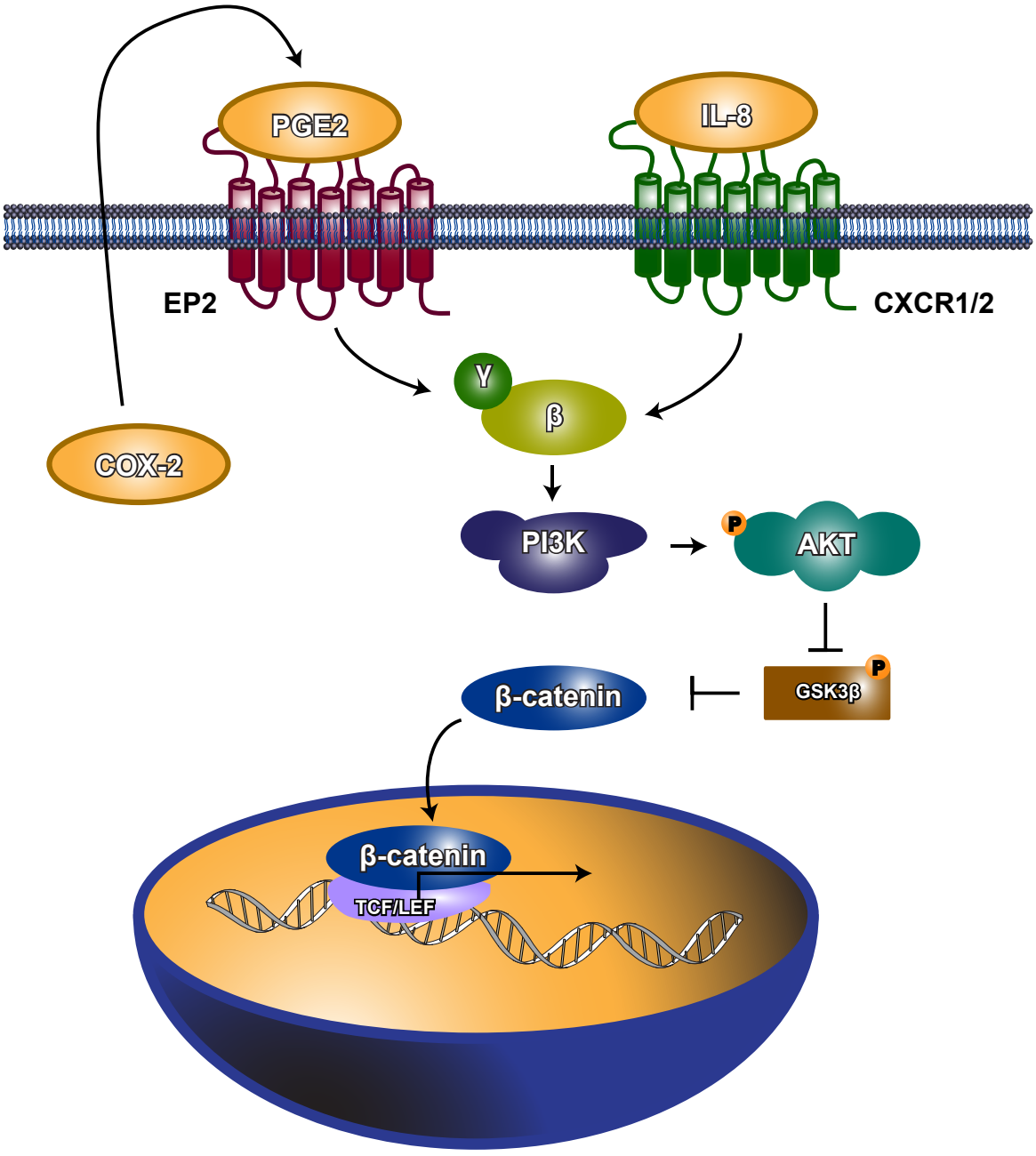
PGE2
IL-8
EP2
CXCR1/2
γ
β
COX-2
PI3K
P
AKT
β-catenin
GSK3β
P
β-catenin
TCF/LEF

Figure 13: Model for RBM3 induced β-catenin signaling adapted from Dorsam and Gutkind. RBM3 overexpression has been shown to increase COX-2 and IL-8 expression at the posttranscriptional level. PGE2 produced by COX-2 and IL-8 can both act through G protein coupled receptors to activate PI3K and AKT. This in turn can suppress GSK3β allowing β-catenin to accumulate and induce transcriptional changes within the nucleus.

Figure 14

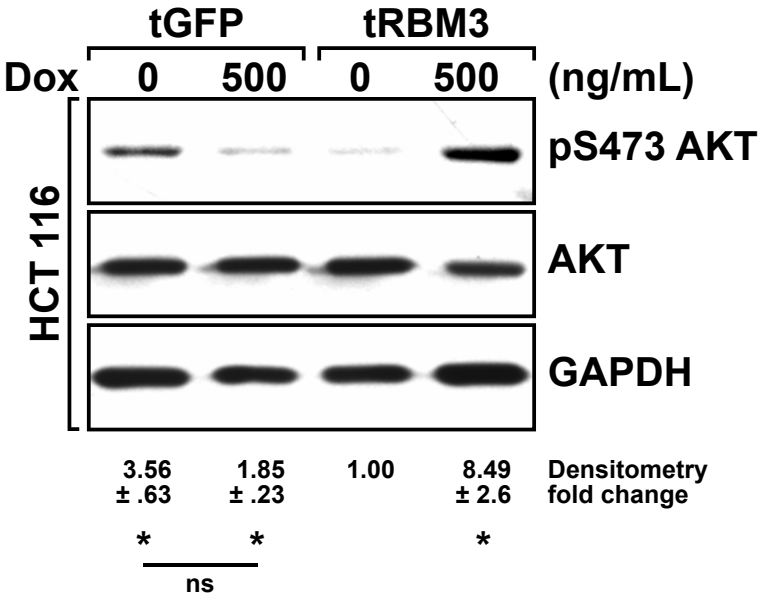
tGFP
tRBM3
Dox
0
500
0
500
(ng/mL)
HCT 116
pS473 AKT
AKT
GAPDH
3.56
± .63
1.85
± .23
1.00
8.49
± 2.6
Densitometry
fold change
*
*
*
ns

Figure 14: HCT 116 cells show increased AKT activity following RBM3 overexpression. Western blot analysis of pS473 AKT and total AKT following induction for 72 hour with indicated concentrations of Dox. pS473 AKT levels are significantly elevated relative to total AKT with RBM3 overexpression. Densitometry represents fold change of pS473 AKT relative to uninduced tRBM3 cells normalized to total AKT. Error represents SEM. *P < 0.05, **P < 0.01, ***P < 0.001 (Student's *t*-test).

Figure 15

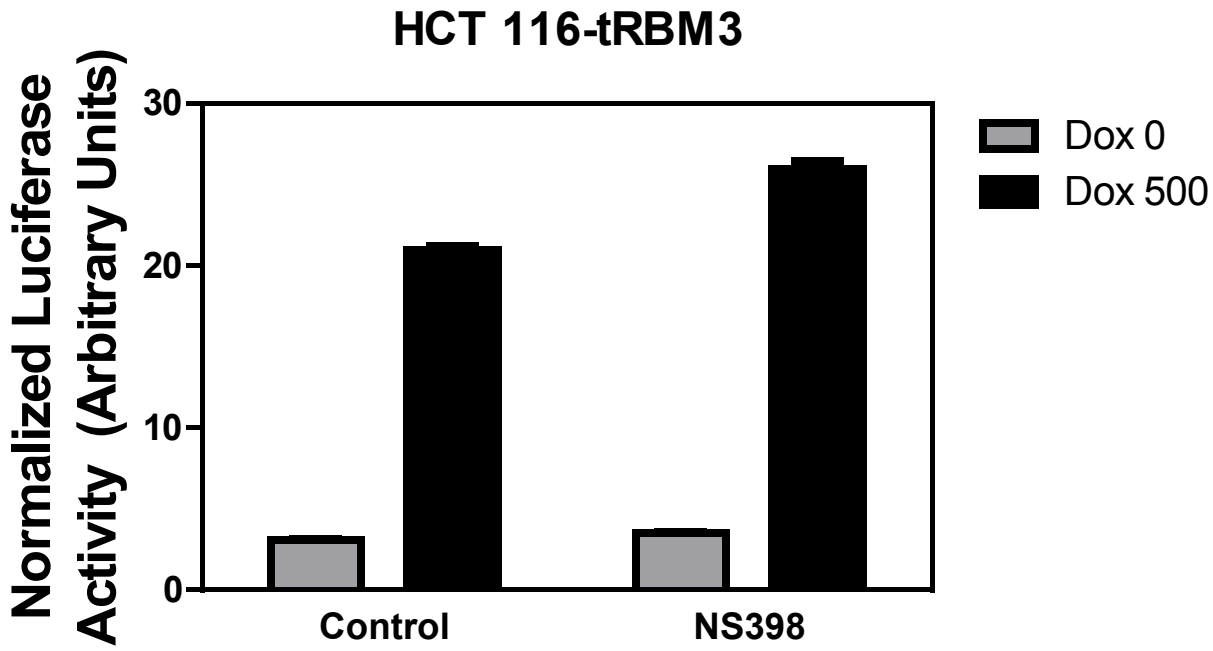
HCT 116-tRBM3
Normalized Luciferase Activity (Arbitrary Units)
30
20
10
0
Control
NS398
Dox 0
Dox 500

Figure 15: COX-2 inhibition does not abrogate RBM3 induced β-catenin activity. HCT 116 tRBM3 cells induced for 48 hours at 500 ng/mL Dox with transient transfection of TOPFlash firefly luciferase and CMV renilla luciferase plasmids. Cells were also treated with 0 or 10 μM NS-398 for 48 hours. Bar graphs represent firefly luciferase luminescence normalized to renilla luciferase luminescence. Error bars represent SEM.

kinases (Meijer et al., 2003). We next examined the effects of pharmacologic GKS3β inhibition using BIO on RBM3 overexpressing cells. HCT 116 cells treated with BIO showed increase in both total and nuclear β-catenin levels similar to that of RBM3 overexpression (Figure 16). Additionally, BIO treatment induced c-MYC expression in both GFP and RBM3 overexpressing cells similar to RBM3 overexpression (Figure 17A). In addition, there was increased TOPFlash luciferase activity following BIO treatment (Figure 17B). Moreover, the combination of RBM3 overexpression and BIO treatment generated an even more robust increase in β-catenin signaling as measured through total β-catenin, nuclear β-catenin, c-MYC protein expression and TOPFlash luciferase activity (Figures 16 & 17). These data further demonstrate that RBM3 regulates β-catenin signaling pathway by affecting GSK3β activity. On the other hand, it also implicates a secondary signaling mechanism through which RBM3 may be acting.

Notch signaling is another signaling cascade that ISCs rely on to maintain stem cell homeostasis (VanDussen et al., 2012). The transmembrane Notch receptor is activated upon binding with one of several ligands including those of the Jagged family or the Delta-like (DLL). Following binding, the extracellular portion of Notch is cleaved. Subsequently, the intracellular portion of the Notch receptor is cleaved by the γ-secretase complex allowing the Notch intracellular domain (NICD) to translocate to the nucleus, associate with transcription factors and induce transcriptional changes within the cell (Vooijs et al., 2011). Previous studies have demonstrated a significant amount of crosstalk between the β-catenin and Notch signaling cascades, with some studies showing that the two are mutually agonistic, while others suggest some level of antagonism between them (Kim et al., 2012a; Kwon et al., 2011; Nakamura et al., 2007). We therefore decided to examine whether Notch activation might play a role in RBM3 induced β-catenin signaling. We observed that treatment with DAPT, a γ-secretase inhibitor used to

Figure 16

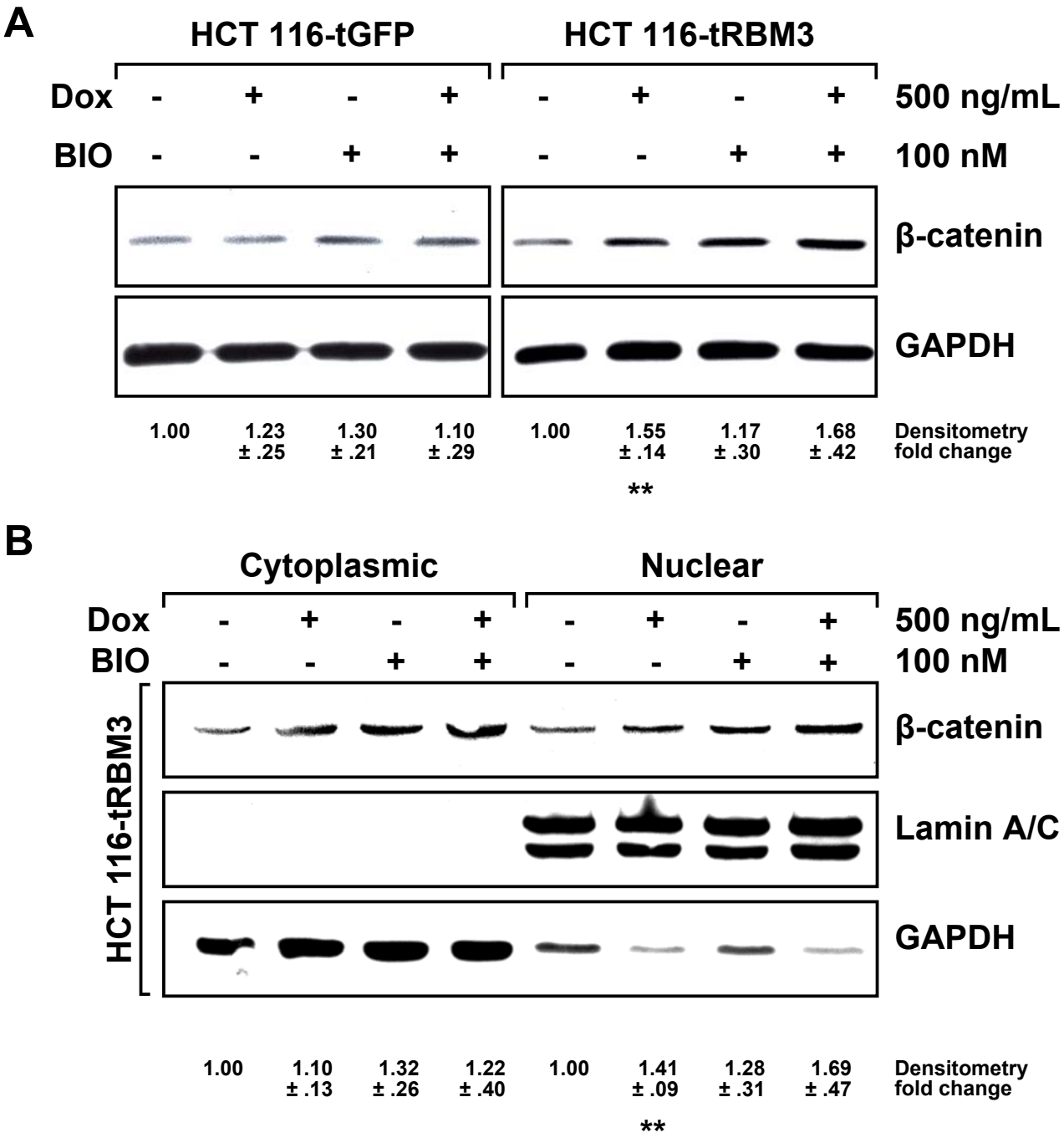
A
HCT 116-tGFP
HCT 116-tRBM3
Dox - + - + - + - + 500 ng/mL
BIO - - + + - - + + 100 nM
β-catenin
GAPDH
1.00 1.23 ± .25 1.30 ± .21 1.10 ± .29 1.00 1.55 ± .14 1.17 ± .30 1.68 ± .42 Densitometry fold change
**
B
Cytoplasmic
Nuclear
Dox - + - + - + - + 500 ng/mL
BIO - - + + - - + + 100 nM
HCT 116-tRBM3
β-catenin
Lamin A/C
GAPDH
1.00 1.10 ± .13 1.32 ± .26 1.22 ± .40 1.00 1.41 ± .09 1.28 ± .31 1.69 ± .47 Densitometry fold change
**

Figure 16: BIO treatment phenocopies RBM3 induced increases in β-catenin. **(A)** Western blot analysis of total β-catenin in HCT 116-tGFP and HCT 116-tRBM3 cells following 72 hour treatment with indicated concentrations of Dox and BIO. **(B)** Western blot analysis of nuclear and cytoplasmic fractions of HCT 116-tRBM3 cells following 72 hour treatment with indicated concentrations of Dox and BIO. BIO or RBM3 show similar increases in β-catenin. Combined RBM3 and BIO show a trend towards a further increase in total β-catenin. Densitometry represents fold change of total β-catenin relative to uninduced tRBM3 cells normalized to GAPDH for total cell lysate or cytoplasmic fraction and Lamin A/C for nuclear fraction. Error represents SEM. *P < 0.05, **P < 0.01, ***P < 0.001 (Student's *t*-test).

Figure 17

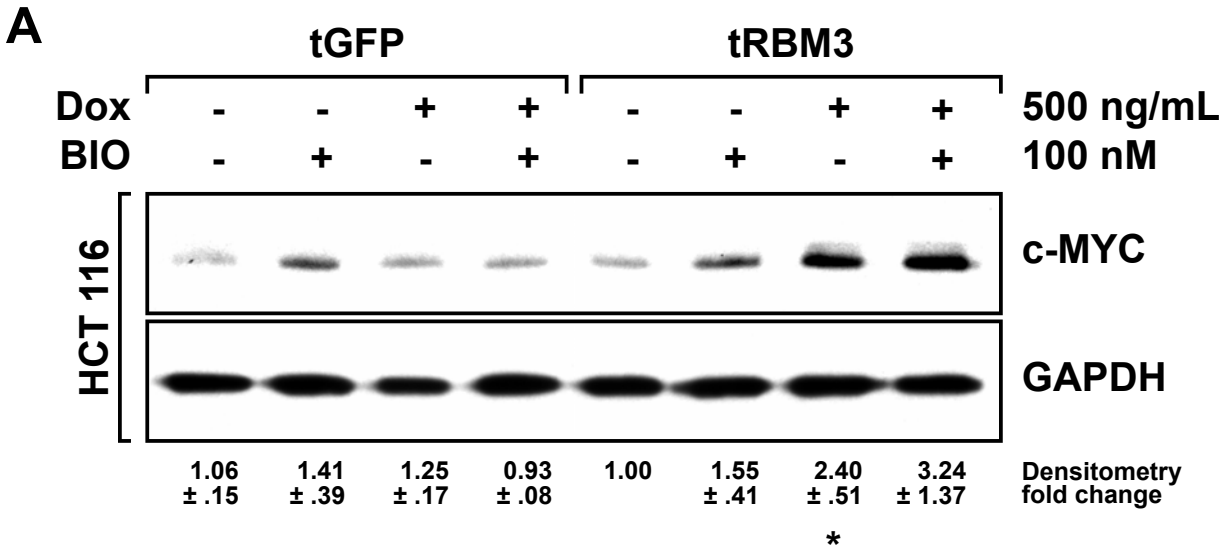
A
tGFP
tRBM3
Dox - - + + - - + + 500 ng/mL
BIO - + - + - + - + 100 nM
HCT 116
c-MYC
GAPDH
1.06 ± .15
1.41 ± .39
1.25 ± .17
0.93 ± .08
1.00
1.55 ± .41
2.40 ± .51
3.24 ± 1.37
Densitometry fold change
*

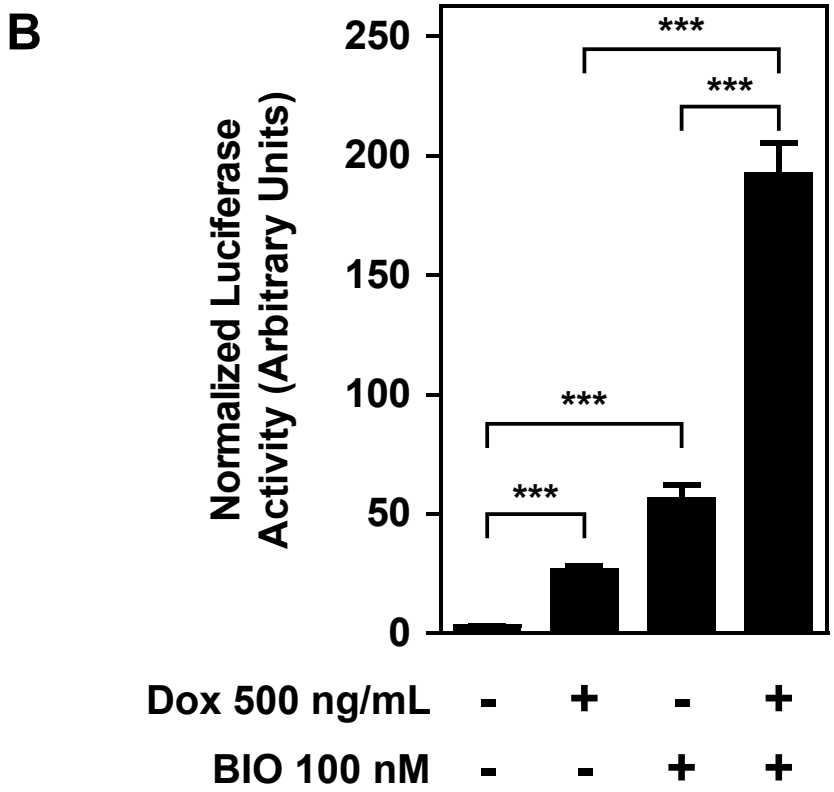
B
Normalized Luciferase Activity (Arbitrary Units)
250
200
150
100
50
0
***
***
***
***
Dox 500 ng/mL - + - +
BIO 100 nM - - + +

Figure 17: BIO treatment phenocopies RBM3 induced β-catenin transcriptional activity. **(A)** Western blot analysis for c-MYC protein in HCT 116 tGFP and tRBM3 cells following 72 hours of treatment with indicated concentrations of Dox and BIO. **(B)** HCT 116 tRBM3 cells treated for 48 hours at indicated concentrations of Dox and BIO with transient transfection of TOPFlash firefly luciferase and CMV renilla luciferase plasmids. Densitometry represents fold change of c-MYC relative to uninduced tRBM3 cells normalized to GAPDH. Error represents SEM. Bar graphs represent firefly luciferase luminescence normalized to renilla luciferase luminescence. Error bars represent SEM. *P < 0.05, **P < 0.01, ***P < 0.001 (Student's *t*-test).

suppress Notch activation, showed a minor increase in RBM3 induced β-catenin activity in DLD-1 cells, but showed no significant change in HCT 116 cells (Figure 18A). Furthermore, overactivation of Notch1 through transient transduction of free N1ICD demonstrated an antagonistic effect in uninduced RBM3 cells that was present proportionally in RBM3 overexpressing cells implying that Notch overactivation provides no significant effect on RBM3 induced β-catenin activity in these two colon cancer cell lines (Figure 18B).

Discussion

In the previous chapter, we showed that RBM3 is capable of inducing an increase in the population of stem cells within colon cancer cells. Here, we report that RBM3 overexpression results in a profound increase in β-catenin transcriptional activity, which is a critical factor in maintaining stem cells in both normal intestine and colon cancer. Previous studies have implicated that RBM3 is upregulated in the stem cell compartment (Baghdoyan et al., 2000). However, this is the first study to demonstrate a mechanism through which RBM3 plays a role in maintaining stem cell self-renewal. Specifically, we show that RBM3 overexpression results in a significant increase in both total β-catenin and nuclear β-catenin with no significant increases in cytoplasmic β-catenin levels implying increases in transcriptionally active β-catenin. This observation correlates with decreased activity of GSK3β thereby inhibiting the β-catenin degradation pathway allowing it to accumulate, translocate to the nucleus and induce transcriptional changes.

Our study also suggests that there must be a second mechanism by which RBM3 activates β-catenin signaling as overexpression of RBM3 combined with inhibition of GSK3β was capable

Figure 18

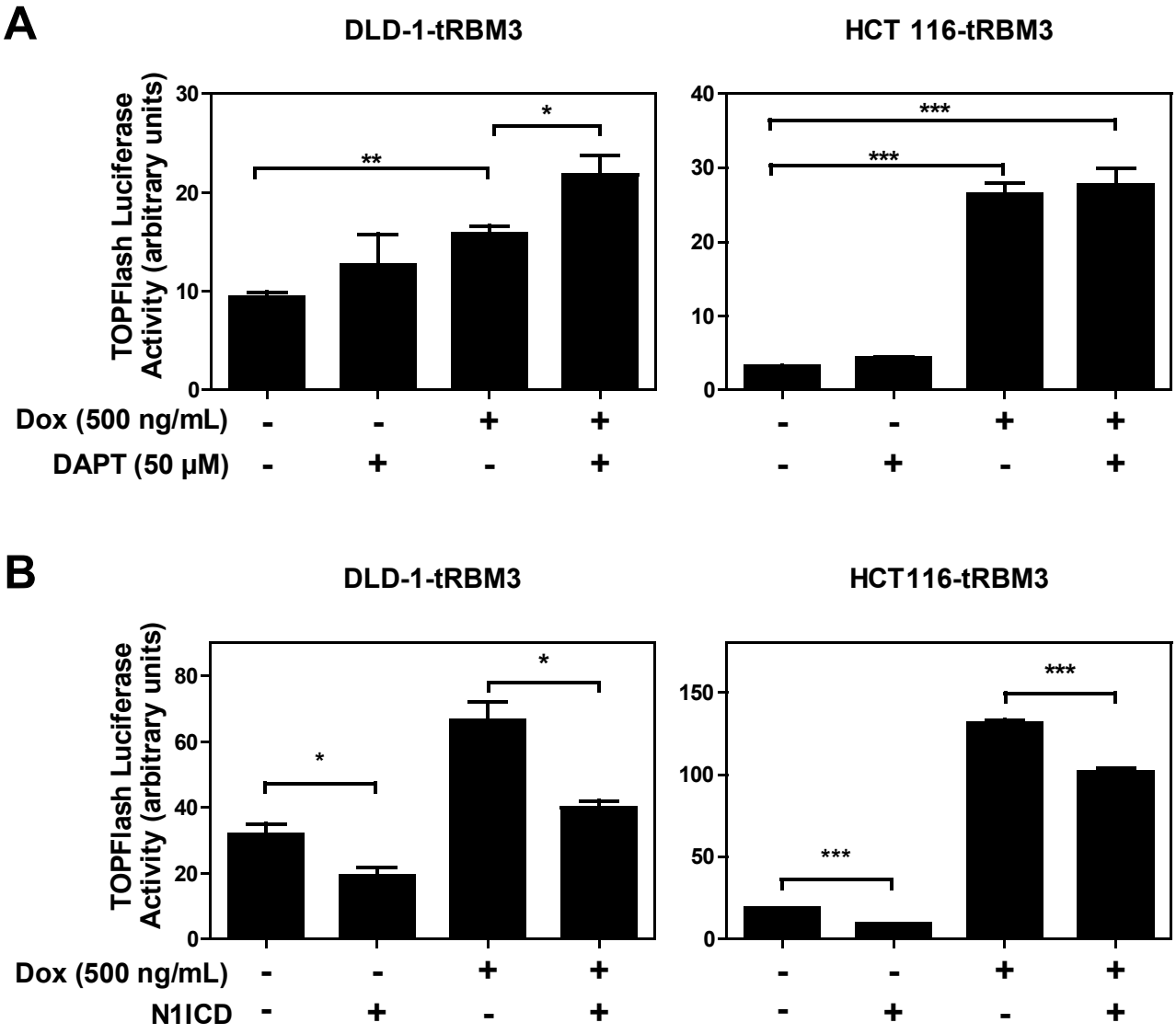
A
DLD-1-tRBM3
HCT 116-tRBM3
TOPFlash Luciferase Activity (arbitrary units)
Dox (500 ng/mL)
DAPT (50 μM)
B
DLD-1-tRBM3
HCT116-tRBM3
TOPFlash Luciferase Activity (arbitrary units)
Dox (500 ng/mL)
N1ICD

Figure 18: RBM3 induced β-catenin transcriptional activity is independent of crosstalk with Notch signaling. **(A)** DLD-1 and HCT 116 tRBM3 cells treated for 48 hours at indicated concentrations of Dox and DAPT with transient transfection of TOPFlash firefly luciferase and CMV renilla luciferase plasmids. **(B)** DLD-1 and HCT 116 tRBM3 cells treated for 48 hours at indicated concentrations of Dox with transient transfection of CMV-GFP-N1ICD or CMV-GFP, TOPFlash firefly luciferase and CMV renilla luciferase plasmids. Bar graphs represent firefly luciferase luminescence normalized to renilla luciferase luminescence. Error bars represent SEM. *P < 0.05, **P < 0.01, ***P < 0.001 (Student's *t*-test).

of increasing nuclear β-catenin and TOPFlash activity beyond that of either one alone. Furthermore, HCT 116 cells are known to contain wild type *APC* with a heterozygous activating mutation in β-catenin, while DLD-1 cells contain a truncating loss of function mutation in *APC* (Yang et al., 2006). This implies that if RBM3 were only acting through inhibition of GSK3β activity, then DLD-1 cells should show no significant upregulation of β-catenin activity and HCT 116 should only show modest increases in β-catenin activity due to one allele containing the wild type β-catenin. However, our studies show that DLD-1-tRBM3 cells show a 1.7-fold change and HCT 116-tRBM3 cells an 8.6-fold increase in TOPFlash activity. These findings reveal that while RBM3 overexpression results in phosphorylation of GSK3β, thereby attenuating β-catenin degradation, this is only a partial mechanism and there is an as yet unknown role that RBM3 plays in modulating β-catenin signaling.

In both IHC for free overexpressed RBM3 and fluorescent microscopy for overexpressed GFP-RBM3 fusion protein, we note that RBM3 is primarily localized within the nucleus. However, while the bulk of RBM3 appears to exist within the nucleus, it has also been observed to display nuclear-cytoplasmic shuttling activity (Sureban et al., 2008b). RBM3 has also been shown to be associated with the RNA binding protein HuR, a protein that has been shown to display direct protein-protein interaction with β-catenin (D'Uva et al., 2013; Kim et al., 2012b; Sureban et al., 2008b). We propose, as a direction for further study, that RBM3 has either direct or indirect interaction with β-catenin protein and that its strong nuclear localization may serve as shuttling mechanism to further enhance nuclear translocation of cytoplasmic β-catenin. Additional studies are also required to determine whether RBM3 plays a role in β-catenin/TCF transcriptional activity.

Also of note is the correlation between hypoxia induction of RBM3 as previously described and the link between hypoxia and stem cells (Kaidi et al., 2007; Mazumdar et al., 2010; Wellmann et al., 2004; Yoshida et al., 2013). Although previous studies have reported that hypoxia is capable of affecting the stem cell population in various cancers, these studies focused on the HIF1α as the primary mechanism of modulating stem cell signaling pathways such as WNT/β-catenin (Kaidi et al., 2007; Mazumdar et al., 2010; Yoshida et al., 2013). Studies have demonstrated that hypoxia also suppresses GSK3β activity (Mottet et al., 2003). Our study demonstrates that increased RBM3 expression affects GSK3β activity thereby enhancing β-catenin signaling. As RBM3 is shown to be regulated by hypoxia in a HIF1α independent mechanism, this implies that RBM3 could be upstream of HIF1α or demonstrates a novel link between hypoxia and enrichment of stem cells. Furthermore, as GSK3β is important for controlling numerous biologic processes within the cell, it could be that altering RBM3 expression has far reaching consequences on the phenotype of the cell that remains to be elucidated.

Chapter IV: RBM3 induces a quiescent state in colon cancer cells

Introduction

A major stressor of tissues within an organ is aging. Aging places a great demand on genomic integrity, telomere stability and long term viability. A potential mechanism by which intestinal epithelial renewal is maintained over the lifespan of an organism is through maintenance of cellular quiescence within a subset of stem cells allowing for decreased impact from the stress of aging. Cellular quiescence is the capability of exiting the cell cycle and remaining within a G0 state with the capability to re-enter a cycling state depending upon the needs of the surrounding tissue. It has been demonstrated that the +4 LRC of the adult intestinal crypt maintains quiescence. +4 LRCs show remarkably long lived levels of nucleoside analog levels following pulse chase experiments giving rise to their name (Potten et al., 1978). Additionally +4 LRCs have been shown to be insensitive to loss of cell cycle regulators (Lee et al., 2009). However, these quiescent stem cells are able to regain the ability to divide following injury (Tian et al., 2011).

Interestingly, while the Wnt/β-catenin signaling pathway is normally associated with increased proliferation in cancer, it has also been shown to paradoxically maintain quiescence within the hepatocyte, myocyte and hematopoietic cells (Gougelet and Colnot, 2012; Povinelli and Nemeth, 2014; Subramaniam et al., 2013). This complex interplay between Wnt induced proliferation and Wnt induced stem cell maintenance and its relevance in ISCs and colonic CSCs is as yet unclear.

Important to note is that quiescence is one of the many mechanisms that CSCs utilize to subvert the effects of genotoxic chemotherapies. As most classical chemotherapies are designed to induce genotoxic insult to rapidly proliferating cells, quiescent CSCs often remain unaffected by these therapies. Recent studies have shown that hematopoietic and colonic CSCs display a

remarkable level of resistance to cytotoxic agents by entering a quiescent state (Cheng et al., 2000; Dick, 2008; Touil et al., 2013).

Here, we examine the phenotypic effect of RBM3 on cell cycle control. Specifically we show that overexpression of RBM3 generates decreased cell proliferation in colon cancer cells. Additionally, this decreased proliferation is maintained *in vivo* in tumor xenografts over long periods of time. Interestingly, RBM3 overexpression only yields minor changes in cell cycle progression. To further elucidate the effects of RBM3 on cellular quiescence, we use nucleotide analog labeling to show that RBM3 overexpression induces a marked increase in the percentage of quiescent cells. These results implicate yet another modality through which RBM3 may play a role in chemoresistance.

Materials and Methods

Cell culture

HCT 116 cells were obtained from ATCC and cultured under conditions of 5% CO_2 in DMEM (Corning) containing 10% FBS (Sigma-Aldrich) and 1% antibiotic/antimycotic solution (Corning). Following transduction of tGFP or tRBM3 virus, cells were cultured as mentioned above with additional 1 mg/mL G 418 (Santa Cruz Biotechnology) and 1μg/mL puromycin (Life Technologies).

Western blotting

Western blot were performed using poly-acrylamide gel electrophoresis within a Miniprotean Tetracell apparatus (BioRad) followed by blotting onto 0.45μm pore size Immobilon polyvinyl difluoride membrane (Millipore) using a mini Transblot module (BioRad). Antibodies for p21CIP1/WAF1 were obtained from Cell Signaling (Cell Signaling Technology).

Real time RT-PCR

Total cellular RNA was isolated using TRIzol reagent followed by reverse transcription using SuperScript II in the presence of random hexonucleotide primers (Life Technologies). cDNA was then analyzed by real-time RT-PCR using Jumpstart Taq polymerase (Sigma Aldrich) and SYBR Green nucleic acid stain (Life Technologies). Threshold crossing values for each gene were normalized to glyceraldehyde phosphate dehydrogenase (GAPDH) gene expression. mRNA expression was then normalized to fold change relative to uninduced controls. Primers used in this study are as follows:

p21CIP1/WAF1: 5'-CCATGTGGACCTGTCACTGT-3' / 5'-TGGTAGAAATCTGTCATGCTGGTC-3'

GAPDH: 5'-CAGCCTCAAGATCATCAGCA-3' / 5'-GTCTTCTGGGTGGCAGTGAT-3'

Microarray analysis

RNA was harvested using TRIzol (Life Technologies) according to manufacturer recommendations. Microarray analysis was performed using the Human Transcriptome Array 2.0 (Affymetrix) according to manufacturer recommendations. Data were analyzed using

Transcriptome Analysis Console (Affymetrix). Results were screened for coding genes with FDR corrected P values less than 0.05.

Proliferation assay

Cells were plated at 50,000 cells per mL into 96 well plates and allowed to adhere overnight followed by treatment with indicated treatments. Following treatment for the indicated time, cells were assayed for proliferation using the hexoseaminidase assay as previously described (Subramaniam et al., 2008). Briefly, cell culture medium was removed followed by addition of 75µL hexoseaminidase substrate buffer (7.5 mM sodium citrate, pH 5.0, 3.75 mM 4-nitrophenyl-N-acetyl-β-D-glucosaminide, 0.25% Triton) per well and incubation at 37°C for 30 minutes. The reaction was quenched using 112.5 µL of hexoseaminidase developer solution (50 mM glycine, 5 mM EDTA, pH 10.4) and absorbance at 405 nm was read on a plate reader. Percentage proliferation was calculated as absorbance relative to untreated control and curves for inhibitory response were fit using GraphPad Prism software (GraphPad).

Spheroid formation assay

Cells were appropriately treated in 2D culture, trypsinized followed by a wash in PBS to remove residual serum. Cells were then resuspended in spheroid media containing 1x B27 supplement, 20 ng/mL bFGF and 20 ng/mL recombinant EGF (Life Technologies) in DMEM. Cells were passed through a 35 µm sieve, counted and plated onto ultra-low attachment surface plates

(Corning). Spheroid formation was allowed to proceed for 10-14 days followed by spheroid quantification and analysis using a Celigo Cyntellect embryoid body counter.

Tumor Xenografts

Cells were grown with 500 ng/mL Dox for 72 hours in 2D culture. Cells were then trypsinized and 1 million cells were injected suspended in PBS into the flanks of nude mice. Tumor formation was measured once per week using Vernier calipers for volume measurement. Volume was calculated as

$$\frac{L^2 \times W}{2}$$

where L represents length and W represents width. If injection sites had no palpable tumor at time of measurement, tumor volume was recorded as 0 cm^3. Mice were euthanized at 35 days and tumors were harvested and weighed.

Cell Cycle

Cells were plated and treated with indicated concentrations of Dox for 72 hours. Cells were then trypsinized, washed and fixed in 70% ethanol/30% PBS overnight. Fixed cells were then washed and stained in cell cycle staining buffer containing 1% propidium iodide (Life Technologies, Inc.) and 3% RNAseA (Sigma-Aldrich) in PBS and analyzed by flow cytometry.

Quiescence assay

Cellular quiescence was measured as previously described with minor alterations (Coller et al., 2006). Cells were cultured at extremely low seeding density (35,000 cells/mL) in indicated concentrations of Dox. At 48 hours of induction, cells were given either normal culture medium with selection antibiotics or serum free culture medium with selection antibiotics and fresh Dox as appropriate. Serum deprivation was a positive control for induced quiescence. Following 72 hours with appropriate Dox treatment, cells were treated with 100 μM bromo-deoxy uridine (BrdU). Cells were harvested with trypsin/EDTA, washed and fixed overnight at -20°C in fixation solution (70% ethanol, 50 mM glycine, pH 2.0). Nuclei were denatured using 4 M HCl treatment for 15 minutes followed by neutralization with PBS. Cells were then blocked for 30 minutes (2% bovine serum albumin in PBS) and incubated for 1 hour at room temperature with alexafluor-488 (AF488) conjugated anti-BrdU antibody (Life Technologies). Cells were washed and resuspended in cell cycle staining solution containing 1% propidium iodide (Life Technologies, Inc.) and 3% RNAseA (Sigma-Aldrich) and analyzed by flow cytometry.

Results

We first observed that RBM3 overexpression induces significant chemoresistance against paclitaxel and modest chemoresistance against ADM (Chapter 2 Figures 15 & 16). Interestingly, the mechanism of action of paclitaxel is thought to be cell cycle specific while ADM is thought to be partially cell cycle non-specific (Pommier et al., 2010). We reasoned that RBM3 may confer multiple modalities of drug resistance with quiescence explaining the large difference between resistances in paclitaxel versus ADM.

We initiated these studies by investigating the effect on RBM3 overexpression in overall proliferation in HCT 116 tRBM3 cells. We observed that as expected, RBM3 overexpression in a dose and time dependent manner progressively decreases proliferation (Figure 1). This effect was replicated through RBM3 overexpression in a p53 null variant of HCT 116 (HCT $116^{p53-/-}$) (Figure 2). Both HCT 116 with wild type p53 and HCT $116^{p53-/-}$ show decreased proliferation following Dox induction. The overall curves between the two cell lines differ somewhat but we attribute this to differences between RBM3 induction characteristics following transduction of the different cell lines. Interestingly, the cell cycle regulator *p21CIP1/WAF1* showed a significant increase in our whole transcriptome analysis of RBM3 overexpressing HCT 116 cells (Table 1). p21CIP1/WAF1 is a downstream target of p53 and is necessary for maintaining HSCs in a quiescent state (Cheng et al., 2000; Porlan et al., 2013; van Os et al., 2007). We further validated the microarray finding by showing that RBM3 overexpression increases p21CIP1/WAF1 protein and mRNA significantly in HCT 116 tRBM3 cells with no appreciable change in vector control (Figure 3A). Interestingly, this effect was independent of inhibition of GSK3β using BIO implying that RBM3 overexpression induces an upregulation in p21CIP1/WAF1 independent of RBM3 induced β-catenin overactivation (Figure 3B).

We next presumed that if RBM3 overexpression were to modulate the proliferative capacity of colon cancer cells, there may be an effect on the size of spheroid formation *in vitro* and tumor formation *in vivo* following RBM3 overexpression. We initially observed that RBM3 overexpression confers increased capacity to form spheroids in ultra-low attachment conditions (Figure 4B). Interestingly though, while RBM3 overexpressing cells formed a greater number of spheroids, the average diameter of the spheroids formed was smaller than that of uninduced controls (Figure 4A). Additionally, following 72 hours of induction with 500 ng/mL of Dox,

Figure 1

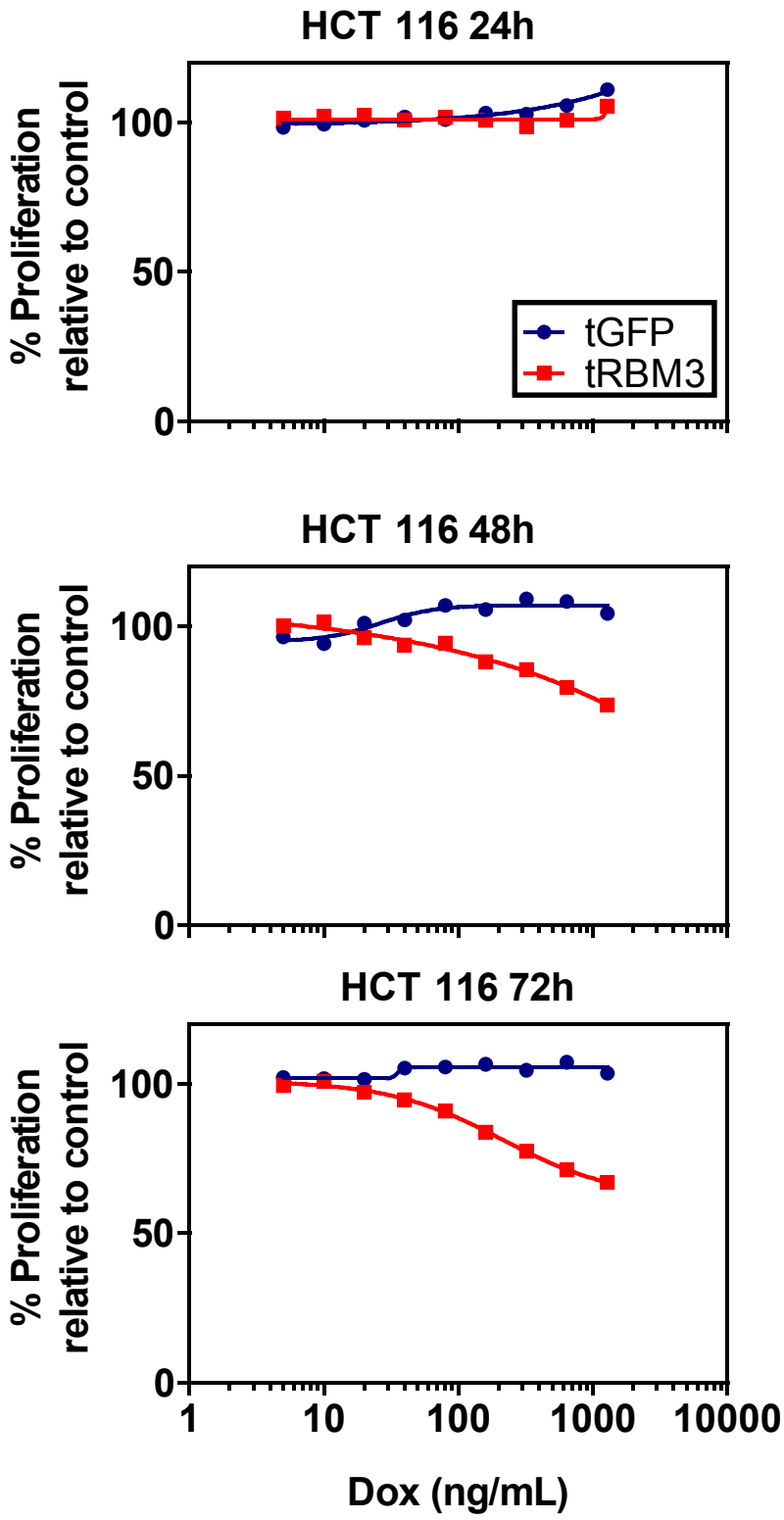
HCT 116 24h
% Proliferation relative to control
100
50
0
tGFP
tRBM3
HCT 116 48h
% Proliferation relative to control
100
50
0
HCT 116 72h
% Proliferation relative to control
100
50
0
1
10
100
1000
10000
Dox (ng/mL)

Figure 1: RBM3 overexpression decreases proliferation in a dose dependent manner. Hexoseaminidase proliferation assay following treatment with Dox showing that RBM3 overexpression decreases proliferation at 48 hours and 72 hours of induction. Proliferation of GFP overexpressing cells remains largely unchanged. Error bars represent SEM.

Figure 2

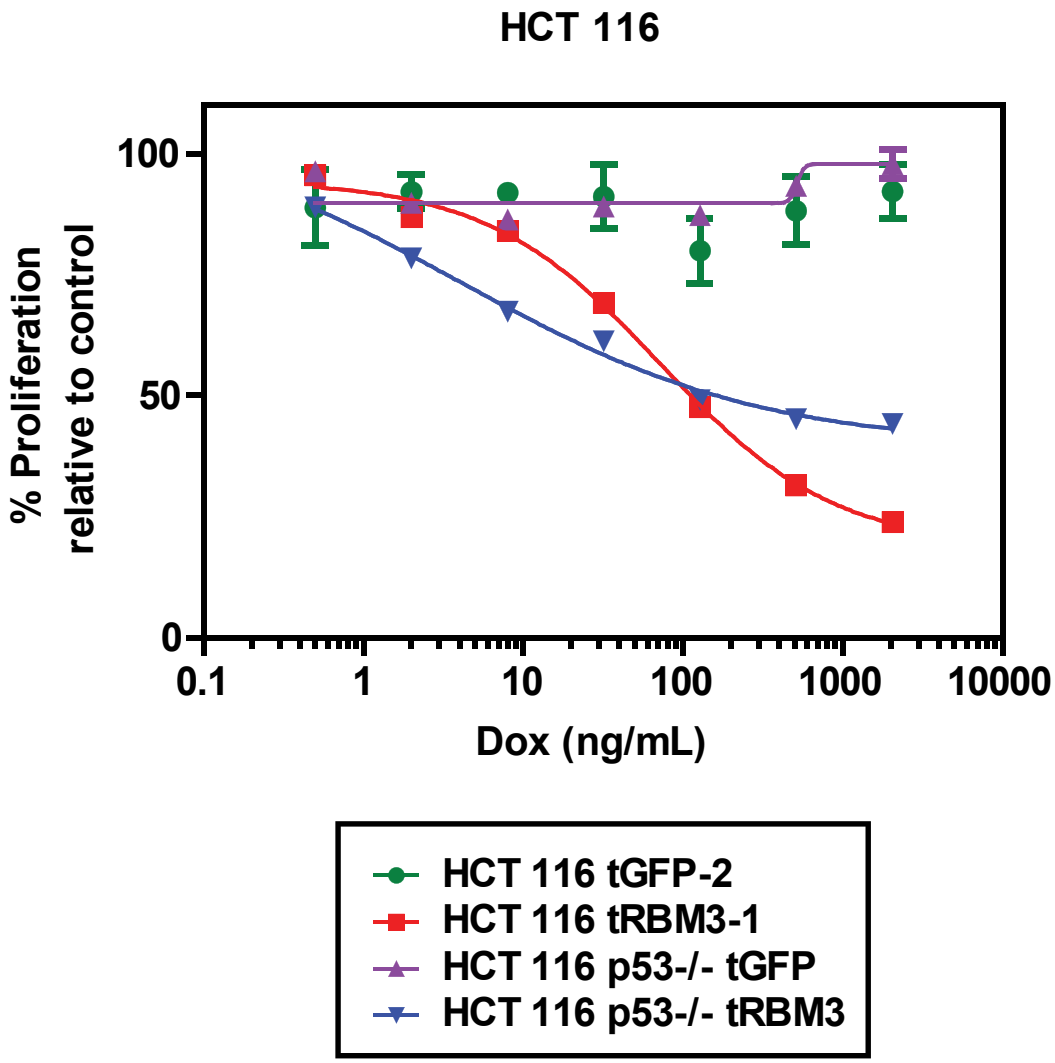
HCT 116
% Proliferation relative to control
100
50
0
0.1
1
10
100
1000
10000
Dox (ng/mL)
HCT 116 tGFP-2
HCT 116 tRBM3-1
HCT 116 p53-/- tGFP
HCT 116 p53-/- tRBM3

Figure 2: RBM3 induced decreases in proliferation are independent of p53. Hexoseaminidase proliferation assay following treatment for 48 hours with Dox showing that RBM3 overexpression decreases proliferation in HCT 116 cells with wild type p53 or p53 knockout. Error bars represent SEM.

Figure 3

Gene Symbol	Description	Fold Change	FDR p-value
CPA4	carboxypeptidase A4	8.73	0.0356
IL8	**interleukin 8**	**2.24**	**0.0298**
TMPRSS11E	transmembrane protease, serine 11E	2.12	0.0326
DUSP5	dual specificity phosphatase 5	2.07	0.0298
RNU6ATAC	RNA, U6atac small nuclear	2.01	0.0495
CTGF	connective tissue growth factor	1.95	0.0437
EMP1	epithelial membrane protein 1	1.84	0.0479
GJB3	gap junction protein, beta 3, 31kDa	1.71	0.0368
SLAMF7	SLAM family member 7	1.67	0.0298
PLK3	polo-like kinase 3	1.64	0.0430
EPHA2	EPH receptor A2	1.61	0.0298
FLNC	filamin C, gamma	1.58	0.0368
MYC	**v-myc myelocytomatosis viral oncogene homolog**	**1.54**	**0.0469**
FHL2	four and a half LIM domains 2	1.53	0.0298
CDKN1A	**cyclin-dependent kinase inhibitor 1A (p21, Cip1)**	**1.48**	**0.0401**

Table 1: Representative table of RBM3 induced genes. The table is a selected list of genes upregulated in HCT 116-tRBM3 cells compared to HCT 116-tGFP cells following 72 hours of induction with 500 ng/mL Dox. mRNA was harvested and analyzed using Human Transcriptome Microarray 2.0 analysis. Shown in bold are genes validated in this study. P values are obtained using ANOVA with false discovery rate correction.

Figure 4

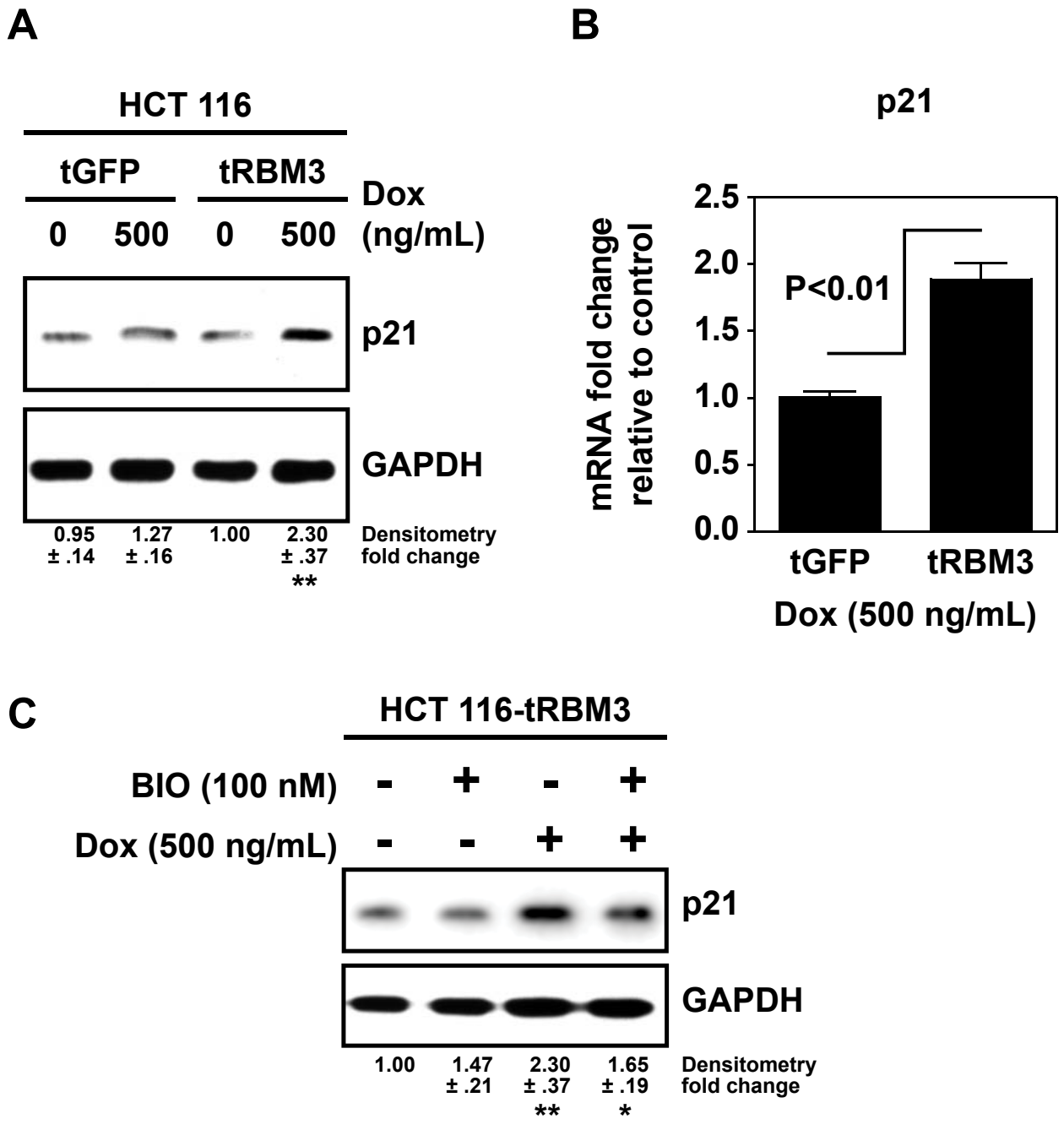
A
HCT 116
tGFP
tRBM3
Dox
0
500
0
500
(ng/mL)
p21
GAPDH
0.95
± .14
1.27
± .16
1.00
2.30
± .37
**
Densitometry
fold change
B
p21
mRNA fold change
relative to control
2.5
2.0
1.5
1.0
0.5
0.0
P<0.01
tGFP
tRBM3
Dox (500 ng/mL)
C
HCT 116-tRBM3
BIO (100 nM)
Dox (500 ng/mL)
- + - +
- - + +
p21
GAPDH
1.00
1.47
± .21
2.30
± .37
**
1.65
± .19
*
Densitometry
fold change

Figure 3: RBM3 overexpression increases p21 expression. **(A)** Western blot analysis of p21CIP1/WAF1 following RBM3 induction with 500 ng/mL Dox for 72 hours showing a significant increase in p21 levels with RBM3 overexpression. **(B)** Real time RT-PCR of *p21CIP1/WAF1* following Dox induction for 72 hours. **(C)** Western blot analysis of p21CIP1/WAF1 following treatment with 500 ng/mL Dox or 100 nM BIO for 72 hours showing a significant increase in p21 levels with RBM3 overexpression but not BIO treatment. Bar graphs represent fold change relative to control. Error bars represent SEM. P values shown are obtained with Student's t-test. Densitometry represents fold change of p21 relative to uninduced tRBM3 cells normalized to GAPDH. Error represents SEM. *P < 0.05, **P < 0.01, ***P < 0.001 (Student's *t*-test).

Figure 5

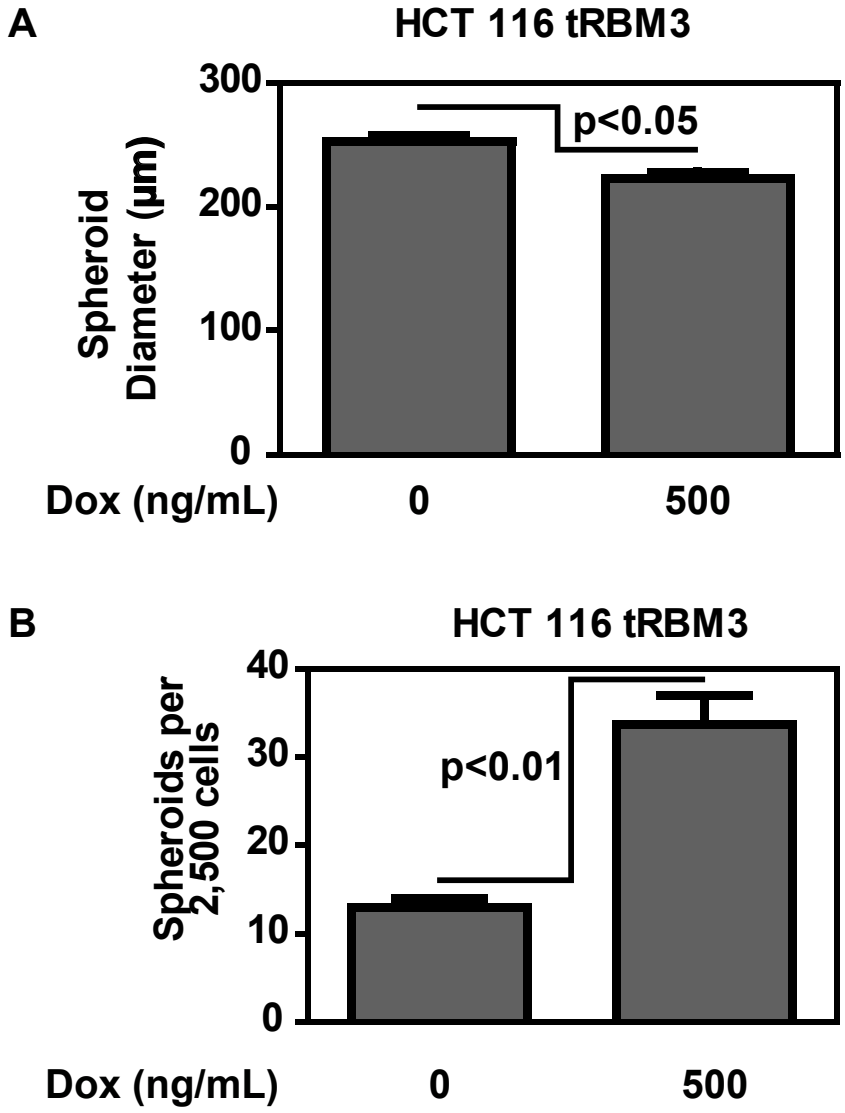
A
HCT 116 tRBM3
300
200
100
0
Spheroid Diameter (µm)
p<0.05
Dox (ng/mL)
0
500
B
HCT 116 tRBM3
40
30
20
10
0
Spheroids per 2,500 cells
p<0.01
Dox (ng/mL)
0
500

Figure 4: RBM3 overexpressing spheroids are greater in number but smaller in size. **(A)** Quantification of average spheroid diameter as performed by Celligo embryoid body counting system. Cells were grown in monolayer culture for 72 hours with inidicated Dox concentration then grown as spheroids for 14 days. Bar graph shows average of the average spheroid diameter of each sample. **(B)** Quantification of average spheroid number following RBM3 induction. Bar graph shows spheroid number from 2,500 seeded cells. Error bars represent SEM. P values shown are obtained with Student's *t*-test.

Figure 6

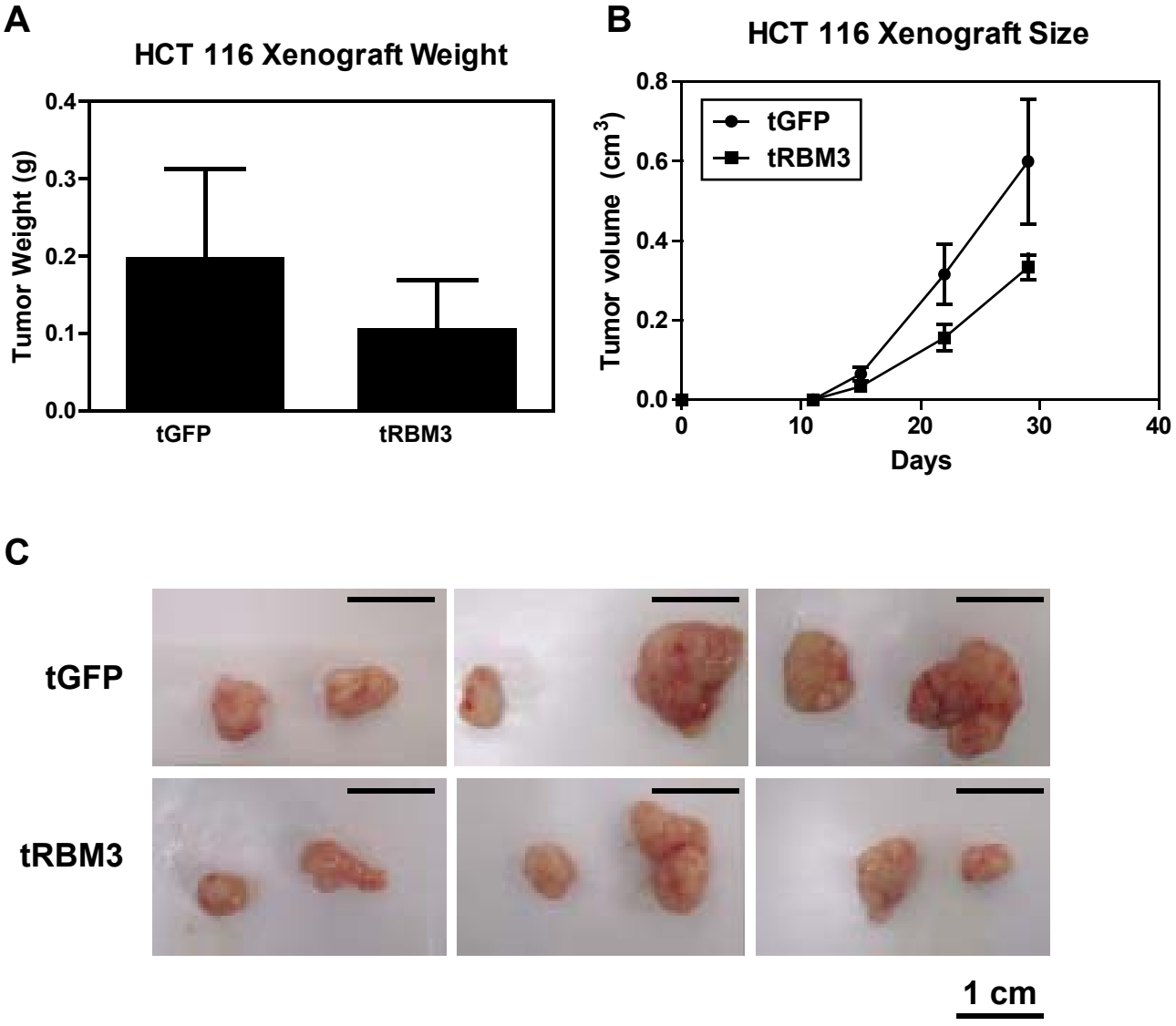
A
HCT 116 Xenograft Weight
Tumor Weight (g)
0.4
0.3
0.2
0.1
0.0
tGFP
tRBM3
B
HCT 116 Xenograft Size
Tumor volume (cm3)
0.8
0.6
0.4
0.2
0.0
tGFP
tRBM3
0
10
20
30
40
Days
C
tGFP
tRBM3
1 cm

Figure 5: RBM3 overexpression decreases proliferation in tumor xenografts. **(A)** Tumor xenograft volume measured at 35 days. HCT 116 tGFP and tRBM3 cells were grown in 500 ng/mL Dox for 72 hours then injected into the flanks of nude mice. **(B)** Tumor xenograft size of HCT 116 cells injected into the flanks of nude mice. **(C)** Images of xenografts collected from mice following 35 days of growth. Scale bar represents 1 cm.

HCT 116 tRBM3 or tGFP cells were injected into the flanks of nude mice to assess tumor xenograft formation. We observed that RBM3 overexpression compared to GFP overexpression generated tumors of decreased size over time and decreased weight following 35 days of tumor formation (Figure 5). This implies that RBM3 decreases cell proliferation *in vitro* and *in vivo*.

We next investigated how RBM3 overexpression alters cell cycle progression. As no significant proliferative changes were observed in HCT 116 tGFP cells following Dox induction, we opted not to investigate cell cycle progression on these cells. We analyzed the cell cycle profile of RBM3 overexpressing HCT 116 tRBM3 cells following 72 hours of induction. Interestingly, RBM3 overexpression generated modest increases in the G0/G1 phase (Figure 6). To further elucidate the effects of RBM3 induction on progression through cell cycle, we used a method established by Coller, *et al.* to discriminate G0 from G1 phase. Treatment with the nucleoside analog BrdU was initiated for 6 hours following 72 hours of RBM3 induction so that only cells which have actively cycled over the past 6 hours will have BrdU incorporated into DNA. Serum starvation was used as a positive control for quiescence. Following 6 hours of BrdU treatment, we observed that RBM3 overexpressing cells had significantly higher levels of quiescent cells and far fewer actively cycling cells (Figure 7). Additionally, DLD-1-tRBM3 cells also showed an increase of quiescent cells with a corresponding decrease in the percentage of cycling cells (Figure 8).

Discussion

Here we show evidence implicating RBM3 in the induction of a quiescent phenotype. It should be noted that previous studies have shown that loss of RBM3 through siRNA mediated

Figure 7

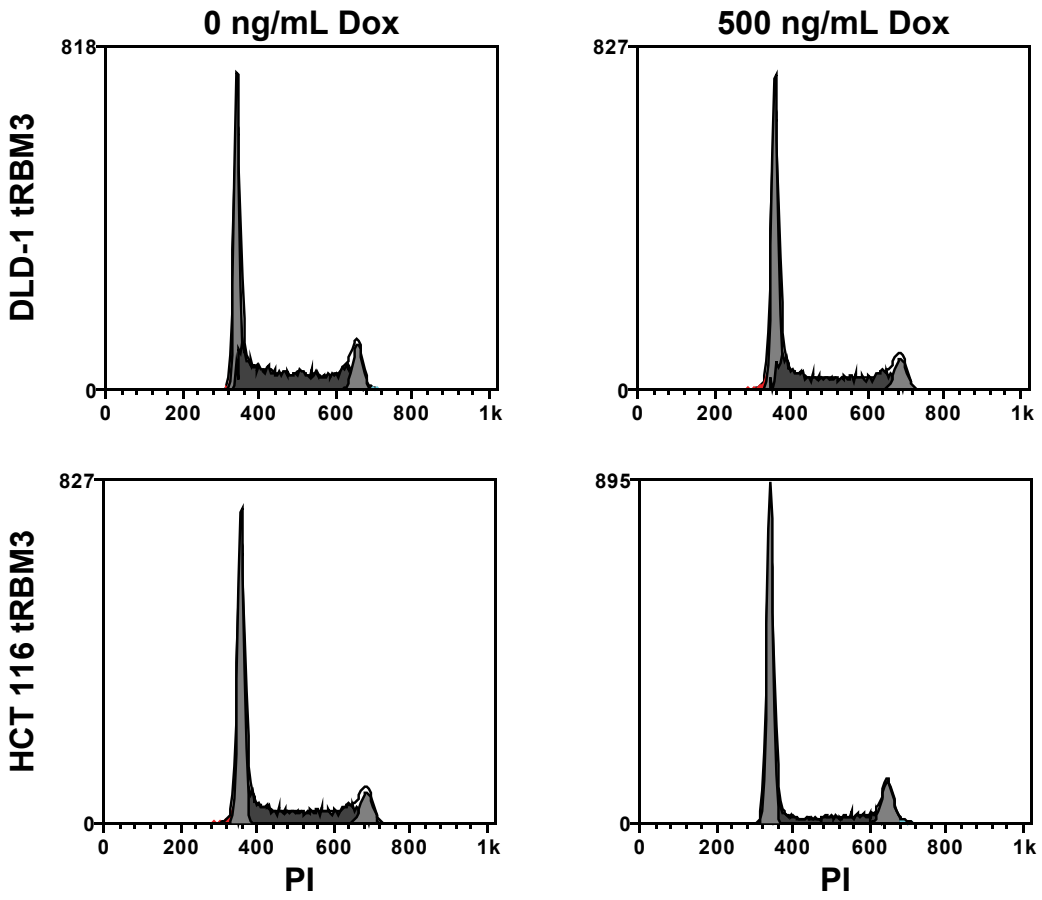
0 ng/mL Dox
500 ng/mL Dox
DLD-1 tRBM3
HCT 116 tRBM3
818
827
827
895
0
0
0
0
0
200
400
600
800
1k
PI
PI

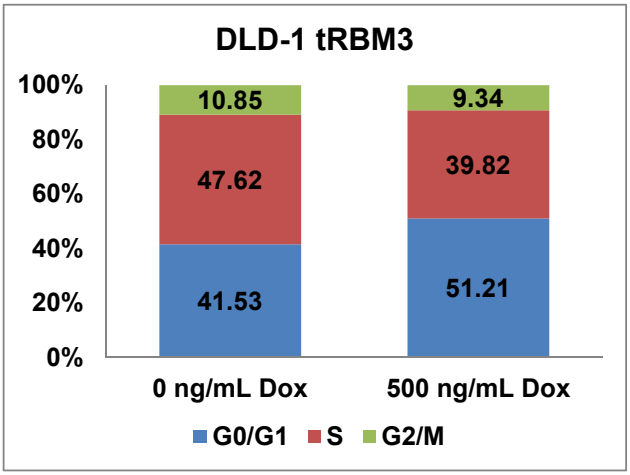
DLD-1 tRBM3
100%
80%
60%
40%
20%
0%
10.85
47.62
41.53
9.34
39.82
51.21
0 ng/mL Dox
500 ng/mL Dox
G0/G1
S
G2/M

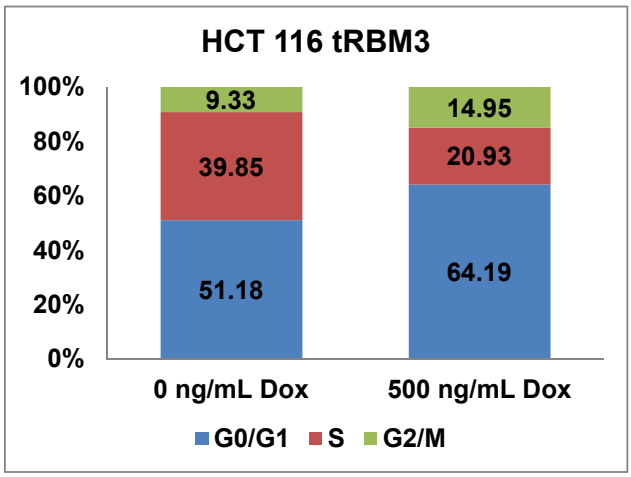
HCT 116 tRBM3
100%
80%
60%
40%
20%
0%
9.33
39.85
51.18
14.95
20.93
64.19
0 ng/mL Dox
500 ng/mL Dox
G0/G1
S
G2/M

Figure 6: RBM3 overexpression induces accumulation of cells at G0/G1 phase. Cell cycle analysis histograms showing that RBM3 overexpressing cells show modest accumulation at G0/G1 phase. Cells were induced with indicated concentrations of Dox for 72 hours then had DNA stained using PI. Cells were then analyzed by flow cytometry for cell cycle. Histogram represents whole and single cells.

Figure 8

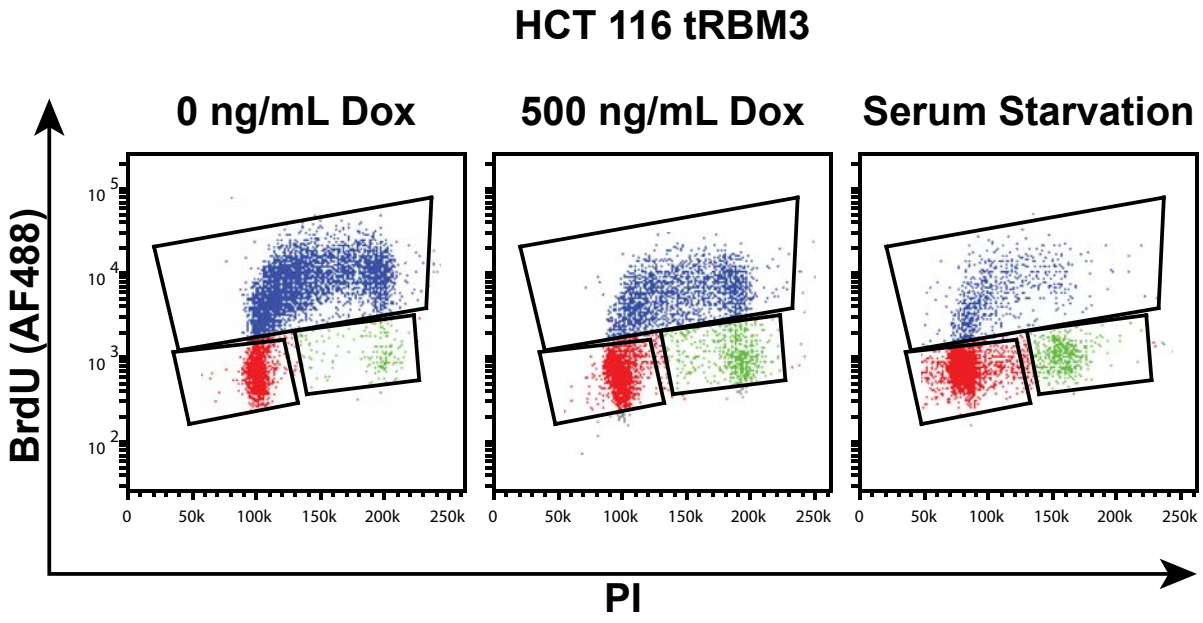
HCT 116 tRBM3
0 ng/mL Dox
500 ng/mL Dox
Serum Starvation
BrdU (AF488)
PI
10 5
10 4
10 3
10 2
0
50k
100k
150k
200k
250k

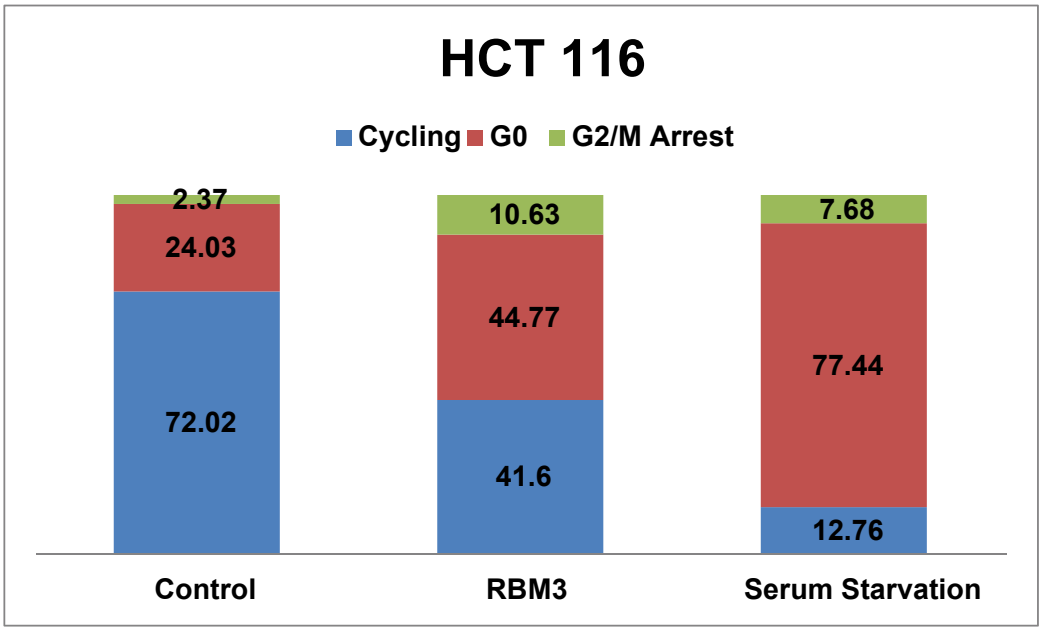
HCT 116
Cycling
G0
G2/M Arrest
2.37
24.03
72.02
10.63
44.77
41.6
7.68
77.44
12.76
Control
RBM3
Serum Starvation

Figure 7: RBM3 overexpression increases quiescence in HCT 116 tRBM3 cells. Cells were induced with indicated concentrations of Dox for 72 hours then treated with BrdU for 6 hours. Cells were then stained for BrdU uptake (AF488). Cycling cells (blue) represent fraction of cells which take up BrdU over 6 hours, quiescent cells (red) represent cells which take up no BrdU over 6 hours. Bar graph shows percentage of gated cells. Serum deprivation is used as a positive control for quiescence.

Figure 11

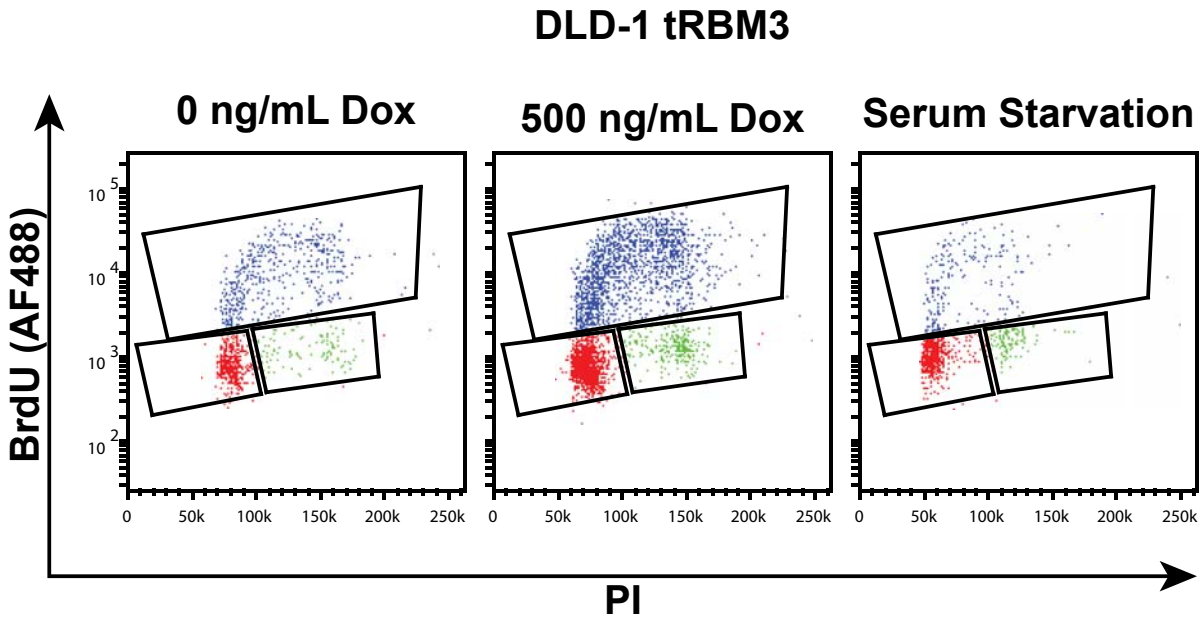
DLD-1 tRBM3
0 ng/mL Dox
500 ng/mL Dox
Serum Starvation
BrdU (AF488)
PI
10 5
10 4
10 3
10 2
0
50k
100k
150k
200k
250k

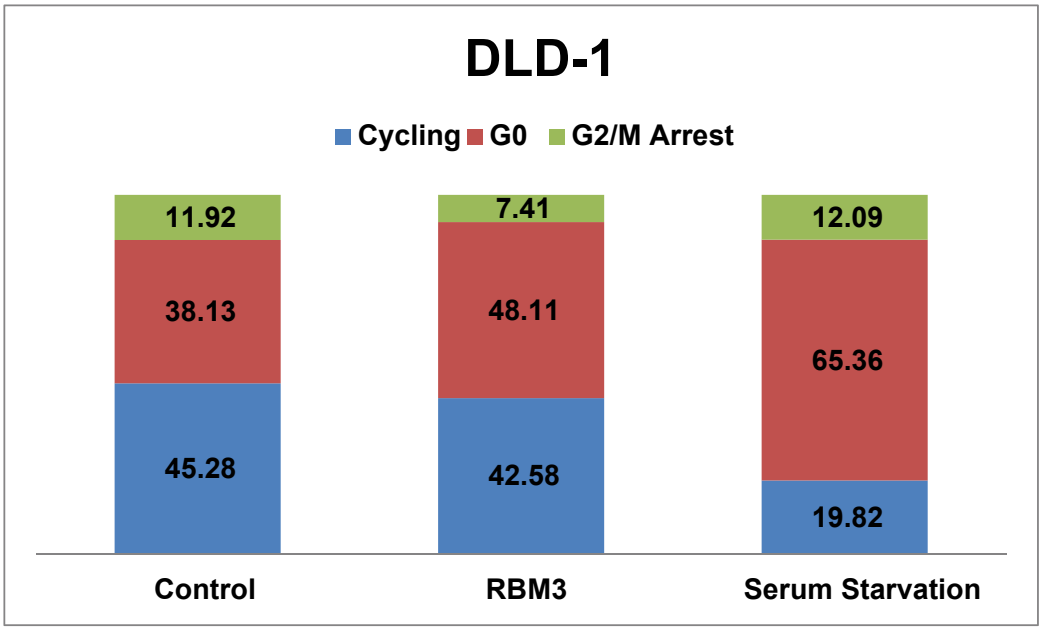
DLD-1
Cycling
G0
G2/M Arrest
11.92
38.13
45.28
7.41
48.11
42.58
12.09
65.36
19.82
Control
RBM3
Serum Starvation

Figure 8: RBM3 overexpression increases quiescence in DLD-1 tRBM3 cells. Cells were induced with indicated concentrations of Dox for 72 hours then treated with BrdU for 6 hours. Cells were then stained for BrdU uptake (AF488).Cycling cells (blue) represent fraction of cells which take up BrdU over 6 hours, quiescent cells (red) represent cells which take up no BrdU over 6 hours. Bar graph shows percentage of gated cells. Serum deprivation is used as a positive control for quiescence.

knockdown results in cells undergoing mitotic catastrophe (Sureban et al., 2008b). Mitotic catastrophe is a phenomenon where cells enter the G2/M phase of cell cycle promiscuously and undergo apoptosis. This implies that the levels of RBM3 show a dose dependent correlation with the overall levels of proliferation and cell cycle progression and that RBM3 could be heavily involved in cell cycle regulation.

While the mechanism behind RBM3 induced quiescence is still unclear, it is possible that RBM3 directly regulates p21CIP1/WAF1, a cell cycle regulatory protein that is critical for inducing quiescence (Cheng et al., 2000; Porlan et al., 2013; van Os et al., 2007). p21CIP1/WAF1 also plays a role in halting cell cycle progression to allow for DNA repair, thereby increasing resistance to genotoxic insults (Abbas and Dutta, 2009). Additionally, it appears that the RBM3 induced quiescent phenotype persists in the absence of p53 further implicated a direct interaction between RBM3 and p21CIP1/WAF1. It is interesting to observe that RBM3 induced quiescence appears independent of p53. However, p21 a downstream target of p53 is induced implying that RBM3 may alter p21 levels at the post-transcriptional level (Beckerman and Prives, 2010). This theory is not without precedent. Previous studies have shown that the RNA binding protein HuR shares similar mRNA binding clients as RBM3 and both seem to have affinity towards AU-rich sequence elements (Sureban et al., 2008b; Young et al., 2009). Notably, one study has shown that following stress conditions, HuR can bind to p21CIP1/WAF1 mRNA and increase mRNA half-life and protein levels (Wang et al., 2000). As RBM3 seems to upregulate p21CIP1/WAF1 expression, it is possible that RBM3 overexpression alters mRNA stability or translation rate of p21CIP1/WAF1 to induce cellular quiescence.

We also note that in the previous chapter, we showed that RBM3 overexpression can generate an increase in the migratory phenotype in HCT 116 cells (Chapter 3, Figure 6). It has been

previously demonstrated that nuclear β-catenin levels are highly correlative with invasiveness (Brabletz et al., 1998). Interestingly, these invasive cells also show a decrease in proliferative index implying that the invasiveness program is also associated with quiescence (Jung et al., 2001). However, as RBM3 induced p21CIP1/WAF1 expression is not phenocopied by BIO treatment to overeactivate β-catenin, it may be that RBM3 induced β-catenin activation and quiescence may be independent effects which may act in parallel to accentuate certain phenotypes such as invasion and migration. Taken together, our findings indicating that RBM3 overexpression increases both invasiveness and quiescence implies that RBM3 induction may be associated with more phenotypic characteristics that have yet to be observed.

Hypoxia has also been shown to induce quiescence in a HIF-1α dependent manner (Takubo et al., 2010). It is possible that RBM3 is also involved in hypoxia induced quiescence either acting through HIF-1α regulation or in parallel with it. It is reasonable to infer that because RBM3 generates protective effects to stressors such as hypoxia, cold shock and serum deprivation, it may play a role in inducing quiescence to preserve cell function in a nutrient deprived environment through decreased cellular activity and nutrient consumption. By doing so, RBM3 may serve as a double edged sword which decreases proliferation of a tumor, but increases its resistance to genotoxic therapies. It would be interesting to investigate if siRNA mediated knock down of *p21CIP1/WAF1* could attenuate the RBM3 mediated chemoresistance to cell cycle specific therapies such a paclitaxel. Further studies are needed to validate this idea.

Chapter V: Conclusions and Significance

The intestinal epithelium is one of the fastest renewing tissues within the adult. This renewal is driven by the proliferation of a transit amplifying compartment which is in turn derived from stem cells residing within the intestinal crypts. The homeostasis of the ISC compartment needs to be tightly regulated and loss of this regulation often leads to the formation of malignant neoplasia. These transformed adenomas and adenocarcinomas harbor a small CSC population that displays characteristics implicating more aggressive disease such as tumor initiation capacity and multidrug resistance. A thorough understanding of the mechanisms that govern the behavior of the CSC pool may lead to more effective therapies for combating colon cancer.

The β-catenin signaling cascade is a critical pathway involved in the maintenance of self-renewal in the ISC (Brabletz et al., 2009; Burgess et al., 2011; Medema and Vermeulen, 2011; van der Flier and Clevers, 2009). Loss of regulation of β-catenin signaling, either through truncating mutation of *APC* or overactivating mutation of β-catenin, has been shown to be present in the majority of colon cancers implicating it as the initiating step in neoplastic transformation (Fearon and Vogelstein, 1990; Groden et al., 1991; Kinzler and Vogelstein, 1997; Morin et al., 1997; Moser et al., 1990). Moreover, knocking out the tumor suppressor *Apc* in ISCs compared to epithelium fated to terminally differentiate, results in a more profound tumorigenesis in the mouse intestine (Barker et al., 2009). This overactivation of β-catenin has been implicated in the progression of colon cancers by increasing characteristics such as invasiveness and chemoresistance (Brabletz et al., 2009; Kanwar et al., 2010).

The RNA binding protein RBM3 has been shown to induce oncogenic transformation *in vitro* and has been shown to be a necessary component in the maintenance of tumor xenografts *in vivo* (Sureban et al., 2008b). RBM3 has been shown to be upregulated as neoplasias progress to higher stages in astrocytoma, colon and prostate cancer implicating significant correlation

between RBM3 expression and cancer aggressiveness (Shaikhibrahim et al., 2013; Sureban et al., 2008b; Zhang et al., 2013). In prostate cancer, it has also been shown to be an independent prognostic factor linked to increased chemical recurrence and decreased overall survival (Grupp et al., 2013). RBM3 also appears to be closely related to stem cells as it is observed to be upregulated in HSC (Baghdoyan et al., 2000). Moreover, similar to CSCs being enriched in hypoxic environments, RBM3 is induced by hypoxia (Wellmann et al., 2004). However, these studies fall short in examining the exact causative role of RBM3 in modulating the behavior of cancers in general and more specifically CSCs.

In this study, we investigated the link between RBM3 and the colon CSC. We initiated these studies by validating that exogenous RBM3 overexpression increased the percentage of cells that behave with stem cell characteristics. We verified this using two separate functional assays as well as measuring changes in the expression of putative stem cell markers. As a secondary consequence of the stem cell phenotype, we showed that RBM3 overexpression generates chemoresistance through the upregulation of multidrug efflux activity. We went on to demonstrate that RBM3 is capable of modulating the β-catenin signaling pathway through alteration of GSK3β activity and implicated the PI3K-AKT axis as a potential mechanistic explanation. Finally, we investigated a paradoxical effect of RBM3 overexpression which induces the phenotype of quiescence, a primary characteristic of CSCs and an additional mechanism of chemoresistance. The findings presented here further our understanding of the factors that govern stem cell behavior by demonstrating a novel role for RBM3 in modulating the population colon CSC population. Additionally these findings present new avenues to explore for predicting and potentially overcoming recurrences and chemotherapy refractory malignant neoplasias.

Chapter II: Overexpression of RBM3 increases stem cell characteristics and chemoresistance in colon cancer cells

Previous studies have demonstrated that RBM3 is overexpressed in neoplastic tissue compared to normal adjacent controls (Grupp et al., 2013; Shaikhibrahim et al., 2013; Sureban et al., 2008b; Zhang et al., 2013). To establish a causative link between RBM3 and cancer, we exogenously overexpressed RBM3 in HCT 116 and DLD-1 colon cancer cells and characterized the expression kinetics with the Dox inducible system.

First, we showed that Dox induction of RBM3 induced an increase in the SP percentage in both DLD-1 and HCT 116 cells implying that RBM3 overexpression generates an increased population of cells with efflux capacity. We validated this finding by demonstrating that RBM3 overexpression results in decreased ADM uptake and increased ADM efflux in HCT 116 cells and that this efflux appears to be largely attributed to a small subset of cells. This was consistent with our finding that RBM3 induction also generated an increase in mRNA transcripts for MRP2 and Pgp efflux transporters. This is finally confirmed by the finding that RBM3 overexpressing cells are resistant to treatment with paclitaxel and ADM which are substrates of Pgp and MRP2.

Second, we showed that RBM3 overexpression generated an increase in spheroid formation capacity in both DLD-1 and HCT 116 cells. As spheroid formation capacity is an *in vitro* marker of "stemness", this further confirmed that RBM3 induces a stem cell phenotype. Finally, we showed that RBM3 overexpression increased the percentage of cells with expression of the putative stem cell markers DCLK1, LGR5 and CD44.

Taken together, we conclude that RBM3 overexpression increases the percentage of stem-like cells within a given population of colon cancer cells and that this is correlated with an increase in resistance to classical chemotherapies through increase of efflux. This implies that the increased expression of RBM3 that has been observed in various solid tumors may serve a role in altering the regulation of the CSC population to generate a more aggressive and more chemoresistant tumor.

Chapter III: RBM3 overexpression generates an increase in β-catenin signaling

β-catenin signaling is a critical pathway for colon CSCs and is also known to drive transcription of LGR5 and CD44 mRNA (Barker et al., 2007; Kanwar et al., 2010; Wielenga et al., 1999). To establish a potential signaling mechanism through which RBM3 overexpression may generate an increased stem cell phenotype, we overexpressed RBM3 in HCT 116 and DLD-1 cells and measured changes in β-catenin activity.

We observed that RBM3 overexpression in both DLD-1 and HCT 116 cell lines resulted in a significant increase in total and nuclear β-catenin levels with no significant changes in cytoplasmic β-catenin levels. This was validated through IF and IHC staining of RBM3 overexpressing cells demonstrating that cells with high levels of nuclear RBM3 also had increased nuclear localization of β-catenin. We also observed that prolonged overexpression of RBM3 generated an increase in wound healing capacity, a known phenotype of β-catenin induced EMT. We also validated that this RBM3- induced upregulation in nuclear β-catenin results in increased transcriptional activity by demonstrating higher levels of *c-MYC*, *LGR5* and

CD44 mRNA. Moreover, we showed that RBM3 overexpression increases TOPFlash luciferase reporter activity in both DLD-1 and HCT 116 cells.

To elucidate a potential molecular mechanism for this RBM3 induced β-catenin activity, we showed that RBM3 overexpression results in increased AKT activity and a decreased GSK3β activity. In confirmation of this, we showed that pharmacologic inhibition of GSK3β using BIO was capable of phenocopying the RBM3 induced β-catenin activity as measured by nuclear β-catenin and TOPFlash activity. Interestingly however, we also observed that concurrent RBM3 overexpression and pharmacologic GSK3β inhibition using BIO further increases β-catenin activity implying a second molecular mechanism.

Taken together, we conclude from these studies that RBM3 overexpression is a novel regulatory factor of the β-catenin signaling cascade. While further studies are needed to further understand the mechanism of RBM3 action, we implicate the enhanced β-catenin activity as a causative mechanism in the increases observed in stem cell phenotype following RBM3 induction.

Chapter IV: RBM3 induces a quiescent state in colon cancer cells

Quiescence is a hallmark of physiologic ISCs as well as CSCs (Borst, 2012; Buczacki et al., 2011; Dick, 2008; Li and Bhatia, 2011; Touil et al., 2013). Furthermore, Wnt/β-catenin signaling has been heavily implicated in self-renewal and quiescence for long term maintenance of HSCs (Fleming et al., 2008; Nemeth et al., 2009; Povinelli and Nemeth, 2014). Our previous studies demonstrated RBM3 overexpression increases β-catenin signaling and the CSC population in HCT 116 and DLD-1 colon cancer cells.

Here, we showed that RBM3 overexpression generates a decrease in cell proliferation. This was observed in both monolayer and spheroid cultures. Additionally, we observed a decrease in proliferation in tumor xenografts. This decrease in proliferation appears independent of p53 status. However, RBM3 overexpression did induce an upregulation in the cell cycle control protein p21CIP1/WAF1. Moreover, RBM3 overexpression generated modest accumulation of cells at the G0/G1 phase. Upon resolution of G0 and G1 phases using nucleotide uptake and flow cytometric analysis, we observed that this accumulation appears to be predominantly within the G0 phase. These findings are consistent with earlier findings of RBM3 induced chemoresistance as cellular quiescence is an established mechanism for inducing resistance in CSCs.

Taken together, we conclude that RBM3 induces decreased cellular proliferation in colon cancer cells which is primarily attributed to cellular quiescence and that this may be an additional mechanism of RBM3 induced chemoresistance. As previous studies have also shown that loss of RBM3 is associated with premature entry into cell cycle followed by apoptosis, we infer that RBM3 may play a central role in cell cycle regulation (Sureban et al., 2008b).

Significance

Previous studies have shown that RBM3 appears to be capable of inducing oncogenic transformation and that it is correlated with increased aggressiveness. To our knowledge, we are the first to show causative evidence of RBM3 in the initiation and progression of colon cancer. We demonstrate that RBM3 can induce a CSC phenotype which is thought to be the tumor initiating population. Additionally, we show that RBM3 is a novel factor capable of modulating β-catenin signaling activity, a pathway critical to initiation and progression of colon cancer.

These findings further our understanding of the mechanisms that govern the behavior of tumors, specifically the subpopulation of CSCs. With additional research, these findings may have tremendous clinical implications as well. The finding that RBM3 induces resistance to chemotherapies indicates the potential for RBM3 to be used as a predictive marker to evaluate responsiveness to various chemotherapies. Moreover, it may well be a new molecular target to exploit as a treatment strategy for colon cancers.

Chapter VI: References

Abbas, T., and Dutta, A. (2009). p21 in cancer: intricate networks and multiple activities. Nature reviews Cancer *9*, 400-414.

Al-Hajj, M., Wicha, M.S., Benito-Hernandez, A., Morrison, S.J., and Clarke, M.F. (2003). Prospective identification of tumorigenic breast cancer cells. Proc Natl Acad Sci U S A *100*, 3983-3988.

Ambros, V., and Horvitz, H.R. (1984). Heterochronic mutants of the nematode Caenorhabditis elegans. Science *226*, 409-416.

Baghdoyan, S., Dubreuil, P., Eberle, F., and Gomez, S. (2000). Capture of cytokine-responsive genes (NACA and RBM3) using a gene trap approach. Blood *95*, 3750-3757.

Barker, N., Ridgway, R.A., van Es, J.H., van de Wetering, M., Begthel, H., van den Born, M., Danenberg, E., Clarke, A.R., Sansom, O.J., and Clevers, H. (2009). Crypt stem cells as the cells-of-origin of intestinal cancer. Nature *457*, 608-611.

Barker, N., van Es, J.H., Kuipers, J., Kujala, P., van den Born, M., Cozijnsen, M., Haegebarth, A., Korving, J., Begthel, H., Peters, P.J., *et al.* (2007). Identification of stem cells in small intestine and colon by marker gene Lgr5. Nature *449*, 1003-1007.

Barrios-Rodiles, M., Tiraloche, G., and Chadee, K. (1999). Lipopolysaccharide modulates cyclooxygenase-2 transcriptionally and posttranscriptionally in human macrophages independently from endogenous IL-1 beta and TNF-alpha. J Immunol *163*, 963-969.

Beckerman, R., and Prives, C. (2010). Transcriptional regulation by p53. Cold Spring Harb Perspect Biol *2*, a000935.

Bilic, J., Huang, Y.L., Davidson, G., Zimmermann, T., Cruciat, C.M., Bienz, M., and Niehrs, C. (2007). Wnt induces LRP6 signalosomes and promotes dishevelled-dependent LRP6 phosphorylation. Science *316*, 1619-1622.

Bisson, I., and Prowse, D.M. (2009). WNT signaling regulates self-renewal and differentiation of prostate cancer cells with stem cell characteristics. Cell Res *19*, 683-697.

Bixby, D., and Talpaz, M. (2011). Seeking the causes and solutions to imatinib-resistance in chronic myeloid leukemia. Leukemia : official journal of the Leukemia Society of America, Leukemia Research Fund, UK *25*, 7-22.

Borst, P. (2012). Cancer drug pan-resistance: pumps, cancer stem cells, quiescence, epithelial to mesenchymal transition, blocked cell death pathways, persisters or what? Open biology *2*, 120066.

Borst, P., Evers, R., Kool, M., and Wijnholds, J. (1999). The multidrug resistance protein family. Biochim Biophys Acta *1461*, 347-357.

Brabletz, S., Schmalhofer, O., and Brabletz, T. (2009). Gastrointestinal stem cells in development and cancer. J Pathol *217*, 307-317.

Brabletz, T., Herrmann, K., Jung, A., Faller, G., and Kirchner, T. (2000). Expression of nuclear beta-catenin and c-myc is correlated with tumor size but not with proliferative activity of colorectal adenomas. Am J Pathol *156*, 865-870.

Brabletz, T., Jung, A., Hermann, K., Gunther, K., Hohenberger, W., and Kirchner, T. (1998). Nuclear overexpression of the oncoprotein beta-catenin in colorectal cancer is localized predominantly at the invasion front. Pathology, research and practice *194*, 701-704.

Buczacki, S., Davies, R.J., and Winton, D.J. (2011). Stem cells, quiescence and rectal carcinoma: an unexplored relationship and potential therapeutic target. Br J Cancer *105*, 1253-1259.

Buick, R.N., and Pollak, M.N. (1984). Perspectives on clonogenic tumor cells, stem cells, and oncogenes. Cancer Res *44*, 4909-4918.

Burgess, A.W., Faux, M.C., Layton, M.J., and Ramsay, R.G. (2011). Wnt signaling and colon tumorigenesis--a view from the periphery. Exp Cell Res *317*, 2748-2758.

Campeau, E., Ruhl, V.E., Rodier, F., Smith, C.L., Rahmberg, B.L., Fuss, J.O., Campisi, J., Yaswen, P., Cooper, P.K., and Kaufman, P.D. (2009). A versatile viral system for expression and depletion of proteins in mammalian cells. PLoS One *4*, e6529.

Cavallo, R.A., Cox, R.T., Moline, M.M., Roose, J., Polevoy, G.A., Clevers, H., Peifer, M., and Bejsovec, A. (1998). Drosophila Tcf and Groucho interact to repress Wingless signalling activity. Nature *395*, 604-608.

Chau, W.K., Ip, C.K., Mak, A.S., Lai, H.C., and Wong, A.S. (2013). c-Kit mediates chemoresistance and tumor-initiating capacity of ovarian cancer cells through activation of Wnt/beta-catenin-ATP-binding cassette G2 signaling. Oncogene *32*, 2767-2781.

Cheng, H., and Leblond, C.P. (1974). Origin, differentiation and renewal of the four main epithelial cell types in the mouse small intestine. V. Unitarian Theory of the origin of the four epithelial cell types. The American journal of anatomy *141*, 537-561.

Cheng, T., Rodrigues, N., Shen, H., Yang, Y., Dombkowski, D., Sykes, M., and Scadden, D.T. (2000). Hematopoietic stem cell quiescence maintained by p21cip1/waf1. Science *287*, 1804-1808.

Chiba, T., Kita, K., Zheng, Y.W., Yokosuka, O., Saisho, H., Iwama, A., Nakauchi, H., and Taniguchi, H. (2006). Side population purified from hepatocellular carcinoma cells harbors cancer stem cell-like properties. Hepatology *44*, 240-251.

Chikazawa, N., Tanaka, H., Tasaka, T., Nakamura, M., Tanaka, M., Onishi, H., and Katano, M. (2010). Inhibition of Wnt signaling pathway decreases chemotherapy-resistant side-population colon cancer cells. Anticancer Res *30*, 2041-2048.

Chip, S., Zelmer, A., Ogunshola, O.O., Felderhoff-Mueser, U., Nitsch, C., Buhrer, C., and Wellmann, S. (2011). The RNA-binding protein RBM3 is involved in hypothermia induced neuroprotection. Neurobiology of disease *43*, 388-396.

Christgen, M., Ballmaier, M., Bruchhardt, H., von Wasielewski, R., Kreipe, H., and Lehmann, U. (2007). Identification of a distinct side population of cancer cells in the Cal-51 human breast carcinoma cell line. Molecular and cellular biochemistry *306*, 201-212.

Cok, S.J., Acton, S.J., Sexton, A.E., and Morrison, A.R. (2004). Identification of RNA-binding proteins in RAW 264.7 cells that recognize a lipopolysaccharide-responsive element in the 3-untranslated region of the murine cyclooxygenase-2 mRNA. J Biol Chem *279*, 8196-8205.

Coller, H.A., Sang, L., and Roberts, J.M. (2006). A new description of cellular quiescence. PLoS Biol *4*, e83.

D'Uva, G., Bertoni, S., Lauriola, M., De Carolis, S., Pacilli, A., D'Anello, L., Santini, D., Taffurelli, M., Ceccarelli, C., Yarden, Y.*, et al.* (2013). Beta-catenin/HuR post-transcriptional machinery governs cancer stem cell features in response to hypoxia. PLoS One *8*, e80742.

Dalerba, P., Dylla, S.J., Park, I.K., Liu, R., Wang, X., Cho, R.W., Hoey, T., Gurney, A., Huang, E.H., Simeone, D.M.*, et al.* (2007). Phenotypic characterization of human colorectal cancer stem cells. Proc Natl Acad Sci U S A *104*, 10158-10163.

Danno, S., Itoh, K., Matsuda, T., and Fujita, J. (2000). Decreased expression of mouse Rbm3, a cold-shock protein, in Sertoli cells of cryptorchid testis. Am J Pathol *156*, 1685-1692.

Danno, S., Nishiyama, H., Higashitsuji, H., Yokoi, H., Xue, J.H., Itoh, K., Matsuda, T., and Fujita, J. (1997). Increased transcript level of RBM3, a member of the glycine-rich RNA-binding protein family, in human cells in response to cold stress. Biochem Biophys Res Commun *236*, 804-807.

Dean, M., Fojo, T., and Bates, S. (2005). Tumour stem cells and drug resistance. Nature reviews Cancer *5*, 275-284.

Deng, S., Yang, X., Lassus, H., Liang, S., Kaur, S., Ye, Q., Li, C., Wang, L.P., Roby, K.F., Orsulic, S.*, et al.* (2010). Distinct expression levels and patterns of stem cell marker, aldehyde dehydrogenase isoform 1 (ALDH1), in human epithelial cancers. PLoS One *5*, e10277.

Derry, J.M., Kerns, J.A., and Francke, U. (1995). RBM3, a novel human gene in Xp11.23 with a putative RNA-binding domain. Hum Mol Genet *4*, 2307-2311.

Dick, J.E. (2008). Stem cell concepts renew cancer research. Blood *112*, 4793-4807.

Ding, L., Ley, T.J., Larson, D.E., Miller, C.A., Koboldt, D.C., Welch, J.S., Ritchey, J.K., Young, M.A., Lamprecht, T., McLellan, M.D.*, et al.* (2012). Clonal evolution in relapsed acute myeloid leukaemia revealed by whole-genome sequencing. Nature *481*, 506-510.

Dontu, G., Abdallah, W.M., Foley, J.M., Jackson, K.W., Clarke, M.F., Kawamura, M.J., and Wicha, M.S. (2003). In vitro propagation and transcriptional profiling of human mammary stem/progenitor cells. Genes Dev *17*, 1253-1270.

Dorsam, R.T., and Gutkind, J.S. (2007). G-protein-coupled receptors and cancer. Nature reviews Cancer *7*, 79-94.

Dresios, J., Aschrafi, A., Owens, G.C., Vanderklish, P.W., Edelman, G.M., and Mauro, V.P. (2005). Cold stress-induced protein Rbm3 binds 60S ribosomal subunits, alters microRNA levels, and enhances global protein synthesis. Proc Natl Acad Sci U S A *102*, 1865-1870.

Dylla, S.J., Beviglia, L., Park, I.K., Chartier, C., Raval, J., Ngan, L., Pickell, K., Aguilar, J., Lazetic, S., Smith-Berdan, S.*, et al.* (2008). Colorectal cancer stem cells are enriched in xenogeneic tumors following chemotherapy. PLoS One *3*, e2428.

Fearon, E.R., and Vogelstein, B. (1990). A genetic model for colorectal tumorigenesis. Cell *61*, 759-767.

Ferry, A.L., Vanderklish, P.W., and Dupont-Versteegden, E.E. (2011). Enhanced survival of skeletal muscle myoblasts in response to overexpression of cold shock protein RBM3. Am J Physiol Cell Physiol *301*, C392-402.

Fialkow, P.J., Jacobson, R.J., and Papayannopoulou, T. (1977). Chronic myelocytic leukemia: clonal origin in a stem cell common to the granulocyte, erythrocyte, platelet and monocyte/macrophage. The American journal of medicine *63*, 125-130.

Flahaut, M., Meier, R., Coulon, A., Nardou, K.A., Niggli, F.K., Martinet, D., Beckmann, J.S., Joseph, J.M., Muhlethaler-Mottet, A., and Gross, N. (2009). The Wnt receptor FZD1 mediates chemoresistance in neuroblastoma through activation of the Wnt/beta-catenin pathway. Oncogene *28*, 2245-2256.

Fleming, H.E., Janzen, V., Lo Celso, C., Guo, J., Leahy, K.M., Kronenberg, H.M., and Scadden, D.T. (2008). Wnt signaling in the niche enforces hematopoietic stem cell quiescence and is necessary to preserve self-renewal in vivo. Cell stem cell *2*, 274-283.

Fodde, R., and Brabletz, T. (2007). Wnt/beta-catenin signaling in cancer stemness and malignant behavior. Current opinion in cell biology *19*, 150-158.

Fodde, R., Edelmann, W., Yang, K., van Leeuwen, C., Carlson, C., Renault, B., Breukel, C., Alt, E., Lipkin, M., Khan, P.M.*, et al.* (1994). A targeted chain-termination mutation in the mouse Apc gene results in multiple intestinal tumors. Proc Natl Acad Sci U S A *91*, 8969-8973.

Gaspar, C., and Fodde, R. (2004). APC dosage effects in tumorigenesis and stem cell differentiation. Int J Dev Biol *48*, 377-386.

Ghosh, M., Aguila, H.L., Michaud, J., Ai, Y., Wu, M.T., Hemmes, A., Ristimaki, A., Guo, C., Furneaux, H., and Hla, T. (2009). Essential role of the RNA-binding protein HuR in progenitor cell survival in mice. J Clin Invest *119*, 3530-3543.

Giannakis, M., Stappenbeck, T.S., Mills, J.C., Leip, D.G., Lovett, M., Clifton, S.W., Ippolito, J.E., Glasscock, J.I., Arumugam, M., Brent, M.R.*, et al.* (2006). Molecular properties of adult

mouse gastric and intestinal epithelial progenitors in their niches. J Biol Chem *281*, 11292-11300.

Goodell, M.A., Brose, K., Paradis, G., Conner, A.S., and Mulligan, R.C. (1996). Isolation and functional properties of murine hematopoietic stem cells that are replicating in vivo. J Exp Med *183*, 1797-1806.

Gougelet, A., and Colnot, S. (2012). A Complex Interplay between Wnt/beta-Catenin Signalling and the Cell Cycle in the Adult Liver. International journal of hepatology *2012*, 816125.

Griffiths, D.F., Davies, S.J., Williams, D., Williams, G.T., and Williams, E.D. (1988). Demonstration of somatic mutation and colonic crypt clonality by X-linked enzyme histochemistry. Nature *333*, 461-463.

Groden, J., Thliveris, A., Samowitz, W., Carlson, M., Gelbert, L., Albertsen, H., Joslyn, G., Stevens, J., Spirio, L., Robertson, M., *et al.* (1991). Identification and characterization of the familial adenomatous polyposis coli gene. Cell *66*, 589-600.

Grupp, K., Wilking, J., Prien, K., Hube-Magg, C., Sirma, H., Simon, R., Steurer, S., Budaus, L., Haese, A., Izbicki, J., *et al.* (2013). High RNA-binding motif protein 3 expression is an independent prognostic marker in operated prostate cancer and tightly linked to ERG activation and PTEN deletions. Eur J Cancer.

Hall, P.A., Coates, P.J., Ansari, B., and Hopwood, D. (1994). Regulation of cell number in the mammalian gastrointestinal tract: the importance of apoptosis. J Cell Sci *107 (Pt 12)*, 3569-3577.

Haraguchi, N., Inoue, H., Tanaka, F., Mimori, K., Utsunomiya, T., Sasaki, A., and Mori, M. (2006). Cancer stem cells in human gastrointestinal cancers. Hum Cell *19*, 24-29.

He, T.C., Sparks, A.B., Rago, C., Hermeking, H., Zawel, L., da Costa, L.T., Morin, P.J., Vogelstein, B., and Kinzler, K.W. (1998). Identification of c-MYC as a target of the APC pathway. Science *281*, 1509-1512.

Heath, J.P. (1996). Epithelial cell migration in the intestine. Cell biology international *20*, 139-146.

Hirschmann-Jax, C., Foster, A.E., Wulf, G.G., Nuchtern, J.G., Jax, T.W., Gobel, U., Goodell, M.A., and Brenner, M.K. (2004). A distinct "side population" of cells with high drug efflux capacity in human tumor cells. Proc Natl Acad Sci U S A *101*, 14228-14233.

Imai, T., Tokunaga, A., Yoshida, T., Hashimoto, M., Mikoshiba, K., Weinmaster, G., Nakafuku, M., and Okano, H. (2001). The neural RNA-binding protein Musashi1 translationally regulates mammalian numb gene expression by interacting with its mRNA. Mol Cell Biol *21*, 3888-3900.

Ishikawa, T., and Ali-Osman, F. (1993). Glutathione-associated cis-diamminedichloroplatinum(II) metabolism and ATP-dependent efflux from leukemia cells.

Molecular characterization of glutathione-platinum complex and its biological significance. J Biol Chem *268*, 20116-20125.

Jogi, A., Brennan, D.J., Ryden, L., Magnusson, K., Ferno, M., Stal, O., Borgquist, S., Uhlen, M., Landberg, G., Pahlman, S., *et al.* (2009). Nuclear expression of the RNA-binding protein RBM3 is associated with an improved clinical outcome in breast cancer. Mod Pathol *22*, 1564-1574.

Jung, A., Schrauder, M., Oswald, U., Knoll, C., Sellberg, P., Palmqvist, R., Niedobitek, G., Brabletz, T., and Kirchner, T. (2001). The invasion front of human colorectal adenocarcinomas shows co-localization of nuclear beta-catenin, cyclin D1, and p16INK4A and is a region of low proliferation. Am J Pathol *159*, 1613-1617.

Kahlert, C., Gaitzsch, E., Steinert, G., Mogler, C., Herpel, E., Hoffmeister, M., Jansen, L., Benner, A., Brenner, H., Chang-Claude, J., *et al.* (2012). Expression analysis of aldehyde dehydrogenase 1A1 (ALDH1A1) in colon and rectal cancer in association with prognosis and response to chemotherapy. Ann Surg Oncol *19*, 4193-4201.

Kaidi, A., Williams, A.C., and Paraskeva, C. (2007). Interaction between beta-catenin and HIF-1 promotes cellular adaptation to hypoxia. Nat Cell Biol *9*, 210-217.

Kanwar, S.S., Yu, Y., Nautiyal, J., Patel, B.B., and Majumdar, A.P. (2010). The Wnt/beta-catenin pathway regulates growth and maintenance of colonospheres. Mol Cancer *9*, 212.

Kawabata, S., Oka, M., Shiozawa, K., Tsukamoto, K., Nakatomi, K., Soda, H., Fukuda, M., Ikegami, Y., Sugahara, K., Yamada, Y., *et al.* (2001). Breast cancer resistance protein directly confers SN-38 resistance of lung cancer cells. Biochem Biophys Res Commun *280*, 1216-1223.

Kim, H.A., Koo, B.K., Cho, J.H., Kim, Y.Y., Seong, J., Chang, H.J., Oh, Y.M., Stange, D.E., Park, J.G., Hwang, D., *et al.* (2012a). Notch1 counteracts WNT/beta-catenin signaling through chromatin modification in colorectal cancer. J Clin Invest *122*, 3248-3259.

Kim, I., Kwak, H., Lee, H.K., Hyun, S., and Jeong, S. (2012b). beta-Catenin recognizes a specific RNA motif in the cyclooxygenase-2 mRNA 3'-UTR and interacts with HuR in colon cancer cells. Nucleic Acids Res *40*, 6863-6872.

Kinzler, K.W., and Vogelstein, B. (1997). Cancer-susceptibility genes. Gatekeepers and caretakers. Nature *386*, 761, 763.

Kita, H., Carmichael, J., Swartz, J., Muro, S., Wyttenbach, A., Matsubara, K., Rubinsztein, D.C., and Kato, K. (2002). Modulation of polyglutamine-induced cell death by genes identified by expression profiling. Hum Mol Genet *11*, 2279-2287.

Korinek, V., Barker, N., Moerer, P., van Donselaar, E., Huls, G., Peters, P.J., and Clevers, H. (1998). Depletion of epithelial stem-cell compartments in the small intestine of mice lacking Tcf-4. Nat Genet *19*, 379-383.

Korinek, V., Barker, N., Morin, P.J., van Wichen, D., de Weger, R., Kinzler, K.W., Vogelstein, B., and Clevers, H. (1997). Constitutive transcriptional activation by a beta-catenin-Tcf complex in APC-/- colon carcinoma. Science *275*, 1784-1787.

Kwon, C., Cheng, P., King, I.N., Andersen, P., Shenje, L., Nigam, V., and Srivastava, D. (2011). Notch post-translationally regulates beta-catenin protein in stem and progenitor cells. Nat Cell Biol *13*, 1244-1251.

Lapidot, T., Sirard, C., Vormoor, J., Murdoch, B., Hoang, T., Caceres-Cortes, J., Minden, M., Paterson, B., Caligiuri, M.A., and Dick, J.E. (1994). A cell initiating human acute myeloid leukaemia after transplantation into SCID mice. Nature *367*, 645-648.

Lee, G., White, L.S., Hurov, K.E., Stappenbeck, T.S., and Piwnica-Worms, H. (2009). Response of small intestinal epithelial cells to acute disruption of cell division through CDC25 deletion. Proc Natl Acad Sci U S A *106*, 4701-4706.

Lessard, J., and Sauvageau, G. (2003). Bmi-1 determines the proliferative capacity of normal and leukaemic stem cells. Nature *423*, 255-260.

Li, C., Heidt, D.G., Dalerba, P., Burant, C.F., Zhang, L., Adsay, V., Wicha, M., Clarke, M.F., and Simeone, D.M. (2007). Identification of pancreatic cancer stem cells. Cancer Res *67*, 1030-1037.

Li, L., and Bhatia, R. (2011). Stem cell quiescence. Clin Cancer Res *17*, 4936-4941.

Litman, T., Brangi, M., Hudson, E., Fetsch, P., Abati, A., Ross, D.D., Miyake, K., Resau, J.H., and Bates, S.E. (2000). The multidrug-resistant phenotype associated with overexpression of the new ABC half-transporter, MXR (ABCG2). J Cell Sci *113 (Pt 11)*, 2011-2021.

Liu, C., Li, Y., Semenov, M., Han, C., Baeg, G.H., Tan, Y., Zhang, Z., Lin, X., and He, X. (2002). Control of beta-catenin phosphorylation/degradation by a dual-kinase mechanism. Cell *108*, 837-847.

Liu, K.P., Luo, F., Xie, S.M., Tang, L.J., Chen, M.X., Wu, X.F., Zhong, X.Y., and Zhao, T. (2012). Glycogen Synthase Kinase 3beta Inhibitor (2'Z,3'E)-6-Bromo-indirubin- 3'-Oxime Enhances Drug Resistance to 5-Fluorouracil Chemotherapy in Colon Cancer Cells. Chinese journal of cancer research = Chung-kuo yen cheng yen chiu *24*, 116-123.

Lleonart, M.E. (2010). A new generation of proto-oncogenes: cold-inducible RNA binding proteins. Biochim Biophys Acta *1805*, 43-52.

Longley, D.B., and Johnston, P.G. (2005). Molecular mechanisms of drug resistance. J Pathol *205*, 275-292.

Ma, W.J., Cheng, S., Campbell, C., Wright, A., and Furneaux, H. (1996). Cloning and characterization of HuR, a ubiquitously expressed Elav-like protein. J Biol Chem *271*, 8144-8151.

Mani, S.A., Guo, W., Liao, M.J., Eaton, E.N., Ayyanan, A., Zhou, A.Y., Brooks, M., Reinhard, F., Zhang, C.C., Shipitsin, M., *et al.* (2008). The epithelial-mesenchymal transition generates cells with properties of stem cells. Cell *133*, 704-715.

Mathew, G., Timm, E.A., Jr., Sotomayor, P., Godoy, A., Montecinos, V.P., Smith, G.J., and Huss, W.J. (2009). ABCG2-mediated DyeCycle Violet efflux defined side population in benign and malignant prostate. Cell Cycle *8*, 1053-1061.

May, R., Riehl, T.E., Hunt, C., Sureban, S.M., Anant, S., and Houchen, C.W. (2008). Identification of a novel putative gastrointestinal stem cell and adenoma stem cell marker, doublecortin and CaM kinase-like-1, following radiation injury and in adenomatous polyposis coli/multiple intestinal neoplasia mice. Stem Cells *26*, 630-637.

May, R.J., Sureban, S.M., Lightfoot, S.A., Hoskins, A.B., Brackett, D.J., Postier, R.G., Ramanujam, R., Rao, C.V., Wyche, J.H., Anant, S., *et al.* (2010). Identification of a Novel Putative Pancreatic Stem/Progenitor Cell Marker Dcamkl-1 in Normal Mouse Pancreas. Am J Physiol Gastrointest Liver Physiol.

Mazumdar, J., O'Brien, W.T., Johnson, R.S., LaManna, J.C., Chavez, J.C., Klein, P.S., and Simon, M.C. (2010). O2 regulates stem cells through Wnt/beta-catenin signalling. Nat Cell Biol *12*, 1007-1013.

Meacham, C.E., and Morrison, S.J. (2013). Tumour heterogeneity and cancer cell plasticity. Nature *501*, 328-337.

Medema, J.P., and Vermeulen, L. (2011). Microenvironmental regulation of stem cells in intestinal homeostasis and cancer. Nature *474*, 318-326.

Meijer, L., Skaltsounis, A.L., Magiatis, P., Polychronopoulos, P., Knockaert, M., Leost, M., Ryan, X.P., Vonica, C.A., Brivanlou, A., Dajani, R., *et al.* (2003). GSK-3-selective inhibitors derived from Tyrian purple indirubins. Chemistry & biology *10*, 1255-1266.

Merlos-Suarez, A., Barriga, F.M., Jung, P., Iglesias, M., Cespedes, M.V., Rossell, D., Sevillano, M., Hernando-Momblona, X., da Silva-Diz, V., Munoz, P., *et al.* (2011). The intestinal stem cell signature identifies colorectal cancer stem cells and predicts disease relapse. Cell stem cell *8*, 511-524.

Metcalfe, C., Kljavin, N.M., Ybarra, R., and de Sauvage, F.J. (2013). Lgr5 Stem Cells Are Indispensable for Radiation-Induced Intestinal Regeneration. Cell stem cell.

Molofsky, A.V., Pardal, R., Iwashita, T., Park, I.K., Clarke, M.F., and Morrison, S.J. (2003). Bmi-1 dependence distinguishes neural stem cell self-renewal from progenitor proliferation. Nature *425*, 962-967.

Morin, P.J., Sparks, A.B., Korinek, V., Barker, N., Clevers, H., Vogelstein, B., and Kinzler, K.W. (1997). Activation of beta-catenin-Tcf signaling in colon cancer by mutations in beta-catenin or APC. Science *275*, 1787-1790.

Moser, A.R., Pitot, H.C., and Dove, W.F. (1990). A dominant mutation that predisposes to multiple intestinal neoplasia in the mouse. Science *247*, 322-324.

Moss, E.G., and Tang, L. (2003). Conservation of the heterochronic regulator Lin-28, its developmental expression and microRNA complementary sites. Developmental biology *258*, 432-442.

Mottet, D., Dumont, V., Deccache, Y., Demazy, C., Ninane, N., Raes, M., and Michiels, C. (2003). Regulation of hypoxia-inducible factor-1alpha protein level during hypoxic conditions by the phosphatidylinositol 3-kinase/Akt/glycogen synthase kinase 3beta pathway in HepG2 cells. J Biol Chem *278*, 31277-31285.

Munemitsu, S., Albert, I., Souza, B., Rubinfeld, B., and Polakis, P. (1995). Regulation of intracellular beta-catenin levels by the adenomatous polyposis coli (APC) tumor-suppressor protein. Proc Natl Acad Sci U S A *92*, 3046-3050.

Muraro, M.G., Mele, V., Daster, S., Han, J., Heberer, M., Cesare Spagnoli, G., and Iezzi, G. (2012). CD133+, CD166+CD44+, and CD24+CD44+ phenotypes fail to reliably identify cell populations with cancer stem cell functional features in established human colorectal cancer cell lines. Stem cells translational medicine *1*, 592-603.

Nakamura, T., Tsuchiya, K., and Watanabe, M. (2007). Crosstalk between Wnt and Notch signaling in intestinal epithelial cell fate decision. Journal of gastroenterology *42*, 705-710.

Nakanishi, Y., Seno, H., Fukuoka, A., Ueo, T., Yamaga, Y., Maruno, T., Nakanishi, N., Kanda, K., Komekado, H., Kawada, M., *et al.* (2013). Dclk1 distinguishes between tumor and normal stem cells in the intestine. Nat Genet *45*, 98-103.

Nemeth, M.J., Mak, K.K., Yang, Y., and Bodine, D.M. (2009). beta-Catenin expression in the bone marrow microenvironment is required for long-term maintenance of primitive hematopoietic cells. Stem Cells *27*, 1109-1119.

Newton, R., Seybold, J., Liu, S.F., and Barnes, P.J. (1997). Alternate COX-2 transcripts are differentially regulated: implications for post-transcriptional control. Biochem Biophys Res Commun *234*, 85-89.

Noda, T., Nagano, H., Takemasa, I., Yoshioka, S., Murakami, M., Wada, H., Kobayashi, S., Marubashi, S., Takeda, Y., Dono, K., *et al.* (2009). Activation of Wnt/beta-catenin signalling pathway induces chemoresistance to interferon-alpha/5-fluorouracil combination therapy for hepatocellular carcinoma. Br J Cancer *100*, 1647-1658.

O'Brien, C.A., Pollett, A., Gallinger, S., and Dick, J.E. (2007). A human colon cancer cell capable of initiating tumour growth in immunodeficient mice. Nature *445*, 106-110.

Ozawa, M., Ringwald, M., and Kemler, R. (1990). Uvomorulin-catenin complex formation is regulated by a specific domain in the cytoplasmic region of the cell adhesion molecule. Proc Natl Acad Sci U S A *87*, 4246-4250.

Pilotte, J., Dupont-Versteegden, E.E., and Vanderklish, P.W. (2011). Widespread regulation of miRNA biogenesis at the Dicer step by the cold-inducible RNA-binding protein, RBM3. PLoS One *6*, e28446.

Polakis, P. (2007). The many ways of Wnt in cancer. Curr Opin Genet Dev *17*, 45-51.

Pommier, Y., Leo, E., Zhang, H., and Marchand, C. (2010). DNA topoisomerases and their poisoning by anticancer and antibacterial drugs. Chemistry & biology *17*, 421-433.

Porlan, E., Morante-Redolat, J.M., Marques-Torrejon, M.A., Andreu-Agullo, C., Carneiro, C., Gomez-Ibarlucea, E., Soto, A., Vidal, A., Ferron, S.R., and Farinas, I. (2013). Transcriptional repression of Bmp2 by p21(Waf1/Cip1) links quiescence to neural stem cell maintenance. Nature neuroscience *16*, 1567-1575.

Potten, C.S. (1977). Extreme sensitivity of some intestinal crypt cells to X and gamma irradiation. Nature *269*, 518-521.

Potten, C.S., Booth, C., and Pritchard, D.M. (1997). The intestinal epithelial stem cell: the mucosal governor. International journal of experimental pathology *78*, 219-243.

Potten, C.S., Hume, W.J., Reid, P., and Cairns, J. (1978). The segregation of DNA in epithelial stem cells. Cell *15*, 899-906.

Povinelli, B.J., and Nemeth, M.J. (2014). Wnt5a regulates hematopoietic stem cell proliferation and repopulation through the ryk receptor. Stem Cells *32*, 105-115.

Qing-Bin, M., Jian-Chun, Y., Wei-Ming, K., Zhi-Qiang, M., Wei-Xun, Z., Ji, L., Li, Z., Zhan-Jiang, C., and Shu-Bo, T. (2013). Expression of Doublecortin-like Kinase 1 in Human Gastric Cancer and Its Correlation with Prognosis. Zhongguo yi xue ke xue yuan xue bao Acta Academiae Medicinae Sinicae *35*, 639-644.

Reya, T., and Clevers, H. (2005). Wnt signalling in stem cells and cancer. Nature *434*, 843-850.

Reya, T., Duncan, A.W., Ailles, L., Domen, J., Scherer, D.C., Willert, K., Hintz, L., Nusse, R., and Weissman, I.L. (2003). A role for Wnt signalling in self-renewal of haematopoietic stem cells. Nature *423*, 409-414.

Reynolds, B.A., and Weiss, S. (1996). Clonal and population analyses demonstrate that an EGF-responsive mammalian embryonic CNS precursor is a stem cell. Developmental biology *175*, 1-13.

Ricci-Vitiani, L., Lombardi, D.G., Pilozzi, E., Biffoni, M., Todaro, M., Peschle, C., and De Maria, R. (2007). Identification and expansion of human colon-cancer-initiating cells. Nature *445*, 111-115.

Roshak, A., Sathe, G., and Marshall, L.A. (1994). Suppression of monocyte 85-kDa phospholipase A2 by antisense and effects on endotoxin-induced prostaglandin biosynthesis. J Biol Chem *269*, 25999-26005.

Ryan, J.C., Morey, J.S., Ramsdell, J.S., and Van Dolah, F.M. (2005). Acute phase gene expression in mice exposed to the marine neurotoxin domoic acid. Neuroscience *136*, 1121-1132.

Saigusa, S., Tanaka, K., Toiyama, Y., Yokoe, T., Okugawa, Y., Ioue, Y., Miki, C., and Kusunoki, M. (2009). Correlation of CD133, OCT4, and SOX2 in rectal cancer and their association with distant recurrence after chemoradiotherapy. Ann Surg Oncol *16*, 3488-3498.

Sangiorgi, E., and Capecchi, M.R. (2008). Bmi1 is expressed in vivo in intestinal stem cells. Nat Genet *40*, 915-920.

Scharenberg, C.W., Harkey, M.A., and Torok-Storb, B. (2002). The ABCG2 transporter is an efficient Hoechst 33342 efflux pump and is preferentially expressed by immature human hematopoietic progenitors. Blood *99*, 507-512.

Schmidt, G.H., Winton, D.J., and Ponder, B.A. (1988). Development of the pattern of cell renewal in the crypt-villus unit of chimaeric mouse small intestine. Development *103*, 785-790.

Schwitalla, S., Fingerle, A.A., Cammareri, P., Nebelsiek, T., Goktuna, S.I., Ziegler, P.K., Canli, O., Heijmans, J., Huels, D.J., Moreaux, G., *et al.* (2013). Intestinal tumorigenesis initiated by dedifferentiation and acquisition of stem-cell-like properties. Cell *152*, 25-38.

Shaikhibrahim, Z., Lindstrot, A., Ochsenfahrt, J., Fuchs, K., and Wernert, N. (2013). Epigenetics-related genes in prostate cancer: expression profile in prostate cancer tissues, androgen-sensitive and -insensitive cell lines. Int J Mol Med *31*, 21-25.

Shapiro, A.B., Corder, A.B., and Ling, V. (1997). P-glycoprotein-mediated Hoechst 33342 transport out of the lipid bilayer. Eur J Biochem *250*, 115-121.

Shmelkov, S.V., Butler, J.M., Hooper, A.T., Hormigo, A., Kushner, J., Milde, T., St Clair, R., Baljevic, M., White, I., Jin, D.K., *et al.* (2008). CD133 expression is not restricted to stem cells, and both CD133+ and CD133- metastatic colon cancer cells initiate tumors. J Clin Invest *118*, 2111-2120.

Shyh-Chang, N., and Daley, G.Q. (2013). Lin28: primal regulator of growth and metabolism in stem cells. Cell stem cell *12*, 395-406.

Smart, F., Aschrafi, A., Atkins, A., Owens, G.C., Pilotte, J., Cunningham, B.A., and Vanderklish, P.W. (2007). Two isoforms of the cold-inducible mRNA-binding protein RBM3 localize to dendrites and promote translation. J Neurochem *101*, 1367-1379.

Stappenbeck, T.S., Mills, J.C., and Gordon, J.I. (2003). Molecular features of adult mouse small intestinal epithelial progenitors. Proc Natl Acad Sci U S A *100*, 1004-1009.

Subramaniam, D., May, R., Sureban, S.M., Lee, K.B., George, R., Kuppusamy, P., Ramanujam, R.P., Hideg, K., Dieckgraefe, B.K., Houchen, C.W., *et al.* (2008). Diphenyl difluoroketone: a curcumin derivative with potent in vivo anticancer activity. Cancer Res *68*, 1962-1969.

Subramaniam, S., Sreenivas, P., Cheedipudi, S., Reddy, V.R., Shashidhara, L.S., Chilukoti, R.K., Mylavarapu, M., and Dhawan, J. (2013). Distinct transcriptional networks in quiescent myoblasts: a role for Wnt signaling in reversible vs. irreversible arrest. PLoS One *8*, e65097.

Sureban, S.M., May, R., George, R.J., Dieckgraefe, B.K., McLeod, H.L., Ramalingam, S., Bishnupuri, K.S., Natarajan, G., Anant, S., and Houchen, C.W. (2008a). Knockdown of RNA binding protein musashi-1 leads to tumor regression in vivo. Gastroenterology *134*, 1448-1458.

Sureban, S.M., May, R., Lightfoot, S.A., Hoskins, A.B., Lerner, M., Brackett, D.J., Postier, R.G., Ramanujam, R., Mohammed, A., Rao, C.V., *et al.* (2011). DCAMKL-1 regulates epithelial-mesenchymal transition in human pancreatic cells through a miR-200a-dependent mechanism. Cancer Res *71*, 2328-2338.

Sureban, S.M., Ramalingam, S., Natarajan, G., May, R., Subramaniam, D., Bishnupuri, K.S., Morrison, A.R., Dieckgraefe, B.K., Brackett, D.J., Postier, R.G., *et al.* (2008b). Translation regulatory factor RBM3 is a proto-oncogene that prevents mitotic catastrophe. Oncogene *27*, 4544-4556.

Szakacs, G., Paterson, J.K., Ludwig, J.A., Booth-Genthe, C., and Gottesman, M.M. (2006). Targeting multidrug resistance in cancer. Nature reviews Drug discovery *5*, 219-234.

Szotek, P.P., Pieretti-Vanmarcke, R., Masiakos, P.T., Dinulescu, D.M., Connolly, D., Foster, R., Dombkowski, D., Preffer, F., Maclaughlin, D.T., and Donahoe, P.K. (2006). Ovarian cancer side population defines cells with stem cell-like characteristics and Mullerian Inhibiting Substance responsiveness. Proc Natl Acad Sci U S A *103*, 11154-11159.

Takahashi, S., Kamiyama, T., Tomaru, U., Ishizu, A., Shida, T., Osaka, M., Sato, Y., Saji, Y., Ozaki, M., and Todo, S. (2010). Frequency and pattern of expression of the stem cell marker CD133 have strong prognostic effect on the surgical outcome of colorectal cancer patients. Oncology reports *24*, 1201-1212.

Takubo, K., Goda, N., Yamada, W., Iriuchishima, H., Ikeda, E., Kubota, Y., Shima, H., Johnson, R.S., Hirao, A., Suematsu, M., *et al.* (2010). Regulation of the HIF-1alpha level is essential for hematopoietic stem cells. Cell stem cell *7*, 391-402.

Tamm, I., Wang, Y., Sausville, E., Scudiero, D.A., Vigna, N., Oltersdorf, T., and Reed, J.C. (1998). IAP-family protein survivin inhibits caspase activity and apoptosis induced by Fas (CD95), Bax, caspases, and anticancer drugs. Cancer Res *58*, 5315-5320.

Tetsu, O., and McCormick, F. (1999). Beta-catenin regulates expression of cyclin D1 in colon carcinoma cells. Nature *398*, 422-426.

Tian, H., Biehs, B., Warming, S., Leong, K.G., Rangell, L., Klein, O.D., and de Sauvage, F.J. (2011). A reserve stem cell population in small intestine renders Lgr5-positive cells dispensable. Nature *478*, 255-259.

Touil, Y., Igoudjil, W., Corvaisier, M., Dessein, A.F., Vandomme, J., Monte, D., Stechly, L., Skrypek, N., Langlois, C., Grard, G., *et al.* (2013). Colon cancer cells escape 5FU

chemotherapy-induced cell death by entering stemness and quiescence associated with the c-Yes/YAP axis. Clin Cancer Res.

Uchida, N., Buck, D.W., He, D., Reitsma, M.J., Masek, M., Phan, T.V., Tsukamoto, A.S., Gage, F.H., and Weissman, I.L. (2000). Direct isolation of human central nervous system stem cells. Proc Natl Acad Sci U S A *97*, 14720-14725.

van de Wetering, M., Oosterwegel, M., Dooijes, D., and Clevers, H. (1991). Identification and cloning of TCF-1, a T lymphocyte-specific transcription factor containing a sequence-specific HMG box. The EMBO journal *10*, 123-132.

van de Wetering, M., Sancho, E., Verweij, C., de Lau, W., Oving, I., Hurlstone, A., van der Horn, K., Batlle, E., Coudreuse, D., Haramis, A.P.*, et al.* (2002). The beta-catenin/TCF-4 complex imposes a crypt progenitor phenotype on colorectal cancer cells. Cell *111*, 241-250.

van der Flier, L.G., and Clevers, H. (2009). Stem cells, self-renewal, and differentiation in the intestinal epithelium. Annu Rev Physiol *71*, 241-260.

van der Giessen, K., and Gallouzi, I.E. (2007). Involvement of transportin 2-mediated HuR import in muscle cell differentiation. Molecular biology of the cell *18*, 2619-2629.

van der Wurff, A.A., Vermeulen, S.J., van der Linden, E.P., Mareel, M.M., Bosman, F.T., and Arends, J.W. (1997). Patterns of alpha- and beta-catenin and E-cadherin expression in colorectal adenomas and carcinomas. J Pathol *182*, 325-330.

van Os, R., Kamminga, L.M., Ausema, A., Bystrykh, L.V., Draijer, D.P., van Pelt, K., Dontje, B., and de Haan, G. (2007). A Limited role for p21Cip1/Waf1 in maintaining normal hematopoietic stem cell functioning. Stem Cells *25*, 836-843.

VanDussen, K.L., Carulli, A.J., Keeley, T.M., Patel, S.R., Puthoff, B.J., Magness, S.T., Tran, I.T., Maillard, I., Siebel, C., Kolterud, A.*, et al.* (2012). Notch signaling modulates proliferation and differentiation of intestinal crypt base columnar stem cells. Development *139*, 488-497.

Verissimo, C.S., Cheng, S., Puigvert, J.C., Qin, Y., Vroon, A., van Deutekom, J., Price, L.S., Danen, E.H., van de Water, B., Fitzsimons, C.P.*, et al.* (2012). Combining doublecortin-like kinase silencing and vinca alkaloids results in a synergistic apoptotic effect in neuroblastoma cells. The Journal of pharmacology and experimental therapeutics *342*, 119-130.

Viswanathan, S.R., Daley, G.Q., and Gregory, R.I. (2008). Selective blockade of microRNA processing by Lin28. Science *320*, 97-100.

Viswanathan, S.R., Powers, J.T., Einhorn, W., Hoshida, Y., Ng, T.L., Toffanin, S., O'Sullivan, M., Lu, J., Phillips, L.A., Lockhart, V.L.*, et al.* (2009). Lin28 promotes transformation and is associated with advanced human malignancies. Nat Genet *41*, 843-848.

Vooijs, M., Liu, Z., and Kopan, R. (2011). Notch: architect, landscaper, and guardian of the intestine. Gastroenterology *141*, 448-459.

Wagers, A.J., and Weissman, I.L. (2004). Plasticity of adult stem cells. Cell *116*, 639-648.

Wang, C., Xie, J., Guo, J., Manning, H.C., Gore, J.C., and Guo, N. (2012). Evaluation of CD44 and CD133 as cancer stem cell markers for colorectal cancer. Oncology reports *28*, 1301-1308.

Wang, W., Furneaux, H., Cheng, H., Caldwell, M.C., Hutter, D., Liu, Y., Holbrook, N., and Gorospe, M. (2000). HuR regulates p21 mRNA stabilization by UV light. Mol Cell Biol *20*, 760-769.

Wellmann, S., Buhrer, C., Moderegger, E., Zelmer, A., Kirschner, R., Koehne, P., Fujita, J., and Seeger, K. (2004). Oxygen-regulated expression of the RNA-binding proteins RBM3 and CIRP by a HIF-1-independent mechanism. J Cell Sci *117*, 1785-1794.

Wellmann, S., Truss, M., Bruder, E., Tornillo, L., Zelmer, A., Seeger, K., and Buhrer, C. (2010). The RNA-binding protein RBM3 is required for cell proliferation and protects against serum deprivation-induced cell death. Pediatr Res *67*, 35-41.

Wielenga, V.J., Smits, R., Korinek, V., Smit, L., Kielman, M., Fodde, R., Clevers, H., and Pals, S.T. (1999). Expression of CD44 in Apc and Tcf mutant mice implies regulation by the WNT pathway. Am J Pathol *154*, 515-523.

Woodward, W.A., Chen, M.S., Behbod, F., and Rosen, J.M. (2005). On mammary stem cells. J Cell Sci *118*, 3585-3594.

Yamamoto, H., Komekado, H., and Kikuchi, A. (2006). Caveolin is necessary for Wnt-3a-dependent internalization of LRP6 and accumulation of beta-catenin. Dev Cell *11*, 213-223.

Yang, D., Wang, H., Zhang, J., Li, C., Lu, Z., Liu, J., Lin, C., Li, G., and Qian, H. (2013). In vitro characterization of stem cell-like properties of drug-resistant colon cancer subline. Oncology research *21*, 51-57.

Yang, H.Y., Jeong, D.K., Kim, S.H., Chung, K.J., Cho, E.J., Jin, C.H., Yang, U., Lee, S.R., Lee, D.S., and Lee, T.H. (2008a). Gene expression profiling related to the enhanced erythropoiesis in mouse bone marrow cells. J Cell Biochem *104*, 295-303.

Yang, J., Zhang, W., Evans, P.M., Chen, X., He, X., and Liu, C. (2006). Adenomatous polyposis coli (APC) differentially regulates beta-catenin phosphorylation and ubiquitination in colon cancer cells. J Biol Chem *281*, 17751-17757.

Yang, W., Yan, H.X., Chen, L., Liu, Q., He, Y.Q., Yu, L.X., Zhang, S.H., Huang, D.D., Tang, L., Kong, X.N., *et al.* (2008b). Wnt/beta-catenin signaling contributes to activation of normal and tumorigenic liver progenitor cells. Cancer Res *68*, 4287-4295.

Yatabe, Y., Tavare, S., and Shibata, D. (2001). Investigating stem cells in human colon by using methylation patterns. Proc Natl Acad Sci U S A *98*, 10839-10844.

Yoshida, T., Hashimura, M., Mastumoto, T., Tazo, Y., Inoue, H., Kuwata, T., and Saegusa, M. (2013). Transcriptional upregulation of HIF-1alpha by NF-kappaB/p65 and its associations with beta-catenin/p300 complexes in endometrial carcinoma cells. Lab Invest.

Young, L.E., Sanduja, S., Bemis-Standoli, K., Pena, E.A., Price, R.L., and Dixon, D.A. (2009). The mRNA binding proteins HuR and tristetraprolin regulate cyclooxygenase 2 expression during colon carcinogenesis. Gastroenterology *136*, 1669-1679.

Yu, J., Vodyanik, M.A., Smuga-Otto, K., Antosiewicz-Bourget, J., Frane, J.L., Tian, S., Nie, J., Jonsdottir, G.A., Ruotti, V., Stewart, R., *et al.* (2007). Induced pluripotent stem cell lines derived from human somatic cells. Science *318*, 1917-1920.

Zeng, X., Tamai, K., Doble, B., Li, S., Huang, H., Habas, R., Okamura, H., Woodgett, J., and He, X. (2005). A dual-kinase mechanism for Wnt co-receptor phosphorylation and activation. Nature *438*, 873-877.

Zeng, Y., Kulkarni, P., Inoue, T., and Getzenberg, R.H. (2009). Down-regulating cold shock protein genes impairs cancer cell survival and enhances chemosensitivity. J Cell Biochem *107*, 179-188.

Zeng, Y., Wodzenski, D., Gao, D., Shiraishi, T., Terada, N., Li, Y., Griend, D.J., Luo, J., Kong, C., Getzenberg, R.H., *et al.* (2013). Stress-Response Protein RBM3 Attenuates the Stem-like Properties of Prostate Cancer Cells by Interfering with CD44 Variant Splicing. Cancer Res.

Zhang, H.T., Zhang, Z.W., Xue, J.H., Kong, H.B., Liu, A.J., Li, S.C., Liu, Y.X., and Xu, D.G. (2013). Differential expression of the RNA-binding motif protein 3 in human astrocytoma. Chinese medical journal *126*, 1948-1952.

Zhang, T., Otevrel, T., Gao, Z., Gao, Z., Ehrlich, S.M., Fields, J.Z., and Boman, B.M. (2001). Evidence that APC regulates survivin expression: a possible mechanism contributing to the stem cell origin of colon cancer. Cancer Res *61*, 8664-8667.

Zhou, S., Schuetz, J.D., Bunting, K.D., Colapietro, A.M., Sampath, J., Morris, J.J., Lagutina, I., Grosveld, G.C., Osawa, M., Nakauchi, H., *et al.* (2001). The ABC transporter Bcrp1/ABCG2 is expressed in a wide variety of stem cells and is a molecular determinant of the side-population phenotype. Nature medicine *7*, 1028-1034.